Norwegian University of Life Sciences

Master's Thesis 2019 60 ECTS

Faculty of Chemistry, Biotechnology and Food Science
Daniel Straume

A penicillin resistant *Streptococcus pneumoniae* in the making: characterizing resistance development and cell fitness after acquiring low-affinity penicillin-binding proteins and a mosaic MurM

Maria Victoria Heggenhougen
Biotechnology

Acknowledgements

This master thesis was completed as part of the Master programme in Biotechnology at the Norwegian University of Life Sciences (NMBU), in the Molecular Microbiology research group at the Faculty of Chemistry, Biotechnology and Food Science (KBM), between August 2018 and May 2019.

First and foremost, I would like to thank my supervisor, Dr. Daniel Straume, for excellent guidance, both during the laboratory work and the writing process – and for your patience. I have learned so much from you.

My co-supervisor, Prof. Leiv Sigve Håvarstein, for giving me the opportunity to write my master thesis with the Molecular Microbiology research group, and for sharing your knowledge with me.

Everyone in the Molecular Microbiology research group deserves a big thanks for your support and guidance, and for providing such a great work environment. Especially Zhian Salehian for helping me out with challenging PCR reactions and cloning experiments, and Dr. Gro Stamsås for always taking the time to talk science with a confused student and for helping me in the writing process.

Thanks to my fellow master students Kjerstin and Malene, for lab entertainment and moral support, and to Amalie for countless hours at the library. Thank you Helle and Selma for all your help. Also, a big thanks to Marie for saving me when my computer broke down just weeks before the thesis deadline.

Thank you so much to my friends and loved ones for your continued support and encouragement throughout my studies. And thank you, Erik, for always being there.

Maria Victoria Heggenhougen

Ås, May 2019

Abstract

Streptococcus pneumoniae is an important human pathogen, causing about 100 millions of cases of disease and 1 – 2 million deaths every year. The rapid evolution and spread of multi-resistant strains threaten current antibiotic treatments of pneumococcal infections. A continued exploration of the cellular processes in *S. pneumoniae* is essential for the development of novel therapeutic treatments against this pathogen.

β-lactam resistance in *S. pneumoniae* is mediated through alterations in the targets of these antibiotics: the penicillin-binding proteins (PBPs). PBPs are important enzymes in the cell division machinery, catalysing the final steps in the biosynthesis of the cell wall. Resistant pneumococci have PBPs with a reduced affinity for these antibiotics. How different low-affinity PBPs contribute to increased β-lactam resistance was studied in this work by introducing low-affinity versions of PBP2x, PBP1a and PBP2b from the highly penicillin resistant *S. oralis* Uo5 into the sensitive *S. pneumoniae* R6 strain. The results showed that that the transfer of low-affinity PBPs from *S. oralis* Uo5 to *S. pneumoniae* R6 resulted in an increased level of resistance against different β-lactam antibiotics, but not to the level of the donor strain. The results also showed that low-affinity PBPs most likely are transferred sequential in a specific order into sensitive strains. Transformation of the R6 strain with combinations of the low-affinity *pbp2x/1a/2b* genes demonstrated that *pbp2x* was always transferred first. Subsequent addition of either the low-affinity *pbp1a* or *pbp2b* genes did not appear to be critical, although *pbp1a* appeared to be preferred before *pbp2b*. Introduction of all three low-affinity PBPs in the R6 strain provided the highest level of resistance to β-lactams. Cells expressing low-affinity PBPs often have a cell wall enriched in branched stem peptides. HPLC analyses of the stem peptide composition of a selection of the R6 strain expressing different combinations of low-affinity PBPs revealed that the expression of a low-affinity PBP2b is most likely responsible for this phenotype. However, it was not possible to deduce whether this was affected by the presence of a low-affinity PBP2x and/or PBP1a. In addition to low-affinity PBPs, mutated versions of MurM, an enzyme involved in the synthesis of branched stem peptides in the cell wall, is an important resistance-determining factor in *S. pneumoniae*. The transfer of mosaic MurM versions to sensitive strains of *S. pneumoniae* under laboratory conditions does, however, appear to have a toxic effect on the penicillin-sensitive cells, and it has been hypothesized that they are dependent on the presence of low-affinity PBPs. In this work it was shown that transfer of the mosaic MurM from *S. oralis* Uo5 to the sensitive

R6 strain depends on the activity of MurN, which attaches the second L-Ala residue in the branched stem peptides. Surprisingly, the transfer of a mosaic MurM into the R6 strain expressing low-affinity PBPs did not result in increased resistance against β-lactams. Overexpression experiments showed that MurM had a severe toxic effect on the cells in a Δ*murN* background.

Sammendrag

Streptococcus pneumoniae er en viktig humanpatogen bakterie, og forårsaker rundt 100 millioner sykdomstilfeller og mellom 1-2 millioner dødsfall hvert år.

Utviklingen og spredningen av multiresistente stammer truer dagens antibiotikabehandling mot streptokokkinfeksjoner. Videre forskning på de cellulære mekanismene i *S. pneumoniae* er essensielt for å kunne utvikle nye antibiotika mot disse bakteriene.

I *S. pneumoniae* er resistens mot β-laktamer forårsaket av endringer i målproteinene til disse antibiotikaene: de penicillin-bindende proteinene (PBP-er). PBP-er er viktige enzymer i celleveggssyntesen, og katalyserer polymeriseringen og kryssbindingen av peptidoglykan. Resistente pneumokokker har PBP-er med redusert affinitet for disse antibiotikaene. I dette arbeidet ble det studert hvordan ulike versjoner av PBP-er bidrar til resistensutvikling, ved å overføre lavaffinitetsversjoner av PBP2x, PBP2b og PBP1a fra en høyresistens stamme (*S. oralis* Uo5) til den penicillin-sensitive stammen *S. pneumoniae* R6. Resultatene fra dette arbeidet viste at overføringen av disse lavaffinitets-PBP-ene fra *S. oralis* Uo5 førte til et høyere resistensnivå i *S. pneumoniae* R6, men ikke i nærheten av nivået til donorstammen. Resultatene viste også at overføringen av lavaffinitets-PBP-er sannsynligvis overføres i en gitt rekkefølge til sensitive stammer. Transformasjon av *S. pneumoniae* R6 med ulike kombinasjoner av lavaffinitets-PBP-er viste at PBP2x alltid ble overført først. Rekkefølgen på den videre overføringen av PBP2b og PBP1a var ikke like kritisk, men resultatene tyder på at PBP1a foretrekkes over PBP2b. Transformasjon av alle de tre lavaffinitets-PBP-ene førte som forventet til høyest resistensnivå.

Celler som uttrykker lavaffinitets-PBP-er har ofte en cellevegg beriket med forgreinede stempeptider. HPLC-analyse av celleveggen til et utvalg av mutantene med ulike kombinasjoner av lavaffinitets-PBP-er viste at økningen i forgreinede stempeptider sannsynligvis skyldes uttrykket av en lavaffinitetsversjon av PBP2b. Det var dog ikke mulig å bestemme hvorvidt denne fenotypen også ble påvirket av tilstedeværelsen til et lavaffinitets-PBP2x eller -PBP1a.

I tillegg til lavaffinitets-versjoner av PBP-er, er endringer i MurM, som sammen med MurN introduserer dipeptidet i den forgreinede celleveggen, en viktig resistensfaktor i *S. pneumoniae*.

Tidligere arbeider har vist at overføringen av slike muterte MurM-versjoner til penicillin-sensitive pneumokokker kan ha en toksisk effekt på cellene. Det har vært foreslått at de er avhengige av uttrykk av en eller flere lavaffinitets-PBP-er. Basert på resultatene fra dette arbeidet, ble det vist at overføringen av et slikt mutert MurM fra S. oralis Uo5 til S. pneumoniae R6 var avhengig av uttrykket til MurN. Overraskende nok førte ikke tilstedeværelsen av $MurM_{Uo5}$, som er en viktig resistensfaktor i *S. oralis* Uo5, til økt resistens i *S. pneumoniae*. I tillegg ble det vist at overuttrykk av MurM har en alvorlig toksisk effekt i S. pneumoniae i en Δ*murN*-bakgrunn.

Index

1 Introduction 1

1.1 Streptococcus pneumoniae 1

1.2 Natural competence for genetic transformation in *S. pneumoniae* 3

1.2.1 Regulation of the competent state 4

1.2.1 Competence-induced fratricide 5

1.3 Pneumococcal cell wall synthesis and cell division 6

1.3.1 The pneumococcal cell wall 6

1.3.3 Cell division in *S. pneumoniae* 9

1.4 The penicillin-binding proteins 10

1.4.1 High molecular mass PBPs in *S. pneumoniae* 11

1.4.2 Low molecular mass PBPs 13

1.6 Penicillin resistance in *S. pneumoniae* 14

1.6.1 Mechanism of β-lactam antibiotics 15

1.6.2 β-lactam resistance in *S. pneumoniae* 16

1.6.3 Characterization of MurM 19

1.7 Main objectives of this study 21

2 Materials 23

2.1 Strains 23

2.2 Primers 24

2.3 Peptides 26

2.4 Enzymes, molecular weight standards and nucleotides 27

2.5 Antibiotics 27

2.7 Kits 28

2.8 Chemicals 28

2.9 Equipment 30

2.10 Recipes for growth mediums and buffers 30

2.10.1 Solutions for C medium 30

2.10.2 Todd Hewitt (TH) medium 32
2.10.3 Brain Heart Infusion (BHI) medium 32
2.10.4 Buffers and solutions for agarose gel electrophoresis 33
2.10.5 Buffers and gels for SDS-PAGE 34
2.10.6 Buffers for HPLC 35
2.10.7 Other buffers and solutions 36
3 Methods 37
3.1 Growth and storage of *S. pneumonia* and *S. oralis* 37
3.2 The Polymerase Chain Reaction (PCR) 37
3.2.1 PCR-screening of potential transformants 39
3.2.2 Overlap extension PCR 40
3.3 Gel electrophoresis 42
3.3.1 Agarose gel electrophoresis 43
3.3.2 Extraction of DNA from agarose gels 43
3.3.3 SDS-PAGE 44
3.4 Isolation of genomic DNA (gDNA) 46
3.5 DNA sequencing 46
3.5.1 Targeted gene sequencing 47
3.5.2 Whole genome sequencing 47
3.6 Natural transformation of *S. pneumoniae* 47
3.6.1 The Janus cassette 48
3.6.2 Selection on a gradient of penicillin G 49
3.7 Phase contrast microscopy 50
3.8 Cell wall analysis 50
3.8.1 Isolation of bacterial cell wall 51
3.8.2 Analysis of the muropeptide composition using HPLC 52
3.9 Antibiotic sensitivity analysis using E-test® strips 54
3.10 Visualization of PBPs with Bocillin FL 54
3.11 Overexpression of genes using the ComRS system 55
3.12 Growth assay 55
3.13 Temperature sensitivity analysis 56

4 Results 59

4.1 Transferring low-affinity PBPs from *S. oralis* Uo5 to *S. pneumoniae* R6 59

4.1.1 *pbp* replacements using the Janus cassette 59

4.1.2 Selection for transformants using a gradient of penicillin G 61

4.2 Characterization of pneumococcal strains expressing mosaic PBPs 65

4.2.1 Minimal inhibitory concentration of PBP_{mos} mutants 66

4.2.2 Detection of PBPs in RH425 (wild-type) and MH83 ($PBP2x_{mos}/1a_{mos}/2b_{mos}$) 67

4.2.2 Expression of low-affinity PBPs does not inhibit growth, but results in abnormal cell morphologies in *S. pneumoniae* R6. 68

4.2.3 The low-affinity PBP2b is important for building a cell wall with higher content of branched stem peptides in *S. pneumoniae* R6. 71

4.2.4 Will deletion of the native *murMN* genes affect penicillin resistance in *S. pneumoniae* R6 harbouring low-affinity PBPs? 74

4.3 Whole genome sequencing 80

4.4 Why is $murM_{Uo5}$ not tolerated in *S. pneumoniae*? 81

4.4.1 The absence of MurN makes overexpression of MurM toxic in *S. pneumoniae*. 82

4.4.2 Cells overexpressing $murM_{Uo5}$ develop gross morphological abnormalities 86

4.4.3 The presence of $MurM_{Uo5}$ do not further increase penicillin resistance in *S. pneumoniae*. 87

5 Discussion 89

5.1 Transfer of low-affinity PBPs from *S. oralis* Uo5 to *S. pneumoniae* R6 89

5.2 Increased β-lactam resistance in *S. pneumoniae* R6 mutants with mosaic *pbps* 92

5.3 Cell fitness cost of acquiring mosaic *pbps* 93

5.4 Inactivation of *murMN* does not always result in loss of β-lactam resistance 94

5.5 MurM, low-affinity PBPs and the tolerance for temperature-induced stress 95

5.6 $MurM_{Uo5}$ is not tolerated in an R6 background in the absence of MurN 96

6 Concluding remarks and further research 99

Reference list 100

Appendix 107

1 Introduction

1.1 Streptococcus pneumoniae

Streptococcus pneumoniae, also known as pneumococcus, is an important human pathogen. William Osler described it in 1918 as the "captain of the men of death", and *S. pneumoniae* is known to cause everything from mild illnesses, such as middle-ear infections (otitis media) and sinusitis, to severe, life-threatening infections like pneumoniae, meningitis and bacteraemia (Mitchell, 2003, van der Poll and Opal, 2009). Bacterial pneumoniae is recognized as one of the main causes of childhood mortality, with *S. pneumoniae,* as well as *Haemophilus influenzae* type b, being the major causative agents (Wahl et al., 2018). The principal treatment of pneumococcal infections is β-lactam antibiotics, which has been used to treat community-acquired pneumoniae since the 1940's (van der Poll and Opal, 2009). However, *S. pneumoniae* is a highly adaptive pathogen, in large due to its ability to undergo natural genetic transformation, which enables the rapid adaptation to antibiotic and vaccine pressure. (Straume et al., 2015). The mechanisms of antibiotic resistance in *S. pneumoniae* has been extensively studied for over 50 years, since the first penicillin-resistant isolates were identified already in the 1960's (Hansman and Bullen, 1967). Today, antibiotic resistant pneumococci are recognized as a major public health concern, and continued exploration of the molecular mechanisms behind resistance is crucial to combat the development and spread of multi-resistant superstrains (Cornick and Bentley, 2012).

Pneumococci belongs to the genus *Streptococcus* of the low GC Gram-positive bacteria in the phylum Firmicutes. The streptococci are phylogenetically divided into six main groups based on 16S rRNA analysis; the anginosus, bovis, mitis, mutans, salivarius and pyogenic groups (Figure 1.1), of which *S. pneumoniae* belongs to the mitis group (Kawamura et al., 1995).

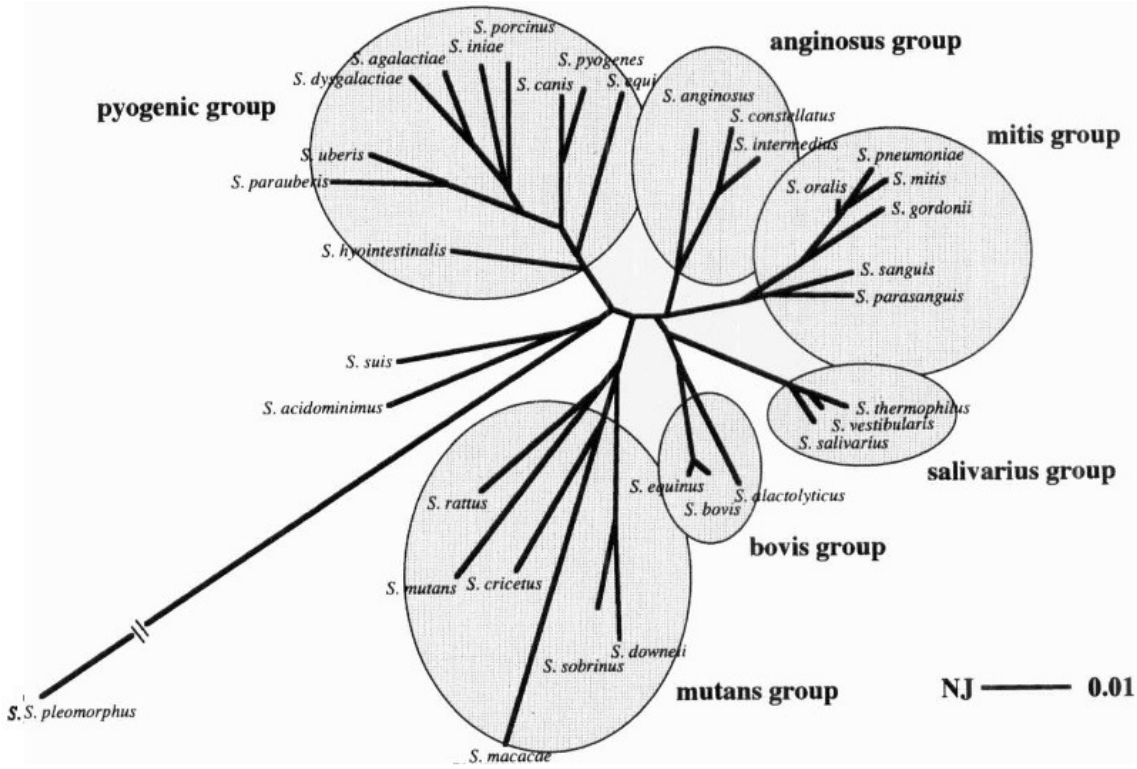

Figure 1.1 Phylogeny of the genus *Streptococcus.* Streptococci are divided into six main groups: the anginosus, bovis, mitis, mutans, salivarius and pyogenic groups. *S. pneumoniae* is found in the mitis group. Figure from (Kawamura et al., 1995).

Streptococci normally inhabit the mucus membrane of humans and other animals (Hardie and Whiley, 1997). The majority of the species in the mitis group are commensal colonizers of the upper respiratory tract in humans, but may act as opportunistic pathogens and cause disease mainly in young children, elderly and immunocompromised individuals (Mitchell, 2003). *S. pneumoniae* generally pursue one of two different colonization strategies; either as a persistent, non-invasive colonizer of the upper airways, most commonly the nasal cavity (nasopharynx), or as an invasive phenotype (van der Poll and Opal, 2009). This strategy enables this bacterium to establish and maintain a natural reservoir in the human host population. At all times, a sub-population are carriers of the pathogen, most frequently young children; approximately 10% of adults, and over 60% of infants are carriers, allowing for a continuous, low-level transmission. The non-invasive colonizer can become invasive upon changes in the host defences, such as viral infections or other diseases that compromise the host immune system, by an unknown mechanism (van der Poll and Opal, 2009).

In the year 2000, pneumococci caused an estimated 14.5 million cases of serious disease, and 826 000 deaths in children under 5 years of age alone, which accounted for approximately half

of the pneumococci-related deaths that year (O'Brien et al., 2009). According to recent estimates, the number of deaths caused by *S. pneumoniae* in children under 5 years of age have declined between the year 2000 and 2015. One recent study estimated a reduction by approximately 50%, to 294 000 pneumococcal-related deaths in young children in 2015 (Wahl et al., 2018). However, Wahl *et al.* (2018) argued that these numbers might be significantly underestimated. Another study found that pneumococcal pneumoniae alone accounted for an estimated 393 000 deaths in children under 5 years of age in 2015 (2017). This would still represent a considerable reduction, which in large can be attributed to the introduction of vaccines and targeted treatment with antibiotics (Troeger, 2017, Wahl et al., 2018).

S. pneumoniae produces a wide array of virulence factors, including a polysaccharide capsule, pneumolysin, autolysin, Ig1a protease, hydrogen peroxide, as well as numerous cell wall surface proteins involved in host interaction (Kilian et al., 2008, Mitchell, 2003). Of these, the polysaccharide capsule is considered the most important helping the bacterium to evade the host's immune system. Over 90 capsular serotypes have been identified so far, of which certain serotypes are more frequently associated with invasive disease than others (Bentley et al., 2006, Maestro and Sanz, 2016). The enormous capsular diversity among pneumococci have most likely evolved due to selection pressure from the immune system of the host, aided by horizontal gene transfer between different strains of pneumococci, and between pneumococci and other species (Bentley et al., 2006). The most potent serotypes have been included in the polyvalent conjugated vaccines developed against *S. pneumoniae*. However, while a reduced disease burden from pneumococcal infections followed the introduction of the vaccines, a rise in the prevalence of non-vaccine serotypes followed shortly thereafter (Weil-Olivier et al., 2012). This highlights the need for additional solutions to combat the global threat of pneumococcal disease, including the search for, and development of novel antibiotics. One of the most important aspect behind the rapid adaptations to vaccine and antimicrobial selection pressure in *S. pneumoniae*, is their ability for natural genetic transformation (Straume et al., 2015).

1.2 Natural competence for genetic transformation in *S. pneumoniae*

Horizontal gene transfer is the transmission of genetic information between different cells, and can even occur between cells of different species. It plays an important role in the adaptability of bacteria to changes in their environment. Three main modes of horizontal gene transfer are recognized today: transduction, conjugation and transformation. Transduction involves the transmission of genetic information through bacteriophages. Transduction is in large limited to

genetic transfer between related bacteria, as the cells involved must possess the specific receptors needed for interaction with the phage (Soucy et al., 2015). Conjugation involves gene transfer through cell-to-cell contact, in which a mobile genetic element such as a plasmid or transposon is transferred from a donor cell to an acceptor cell via a conjugation pilus (Soucy et al., 2015). Transformation involves the uptake of free DNA from the surrounding environment, which can then be incorporated into the genome of the recipient through homologous recombination (Johnsborg et al., 2007).

Among streptococci, natural transformation has been most comprehensively studied in *S. pneumoniae*, but evidence suggest that this ability is prevalent among all the species in the genus (Håvarstein, 2010). The bacteria can undergo natural transformation when they enter a physiological state termed competence. Competence is transiently induced under certain environmental conditions by a quorum-sensing mechanism. When cells enter the competent state, they activate expression of genes involved in the active uptake of free extracellular DNA and its integration into the host genome through homologous recombination, as well as genes involved in a predatory mechanism called fratricide (see section 1.2.2) (Johnsborg et al., 2007, Straume et al., 2015).

1.2.1 Regulation of the competent state

In *S. pneumoniae*, and other streptococci of the mitis and anginous phylogenetic groups, the competent state is regulated by the three-component ComCDE system (Figure 1.2) (Straume et al., 2015). The ComCDE system consists of the competence stimulating peptide (CSP), a CSP specific receptor, ComD, and the transcriptional regulator ComE. In non-competent pneumococci, ComCDE are constitutively expressed at a low level (Straume et al., 2015). As ComC is translocated across the membrane through the ABC transporter ComAB, the N-terminal leader sequence is cleaved off, and the matured CSP is released from the cell. Extracellular CSP binds to its cognate receptor, the transmembrane histidine kinase ComD. This results in the autophosphorylation of ComD, followed by the transfer of the phosphate group from ComD to the cytoplasmic protein ComE. Phosphorylated ComE binds to two direct repeats motifs found in the promoters of so-called early competence genes resulting in transcriptional activation. When the concentration of CSP reaches a critical level, increased transcription of the early competence genes (*comABCDE*) are activated, which generates a positive feedback loop resulting in the induction of the competent state. The factors allowing CSP to accumulate to a concentration required to trigger the autocatalytic loop is not completely

clear, but it is known that different stresses and antibiotics increasing the levels or stability of CSP result in competence induction. (Straume et al., 2015). In addition to the *comABCDE* genes, the early competence genes include a gene encoding ComX. ComX is an alternative σ-factor, and promotes expression of the late competence genes. The ~80 late competence genes encode proteins involved in the acquisition of free extracellular DNA, and its incorporation into the host genome through homologous recombination. The late genes also encode Drpa, which mediates the termination of the competent state by binding phosphorylated ComE, effectively preventing it from activating further transcription of the early genes (Straume et al., 2015). In addition, the late genes encode CbpD, a murein hydrolase involved in the fratricide mechanism (Claverys et al., 2007).

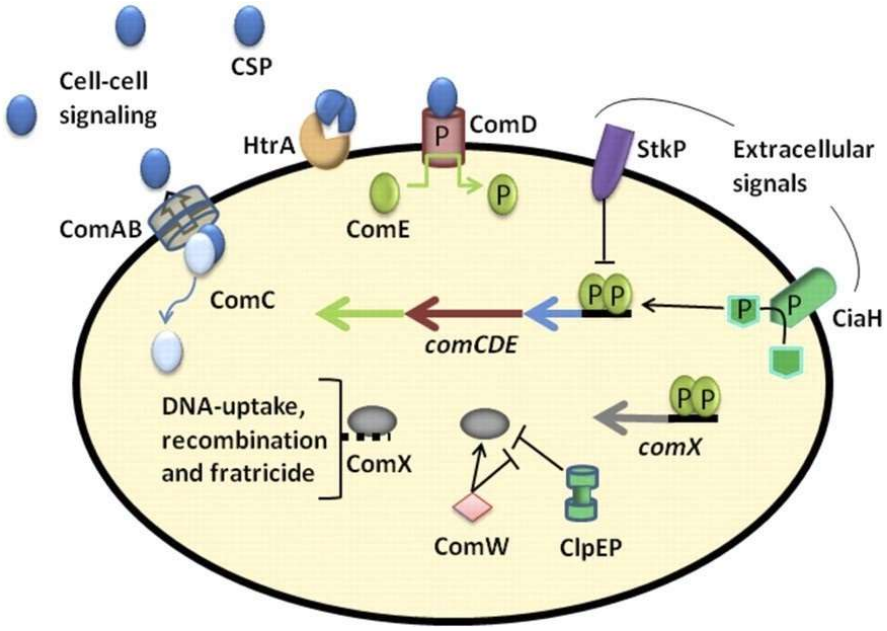

Figure 1.2 Competence regulation in *S. pneumoniae*. In *S. pneumoniae*, competence for natural genetic transformation is regulated by the ComCDE system. Expression of the genes involved in the active uptake of free, extracellular DNA, its integration into the host genome through homologous recombination, and the fratricide mechanism, is induced by a quorum sensing mechanism, when the extracellular concentration of the competence stimulating peptide (CSP) reaches a threshold level. CSP binds its receptor, the transmembrane histidine kinase ComD, which results in the activation of ComD, which regulates transcription of the abovementioned genes. See text for details. Figure from (Berg et al., 2012).

1.2.1 Competence-induced fratricide

Fratricide is a predatory mechanism first described to be executed by *S. pneumoniae* during competence (Guiral et al., 2005). It involves a murein hydrolase called CbpD (choline binding protein D) that is secreted by competent pneumococci. CbpD binds to choline decorated

teichoic acids in the cell wall of non-competent pneumococci or closely related species where it makes cuts in the peptidoglycan layer leading to cell lysis. This results in the release of nutrients and DNA that become available to the competent cells (Berg et al., 2012, Johnsborg et al., 2008). The competent pneumococci protect themselves from CbpD by expressing the early competence gene *comM* (Håvarstein et al., 2006). The fratricide mechanism is not unique to pneumococci, since the presence of competence induced genes encoding fratricins are found within the genomes of all streptococci known to be competent for natural transformation. This suggests that the fratricide mechanism, although not essential for DNA up-take and recombination, is an important aspect of natural transformation in streptococci (Johnsborg et al., 2008, Berg et al., 2012). It is believed to be a mechanism providing homologous DNA to the competent cells, since up-take of foreign DNA can be hazardous to the cells. (Eldholm et al., 2010). Competent pneumococci indiscriminately take up any free DNA from the surrounding environment, but a selective attack on closely related species increases the probability that the DNA taken up by the cells will be homologous (Berg et al., 2012). Bearing in mind that competent pneumococci have been shown to take up and recombine DNA stretches up to 100 kb long from lysed target cells (Cowley et al., 2018), it emphasizes the importance of this DNA being homologous to avoid killing the host. The ability to undergo natural transformation while selectively targeting closely related species through the fratricide mechanism, has been instrumental to the genomic plasticity and adaptability of *S. pneumoniae* (Straume et al., 2015). A good example is how *S. pneumoniae* acquire penicillin resistance. Specific enzymes, called penicillin binding proteins (PBPs), taking part in constructing the bacterial cell wall are usually inhibited by penicillin (see section 1.6). However, the pneumococcus becomes resistant to penicillin by expressing a set of mutated enzymes that are not inhibited by penicillin. Genome sequencing has revealed that *S. pneumoniae* can acquire these penicillin resistance genes from close relatives such as *Streptococcus oralis* and *Streptococcus mitis* through horizontal gene transfer and homologous recombination (Jensen et al., 2015). Natural competence is a major driving force in spreading these resistance genes among pneumococcal strains when put under a penicillin selection pressure in the clinics.

1.3 Pneumococcal cell wall synthesis and cell division

1.3.1 The pneumococcal cell wall

In almost all bacteria, the plasma membrane is enclosed by a cell wall, whose function is to protect the cell from the internal turgor pressure, maintain cellular shape, and function as an anchoring point for proteins, teichoic acids and other cell wall components (Vollmer et al.,

2008). The cell wall associated molecules are involved in various important physiological processes, such as interactions with the outside environment, uptake of nutrients and other substrates, cell division and transformation (Vollmer et al., 2008, Navarre and Schneewind, 1999).

The cell wall is composed of peptidoglycan, also known as murein. It consists of long glycan chains crosslinked via a stem peptide whose composition vary among bacterial species. The stem peptide in pneumococcal peptidoglycan consists of the amino acids L-Ala-D-iGln-L-Lys-D-Ala-D-Ala (Bui et al., 2012). The glycan chain consists of the sugar derivatives *N*-acetylglucosamine (GlcNAc) and *N*-acetylmuramic acid (MurNAc). During peptidoglycan synthesis, alternating GlcNAc and MurNAc residues are connected, forming the glycan chains. The chains are then crosslinked via the stem peptides connected to the carboxyl group on MurNAc (Figure 1.3) (Vollmer et al., 2008).

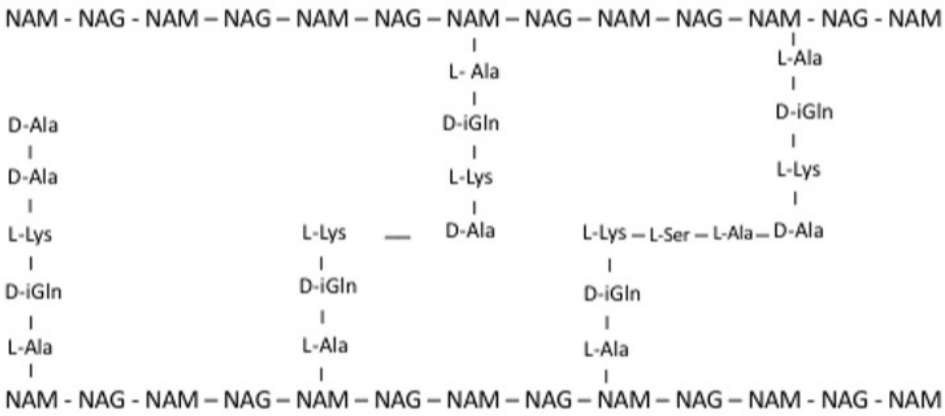

Figure 1.3 Peptidoglycan structure in *S. pneumoniae*. Peptidoglycan consists of long glycan chains, consisting of alternating *N*-acetylglucosamine (GlcNAc) and *N*-acetylmuramic acid (MurNAc) molecules. The glycan chains are interconnected via short stem peptides attached to MurNAc. In *S. pneumoniae*, this stem peptide consists of the five amino acids L-Ala-D-iGln-L-Lys-D-Ala-D-Ala. Figure modified from Zapun (2008a).

Peptidoglycan synthesis involves steps performed by proteins both in the cytoplasm, in the plasma membrane and in the extracellular space (Figure 1.4). The first steps take place in the cytoplasm, and involves the synthesis of peptidoglycan precursors, including the formation of GlcNAc and MurNAc connected to the carrier molecule uridine diphosphate (UDP), and the addition of the stem peptide to MurNAc (Barreteau et al., 2008). The stem peptide is constructed through the subsequent addition of specific amino acids to MurNAc by the MurC, MurD, MurE and MurF enzymes. The MurNAc-pentapeptide complex is then anchored to a membrane carrier lipid (C_{55}) by MraY, which forms Lipid I. The addition of GlcNAc to Lipid I by MurG forms Lipid II, which is translocated across the membrane by a membrane-bound flippase

(Barreteau et al., 2008). Recent evidence has identified MurJ as the lipid II flippase (Sham et al., 2014, Kuk et al., 2019). However, some experimental evidence suggests that the transglycosylases FtsW and RodA might possess flippase activity as well, but this remains uncertain. Further studies are needed to clarify the roles of FtsW and RodA in Lipid II translocation (Teo and Roper, 2015). Finally, on the extracellular side of the membrane, the glycan chains are formed by polymerization of Lipid II via transglycosylation reactions, with concurrent release from the membrane carrier lipid. The glycan chains are then crosslinked via transpeptidation reactions. The PBSs can perform both reactions or transpeptidation only, depending on the type of PBP, while another group of enzymes called SEDS (shape, elongation, division and sporulation) transglycosylases, including FtsW and RodA, work in conjunction with some PBPs to catalyze transglycosylation reactions (Teo and Roper, 2015). Details about the function of PBPs will be further described in section 1.4.

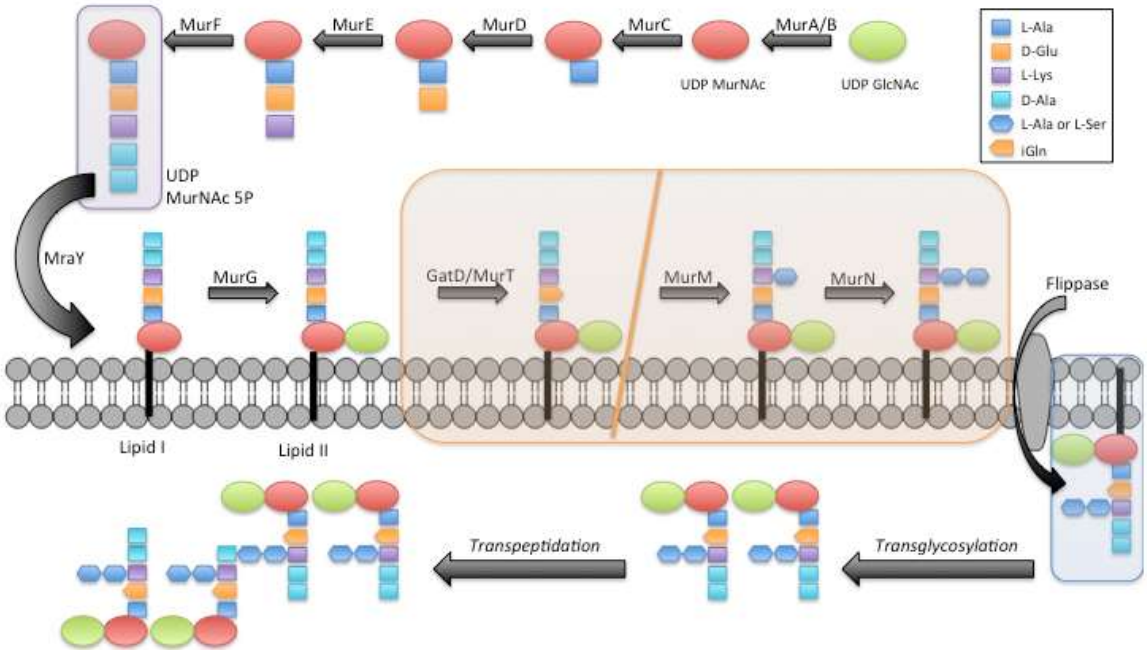

Figure 1.4 Peptidoglycan synthesis in *S. pneumoniae.* Overview over the cytoplasmic, membrane-bound and extracellular steps in peptidoglycan synthesis in *S. pneumoniae*. See text for details. Figure from Rowland (2016).(Severin and Tomasz, 1996, Vollmer et al., 2008)

(Bui et al., 2012)In *S. pneumoniae*, the glycan strands are either crosslinked directly, or branched via an L-Ser-L-Ala or L-Ala-L-Ala dipeptide. The level of branched peptides varies between pneumococcal strains, where a high level of branching is associated with a higher level of resistance against β-lactam antibiotics (Filipe et al., 2001, Fiser et al., 2003). The addition of the L-Ser/Ala-L-Ala dipeptide to the ε-amino group on L-Lys is performed at the Lipid II-level, by the MurM and MurN ligases (Filipe et al., 2001, Lloyd et al., 2008).(Vollmer, 2008) In addition. the position 2 amino acid in the pentapeptide is amidated by GatD/MurT, yielding D-isoglutamine (iGlu) from D-glutamate (Glu) (Zapun et al., 2013). (Filipe et al., 2001, Lloyd et al., 2008)In Figure 1.4, these Lipid II modifications are highlighted in orange.

(Navarre and Schneewind, 1999)Furthermore, the pneumococcal cell wall contains wall teichoic acids (WTA) and lipoteichoic acids (LTA), in which the WTAs are covalently attached to the MurNAC in peptidoglycan, while the LTAs extends through the peptidoglycan layers and attaches to the plasma membrane via a lipid anchor (Denapaite et al., 2012). The pneumococcal WTAs and LTAs are unusual in two ways: first, unlike the teichoic acids in most other Gram-positive bacteria, the chemical structure of the pneumococcal WTAs and LTAs are identical (Navarre and Schneewind, 1999). Secondly, the teichoic acids contain phosphocholine, which are uncommon in bacteria (Maestro and Sanz, 2016, Denapaite et al., 2012). The phosphocholine residues functions as non-covalent attachment sites for choline-binding proteins (CBP), such as the murein hydrolases involved in cell division and fratricide (Maestro and Sanz, 2016, Eldholm et al., 2010).

1.3.3 Cell division in *S. pneumoniae*

Cell division is a highly regulated process. The separation of the daughter cells by murein hydrolases must be coordinated with the synthesis of new peptidoglycan to avoid cell lysis, as well as the other cellular processes such as DNA replication and chromosome segregation (Zapun et al., 2008b). Coccoid bacteria are roughly divided into two morphological groups; truly spherical cocci, and cocci with an ellipsoid shape, like *S. pneumoniae*. The latter are called ovococci, and their ellipsoid shape is the result of a combination of peripheral and septal peptidoglycan synthesis, which is performed by the elongasome and divisome protein complexes, respectively (Zapun et al., 2008b, Philippe et al., 2014).

The working model of pneumococcal cell division involves the initial recruitment of tubulin-like FtsZ protein to the mid-cell, where it polymerases to form the ring-like structure known as the Z-ring, which is anchored to the membrane through FtsA (Massidda et al., 2013). Following

the formation of the Z-ring, proteins involved in the cell division machineries are recruited to the mid-cell division site from which they orchestrate both the peripheral and septal peptidoglycan synthesis. Following the initiation of peripheral cell wall synthesis, the divisome complex synthesize the septal cross wall (Pinho et al., 2013). Finally, the cross-wall is cleaved down the middle by murein hydrolases, yielding two daughter cells (Zapun et al., 2008b). The penicillin-binding proteins are vital players in these multi-protein complex machineries, finalizing the synthesis of the peptidoglycan chains that are incorporated into the growing cell wall. The 5 class A and B PBPs are involved in the polymerization (transglycosylation) and crosslinking (transpeptidation) of the peptidoglycan chains (section 1.4.1), while the class C PBP regulated the level of crosslinking by cleaving the terminal D-Ala of the stem peptide (section 1.4.2). While the class A PBPs possess both transglycosylase and transpeptidase activity, the class B PBPs only function as transpeptidases. However, the two class B PBPs, PBP2b and PBP2x, have been found to work alongside the transglycosylases RodA and FtsW, respectively (Meeske et al., 2016). PBP2x and FtsW are involved in the formation of the septal cross wall, while PBP2b and RodA are involved in the peripheral cell wall synthesis (Berg et al., 2013, Meeske et al., 2016). There are still many unanswered questions regarding the precise workings and regulations of the protein complexes involved in cell division. The further understanding of these proteins and their interactions could provide insight enabling the discovery of novel antibacterial drugs or enhance current β-lactam antibiotics targeting cell wall synthesis.

1.4 The penicillin-binding proteins

As described in section 1.3.1, penicillin-binding proteins (PBPs) are membrane-bound enzymes involved in the late stages of peptidoglycan synthesis; the polymerization and crosslinking of the glycan chains. PBPs belong to the acyl transferase protein family ASPRE (active-site serine penicillin-recognizing enzymes) that are characterized by the presence of a penicillin-binding domain (in which β-lactam antibiotics bind and inhibit) harbouring the three motifs: SXXK, (S/Y)XN and ((K/H)(S/T))G (Zapun et al., 2008a). The penicillin-binding region functions as a carboxypeptidase or a transpeptidase, where the SXXK motif contains the active site serine that forms a covalent acyl-serine intermediate upon binding its substrate, the terminal D-Ala-D-Ala of the peptide stem, before finally cleaving the amide bond between the two D-Ala residues (Zapun et al., 2008a). It is this serine residue of the active site, which is targeted by β-lactam antibiotics domain rendering the enzyme inactive. The mode of action of β-lactam antibiotics are described in more details in section 1.6. The number of PBP's vary between

bacterial species. *S. pneumoniae* have six PBPs, divided into three main classes; class A and B of the high molecular mass (HMM) PBPs and class C of the low molecular mass (LMM) PBPs (Figure 1.5) (Sauvage et al., 2008, Hakenbeck et al., 2012).

1.4.1 High molecular mass PBPs in *S. pneumoniae*

The HMM PBPs are multi-modular proteins consisting of a short cytoplasmic tail, a transmembrane region and larger, extracytoplasmic domains. Class A PBPs are bifunctional performing both transglycosylase and transpeptidase reactions, while class B possess transpeptidase activity only (Hakenbeck et al., 2012).

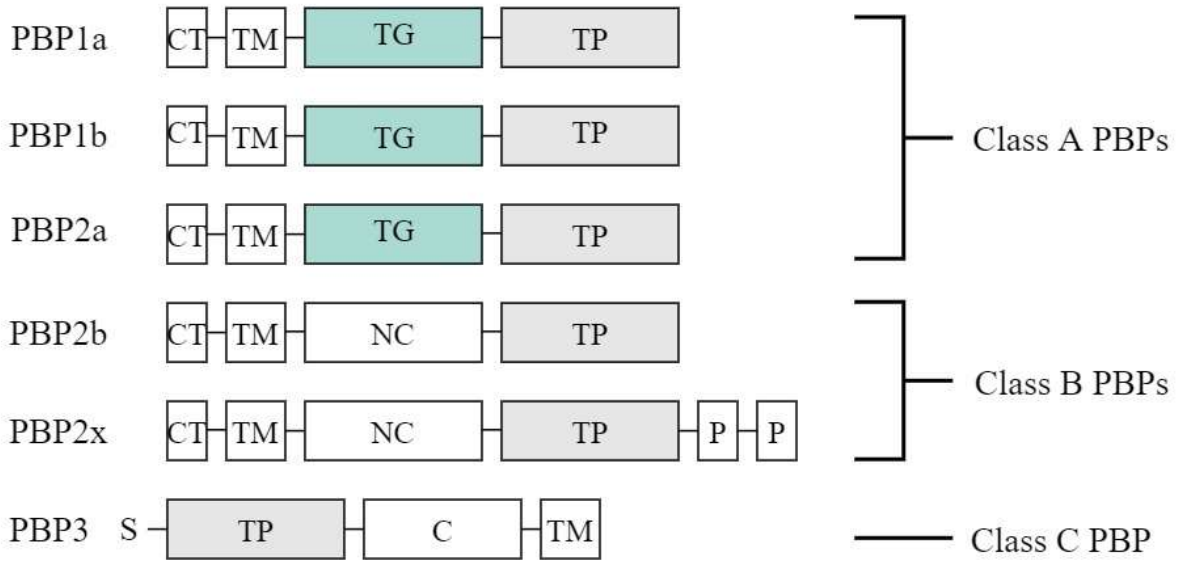

Figure 1.5 Overview of the main domains of the pneumococcal PBPs (N-terminal to C-terminal). *S. pneumoniae* encode six PBPs divided into the HMM class A and B and the LMM class C. The HMM PBPs consist of an N-terminal cytoplasmic tail (CT), a transmembrane (TM) region and two extracytoplasmic domains. The three class A PBPs, PBP1a, 1b and 2a have a transglycosylase (TG) and a transpeptidase (TP) domain, while the class B PBPs PBP2b and 2x have a noncatalytic (NC) domain and a transpeptidase domain. In addition, PBP2x has two small C-terminal PASTA domains. The lone LMM class C PBP PBP3 consists of a C-terminal amphipathic membrane anchor and two extracytoplasmic domains; a C-terminal domain and an N-terminal transpeptidase domain with D,D-carboxypeptidase activity.

The bifunctional class A PBPs, which include PBP1a, PBP1b and PBP2a, have two large extracytoplasmic domains; a transglycosylase domain (catalyses the polymerization of the glycan chains) and a transpeptidase domain (catalyses the crosslinking of the stem peptides of adjacent glycan strands) (Sauvage et al., 2008). They are individually non-essential, but a double Δ*pbp1a*Δ*pbp2a* mutation is lethal (Hakenbeck et al., 2012).

The two monofunctional class B PBPs named PBP2b and PBP2x possess two large extracytoplasmic domains; the C-terminal transpeptidase domain and an N-terminal non-catalytic domain of unknown function. It is postulated that the non-catalytic domain is involved in protein-protein interactions and/or in the spatial positioning of the catalytic transpeptidase domain (Sauvage et al., 2008). A PBP2x crystal structure showed that the non-catalytic domain contains a small hole-like opening, which has been hypothesized to be involved in important interaction mechanisms, either with other proteins in the cell division machinery, or with the peptidoglycan (Zapun et al., 2008a). PBP2x possess two small additional C-terminal PASTA (PBP and Serine/Threonine kinase associated) domains, which are assumed to bind non-crosslinked peptidoglycan (Sauvage et al., 2008). PBP2b and PBP2x are both essential, for the peripheral and septal peptidoglycan synthesis, respectively (Berg et al., 2013). The transmembrane regions of the PBPs function as membrane anchors, but domain swapping and mutation analysis experiments strongly indicate that the transmembrane and cytoplasmic regions are of importance for localization and/or protein-protein interactions as well, as demonstrated for PBP2b and PBP2x (Berg et al., 2014).

1.4.1.1 Transglycosylation and transpeptidation by the HMM PBPs

During peptidoglycan synthesis, the glycan chains are elongated by the polymerization of Lipid II (section 1.3.1). This is accomplished via transglycosylation by the class A PBPs, and the SEDS polymerases FtsW and RodA (Taguchi et al., 2019), where the Lipid II disaccharide-pentapeptide complex is added to the reducing end of the glycan chain, by the formation of a β-glycosidic bond between the GlcNAc of Lipid II and the MurNAc of the elongating glycan chain (Figure 1.4). Concurrent with this reaction, the lipid anchor attached to the MurNAc is cleaved off. (Sauvage and Terrak, 2016, Perlstein et al., 2007). As mentioned above, ranspeptidation is performed by both class A and class B PBPs, and involves the cross-linking of the peptide stems of adjacent glycan chains. (Zapun et al., 2008a)The active-site serine in the transpeptidase domain performs a nucleophilic attack on the amide bond between the stem peptide terminal amino acids, D-Ala-D-Ala. This forms a covalent acyl-serine intermediate between the penultimate D-Ala and the enzyme. Following the cleavage of the amide bond and the release of the terminal D-Ala, the amino group of the position 3 amino acid (L-Lys in *S. pneumoniae*) of an adjacent glycan chain stem peptide attacks the acyl-serine intermediate. The enzyme is released, while the two stem peptides are connected via a peptide bond, forming the finalized cross-linked peptidoglycan (Figure 1.4) (Sauvage et al., 2008, Zapun et al., 2008a). As described in section 1.3.2, some modifications occur at the Lipid II stage. These

modifications can affect the efficiency of the transpeptidase reaction, most notably the amidation of the second amino acid of the stem peptide, from L-Glu to L-iGln, which has been shown to be crucial for efficient cross-linking in *S. pneumoniae* (Zapun et al., 2013). Transglycosylation and transpeptidation are coupled reactions during peptidoglycan synthesis to ensure an efficient and controlled cell wall assembly (Sauvage and Terrak, 2016).

1.4.2 Low molecular mass PBPs

The pneumococcal LMM class C only includes a single PBP; PBP3. PBP3 is a two-domain enzyme, consisting of an N-terminal carboxypeptidase domain and a C-terminal domain of unknown function. It is connected to the cytoplasmic membrane via a C-terminal amphipathic helix (Morlot et al., 2005). PBP3 has D,D-carboxypeptidase activity. As with the transpeptidases, the active site serine of the carboxypeptidase domain forms a covalent acyl-serine intermediate with the penultimate D-Ala of the stem peptide. This is followed by hydrolyzation of the acyl-serine complex, which results in the cleaving of the D-Ala-D-Ala peptide bond and the formation of a tetrapeptide. The resulting tetrapeptide cannot function as a donor in the transpeptidation reaction, and the activity of PBP3 thus regulates the degree of crosslinking in the cell wall (Morlot et al., 2005).

PBP3 is spatially positioned around the entire cell surface, with one notable exception: the future division site, the complete opposite of the localization of the HMM PBPs (Morlot et al., 2004). This leaves an area of untrimmed pentapeptides that can function as both donors and acceptors during the transpeptidation step, which is critical for complete peptidoglycan synthesis, exclusively at the division site. The lack of donor peptides on the remainder of the cell surface is contributing to the inertness of these areas. It is postulated that the presence of untrimmed pentapeptides is involved in the localization of the class A and B PBPs to the division site. When the cell division machinery has initiated peptidoglycan synthesis at the division site, PBP3 repositions itself to this zone and commences trimming of the stem peptides, regulating the degree of crosslinking (Morlot et al., 2005, Morlot et al., 2004). PBP3 is not essential in *S. pneumoniae*, but deletion mutants exhibit a dramatic growth reduction and display irregular morphological phenotype with multiple septa with abnormal positioning (Schuster et al., 1990). Together, this strongly indicate a regulatory role for PBP3 in pneumococcal cell division (Morlot et al., 2005).

1.6 Penicillin resistance in *S. pneumoniae*

The year 2019 marks 90 years since Alexander Fleming first published the discovery of penicillin (Fleming, 1929). Since then, the family of antibiotics has grown substantially, including both naturally isolated and synthetically engineered variants, targeting different features of the cell cycle. For example, aminoglycosides, tetracyclines and macrolides inhibit protein synthesis, quinolones target DNA replication, lipopeptides and polypeptides target the cell membrane, sulphonamides target the biosynthesis of folate, while glycopeptides and β-lactams (penicillins) target cell wall synthesis (Davies and Davies, 2010). Over 20 different classes of antibiotics were identified during the "golden age" of antibiotic discovery between the 1940s and 1970s. However, no new classes have been found since the 1980s (Durand et al., 2019).

Many bacteria possess an intrinsic resistance to certain antibiotics, evolved over millions of years of co-habiting with antibiotic-producing microorganisms. Additionally, microorganisms that produce antibiotics or other toxins frequently produce complementary resistance factors (Durand et al., 2019),These resistance genes can be spread between bacterial species through horizontal gene transfer. Thus, bacterial communities may harbour a reservoir of antibiotic resistance genes that can potentially be acquired by pathogenic bacteria, driven by the selection pressure of antibiotic exposure during therapeutic treatment (Davies and Davies, 2010).

The first penicillin antagonist, a β-lactamase, was discovered already in 1940, years before penicillin became available as a therapeutic drug (Davies and Davies, 2010). The introduction of the various antibiotics as commercially available drugs was soon followed by development and spread of resistance. Today, antibiotic resistance is widely recognized as a major public health concern. The CDC (US centers for disease control and prevention) estimates that approximately 23 000 antimicrobial resistant (AMR) related deaths occur every year in the US (Durand et al., 2019), while the European Union (EU) asserts that 25 000 - 33 000 deaths occur annually in EU nations (EC, 2017). Globally, the annual death toll due to AMR infections has been estimated to be as high as 700 000. It is estimated that the annual number of deaths related to AMR may reach 10 million by 2050, if not sufficiently is done to combat antibiotic resistance (PlosMedicineEditors, 2016).

β-lactam antibiotics is the primary therapeutic treatment of pneumococcal infections (van der Poll and Opal, 2009). The following subchapters will therefore focus on β-lactams, including their mechanism of action and resistance in *S. pneumoniae*.

1.6.1 Mechanism of β-lactam antibiotics

β-lactams are so named due to their primary structure containing a β-lactam ring (highlighted in red in Figure 1.6B). The β-lactam ring is in most cases fused to a five-membered or six-membered heterocyclic ring (Dalhoff et al., 2006). Since the first discovery of penicillin, several subclasses of β-lactams have been discovered, synthetically engineered or modified by adding various side-chains to the core β-lactam structure. The subclasses are characterized by the presence and nature of the second ring (Bycroft and Shute, 1985, Dalhoff et al., 2006).

β-lactam antibiotics function by inhibiting the synthesis of the cell wall, by forming a covalent bond with the active site in the transpeptidase domain of the PBPs (Bycroft and Shute, 1985). Structurally and biochemically, the β-lactams resemble the D-Ala-D-Ala moiety of the stem peptides in peptidoglycan, the substrate of the PBPs (Zapun et al., 2008a, Bycroft and Shute, 1985). A comparison of the structure of the dipeptide (*N*-acyl-D-alanyl-D-alanine) in an elongated form, and the backbone of the β-lactams penicillin and cephalosporin is illustrated in Figure 1.6. The figure also designates the three electrostatic negative regions shared by the dipeptide and the β-lactams (marked by arcs).

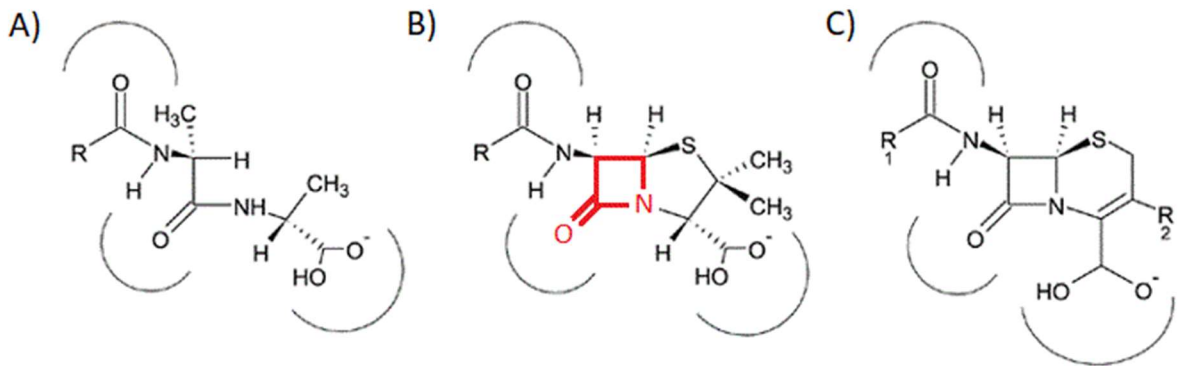

Figure 1.6 Comparison of the structures of the A) peptidoglycan stem peptide D-Ala-D-Ala moiety and the backbone structure of B) penicillins and C) cephalosporins. Arcs highlight the electrostatic negative areas of the molecules. The β-lactam ring marked in red in B). Figure modified from (Zapun et al., 2008a).

The reaction between the β-lactam and the PBPs is equal to the first step of the transpeptidase and D,D-carboxypeptidase reactions (section 1.4.1 and 1.4.2); the active site serine of the PBP performs a nucleophilic attack on the carbonyl of the β-lactam ring, forming a covalent bond between the now open β-lactam ring and the active site serine (Zapun et al., 2008a). During transpeptidation and carboxypeptidation, this bond is subsequently broken. In transpeptidation, the bond is replaced by a peptide bond to the stem peptide of an adjacent glycan chain, while it is hydrolysed in carboxypeptidation. The bond in the β-lactam-PBP complex can also be

hydrolysed, but this reaction is extremely slow, effectively leaving the PBP trapped in an inactive complex with the β-lactam. This results in severe growth inhibition and cell lysis (Zapun et al., 2008a, Sauvage and Terrak, 2016).

1.6.2 β-lactam resistance in *S. pneumoniae*

Resistance against β-lactams are generally divided into four main modes: production of β-lactamases, acquisition of altered PBPs with a lower affinity for the antibiotic, antibiotic efflux pumps and decreased permeability of the outer membrane. The last two are limited to Gram-negative bacteria (Durand et al., 2019). β-lactamases are enzymes that bind and hydrolyse the β-lactam ring, leaving the antibiotic compound inactive (Bycroft and Shute, 1985). These enzymes are often encoded on plasmids, and can thus easily be spread amongst bacterial populations through conjugation. They are of major importance for the rapid spread of antibiotic resistance in both Gram-positive and Gram-negative bacteria, but have so far not been observed in pneumococcus (Zapun et al., 2008a). Resistance in *S. pneumoniae* is in large caused by the presence of low-affinity PBPs (Hakenbeck et al., 2012).

The PBPs of β-lactam-sensitive pneumococci are relatively conserved. In contrast, low-affinity PBPs are characterized by high sequence diversity, often containing large, diverging sequence blocks (Hakenbeck et al., 2012). The presence of low-affinity PBPs results from both point mutations and the acquisition of low-affinity genes or gene fragments through horizontal gene transfer. As described in section 1.2, pneumococci are competent for natural genetic transformation. This has been instrumental for the development of resistance in *S. pneumoniae*. The current theory is that the low-affinity PBP mutations initially developed in commensal streptococci, which then spread to pneumococci through natural transformation events. Supporting this theory is the presence of mosaic blocks in pneumococcal PBP2x and PBP2b that highly resemble PBP gene sequences from the close, commensal relatives *S. mitis* and *S. oralis* (Zapun et al., 2008a, Hakenbeck et al., 2012).

Mosaic variants of PBP1a, PBP2b and PBP2x have been found to be the main determinants of β-lactam resistance (Zapun et al., 2008a). However, the identification of the specific mutations that contribute to resistance is difficult. The combinations of mutations are complex, and often involve changes in multiple PBPs. The most relevant point mutations are often masked by the flanking regions included during transformation of larger sequence blocks. The surrounding mutations, including substitutions upstream or downstream of the *pbp* gene, may not be relevant for resistance at all (Zapun et al., 2008a). Additionally, because the mutations that confer

resistance may also influence the enzymatic function of the PBP, suppressor mutations can occur (Hakenbeck et al., 2012). However, experimental data in combination with sequence analysis of resistant clinical isolates have identified some of the most important mutations and their biochemical effects. The most significant mutations are those affecting the conformation and biochemistry of the active site. Importantly – a point mutation that results in reduced affinity for one β-lactam does not necessarily cause resistance against all β-lactams (Hakenbeck et al., 2012). For example, the T_{550}A/G substitution in PBP2x have been found to cause a high level of resistance against cefotaxime, most likely the result of the loss of a hydrogen bond between T_{550} and the cefotaxime side chain. Simultaneously, the substitution results in a penicillin hypersensitivity (Hakenbeck et al., 2012). Additionally, not all β-lactams react with all PBPs. Most β-lactams have a broad affinity for the different PBPs, while others display a specific affinity for certain PBPs. For example, cefotaxime does not inhibit PBP2b (Hakenbeck et al., 2012).

Resistance often come with a biological cost, such as reduced fitness (Andersson and Levin, 1999). The β-lactam resistance mechanism in *S. pneumoniae* presents an interesting paradox: how do mutations in the PBPs result in reduced affinity for β-lactams, while maintaining their transpeptidase function? The following sections will deal with mutations in PBPs of *S. pneumoniae* that are found to be important for penicillin resistance, and how they affect the structure and function of the PBP.

PBP2x: In the β-lactam sensitive laboratory strain *S. pneumoniae* R6, the three motifs that constitute the transpeptidase active site in PBP2x are S_{337}TMK, S_{395}SN and K_{547}SG (Zerfass et al., 2009). Mutations within and adjacent to these motifs are especially associated with resistance. There have been identified many important resistance-determining substitutions within pbp2x, both as point mutations and in combination with other substitutions. They appear to confer resistance through two main mechanisms: destabilization of the active site, and a narrowing of the active site, which would require that the active site must be opened before acetylation can occur, thus reducing acetylation efficiency (Zapun et al., 2008a, Hakenbeck et al., 2012). For example, the T338A/G/P/S and M339F substitutions within the catalytic STMK motif has been found to be of great importance, postulated to result in active site destabilization (Zerfass et al., 2009, Chesnel et al., 2003). The crystal structure of a strain containing both mutations showed a distortion of the active site serine (S337), in which the hydroxyl group involved in the nucleophilic attack mechanism had been reoriented away from the active site

centre (Zapun et al., 2008a, Hakenbeck et al., 2012). Additionally, mutations affecting the flexibility of the groove surrounding the active site, including the I317T and R384G substitutions, have been hypothesized to leave the active site more accessible and open to accommodate other substrates, such as peptidoglycan monomers with a branched stem peptide (Zapun et al., 2008a, Hakenbeck et al., 2012). As previously stated, a higher level of branching is associated with a higher level of resistance, although the exact mechanism is not understood. In contrast to these, the Q552E substitution have been found to introduce a narrowing of the active site, caused by a displacement of the β-strand containing the KSG motif. Additionally, this substitution introduces a more negative charge to the site, which affects the binding of the negatively charged β-lactams.

PBP2b: In PBP2b there exists a dense network of hydrogen bonds between residues within the three catalytic motifs (S_{386}VVK, S_{443}SN and K_{615}TG in *S. pneumoniae* R6); K_{615}, S_{443}, N_{445}, S_{386} and K_{389} (Contreras-Martel et al., 2009). The crystal structure of PBP2b from the sensitive R6 strain revealed a stable, open active site conformation, while the crystal structure of a low-affinity PBP2b indicated an active site region displaying a high level of flexibility, possibly leading to reduced accessibility of the catalytic serine. This was in part postulated to be caused by two substitutions into glycine (A_{619}G and D_{625}G) in this region, which are small amino acids allowing for more flexibility (Contreras-Martel et al., 2009). The most significant mutations in PBP2b include the T_{446}A/S and E_{476}G substitutions, close to the S_{443}SN motif. The side chain of T_{446} contributes in four important stabilizing polar and hydrophobic interactions with residues surrounding the active site, which are lost in the T_{446}A mutants, resulting in a higher level of flexibility around the active site (Contreras-Martel et al., 2009).

PBP1a: While a certain level of β-lactam resistance can be obtained with low-affinity PBP2b and PBP2x, alterations in PBP1a is critical to achieve a high level of resistance (Smith and Klugman, 1998). However, the mechanisms introduced by altered PBP1a only appears to confer resistance in combination with mosaic PBP2b and/or PBP2x (Hakenbeck et al., 2012). In *S. pneumoniae* R6, the catalytic motifs of the transpeptidase domain include S_{370}TMK, S_{428}RN and K_{557}TG. Some of the major determinants of β-lactam resistance within the PBP1a gene includes the T_{371}A/S substitutions, adjacent to the active site serine S_{370}. This is analogous to the T_{338}A substitution in PBP2x described above (Zapun et al., 2008a). The T_{371}A substitution results in a reorientation of the active site serine, caused by the loss if a hydrogen bond (Job et al., 2008). Another important mutation includes a four-residue substitution, T_{574}SQF → NTGY,

within a loop between two β-strands that constitute one side of the catalytic cleft opening, resulting in a change in polarity and reduced accessibility of the active site (Job et al., 2008). A comparison between the cavities of the active sites of *S. pneumoniae* R6 and the highly resistant pneumococcal isolate 5204, which harbour several mutations including both the $T_{371}A$ and $T_{574}SQF$ → NTGY substitutions, is presented in Figure 1.7, highlighting the reduced accessibility of the active site serine.

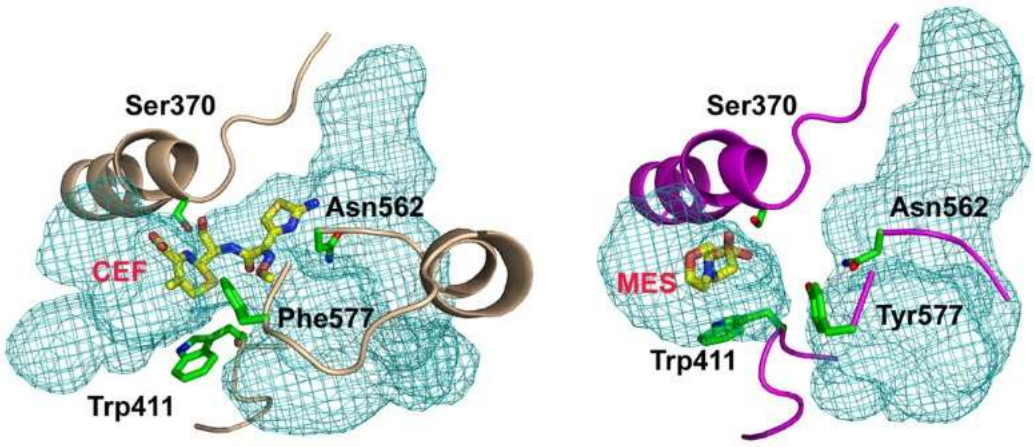

Figure 1.7 The comparison between the active site cavities of PBP1a from *S. pneumoniae* R6 (left) and the highly resistant *S. pneumoniae* 5204 (right). The figure includes a cefotaxime molecule present in the crystal structure of R6, and a MES molecule in 5204. The residues involved in active site narrowing are shown as sticks. Figure modified from (Job et al., 2008).

Alterations in PBP2a have in a few cases been found to contribute to resistance. Notably, a $T_{411}A$ substitution adjacent to the active site serine (S410) (analogous to the PBP2x $T_{338}A$ and PBP1a $T_{471}A$ substitutions) have been found in some resistant clinical isolates (Zapun et al., 2008a, Hakenbeck et al., 2012). So far, alterations in PBP1b and PBP3 have not been expressively associated with increased β-lactam resistance in *S. pneumoniae* (Hakenbeck et al., 2012). While low-affinity PBPs are the major factors behind β-lactam resistance in *S. pneumoniae*, other genes have also been recognized as contributing to resistance. Of these, mosaic varieties of the *murM* gene is one of the most important.

1.6.3 Characterization of MurM

In addition to low-affinity PBPs, alterations in MurM, which is responsible for adding the first L-Ser or L-Lys to the interpeptide bridge in branched muropeptides, is often required for high-level resistance against β-lactam antibiotics (Smith and Klugman, 2001). Studies have shown that many resistant pneumococcal isolates possess a cell wall enriched in branched

muropeptides (Fiser et al., 2003). In fact, the deletion or inactivation of the *murM* gene has been found to result in an almost complete loss of resistance in many clinical isolates of *S. pneumoniae*, even when the presence of low-affinity PBPs remains unchanged (Filipe and Tomasz, 2000). Additionally, the loss of murMN have been shown to increase the sensitivity of the cells against cell wall-inhibitors such as nisin, vancomycin and Fosfomycin (Filipe et al., 2002). The mechanism behind this phenotype is not yet understood, but a similar reduction in β-lactam resistance have also been observed upon the inactivation of branching enzymes in *Staphylococcus aureus* and *Enterococcus faecalis* (Fiser et al., 2003). As with the low-affinity PBPs, the sequences of *murM* in resistant isolates reveal highly mosaic structures, resulting from recombination between closely related species (Filipe et al., 2000). It has been found that specific combinations of mosaic PBPs and MurM variants tend to be preserved in natural populations, suggesting that they have a common origin (del Campo et al., 2006). Additionally, experiments involving the transfer of *murMN* from a resistant pneumococcus to two *S. pneumoniae* R6 derivates which had acquired different versions of mosaic PBPs, only conferred increased resistance in one of them, indicating that the increased resistance conferred by MurM is only effective in combination with the right PBP variants (du Plessis et al., 2002). Kinetic analysis of MurM variants of both penicillin-sensitive and -resistant *S. pneumoniae* isolates revealed that the mosaic MurM variant in the resistant isolate had a much stronger enzymatic activity compared to the MurM of the sensitive strain. This might help explain the increased level of cell wall branching observed in resistant pneumococcal isolates harbouring mosaic *murM* genes (Lloyd et al., 2008).

MurM and MurN are aminoacyl-tRNA ligases, utilizing alanyl-tRNA^{Ala} and seryl-tRNA^{Ser} as substrates, along with Lipid II, for the construction of the peptidoglycan interpeptide branch (Lloyd et al., 2008, De Pascale et al., 2008). However, sometimes these tRNAs are charged with the wrong amino acids. For example, the alanyl-tRNA synthetase (AlaRS) occasionally misactivates serine or glycine, which could disturb correct translation if not corrected (Shepherd and Ibba, 2013). These misactivations are either self-corrected by the synthase in question, or by other proteins such as the highly conserved seryl-tRNA^{Ala}-editing AlaXPs proteins. However, AlaXPs are lacking in *S. pneumoniae*. Interestingly, it was found that MurM can utilize mischarged seryl-tRNA^{Ala} as substrates during peptidoglycan synthesis, and even displayed a high preference for them (Shepherd and Ibba, 2013). It was also found that MurM exhibited a *trans*-editing function in the absence of Lipid II, suggesting that MurM, in addition

to providing the structural integrity of the branched cell wall, is an important factor for translation quality control in *S. pneumoniae* (Shepherd and Ibba, 2013).

At the eve of writing this thesis, the preprint of a study examining the functions of MurM and MurN in a broader context was released on the BioRxciv server (29.04.2019), building on the findings by Shepherd and Ibba (2013). The results from this study strongly suggest that in addition to the abovementioned functions, murMN is involved in the regulation of stringent response pathway activation in pneumococci (Aggarwal et al., 2019). The stringent response is a mechanism utilized by many bacteria to survive periods of environmental or intracellular stress, in which the cellular processes are redirected away from rapid cell proliferation, and towards a state of long-term survival in stationary phase. This new study further highlights the importance of murMN for tolerating both antibiotic and cellular stress in S. pneumoniae (Aggarwal et al., 2019). Considering the very recent and still uncorroborated nature of this discovery, the current thesis has not taken this into account and is thus based on the research and knowledge available prior to this. If the new data presented in the Aggarwal study is found credible and supported by further evidence, the following research findings and discussion found in this thesis must be reassessed in view of the Aggarwal study.

1.7 Main objectives of this study

β-lactam resistance in *S. pneumoniae* is mediated by alterations in the penicillin-binding proteins, which display a reduced affinity for these antibiotics. Additionally, mosaic versions of MurM, which is involved in the biosynthesis of the interpeptide bridge in branched peptidoglycan, have been found to be critical for high-level resistance in many pneumococcal strains (Filipe and Tomasz, 2000). In this work, we wanted to explore the development of penicillin-resistance in *S. pneumoniae* by introducing low-affinity versions of PBP2x, PBP2b and PBP1a, and a mosaic MurM, from the highly resistant *S. oralis* Uo5 strain. Previous studies have shown that the transfer of mosaic MurM versions from resistant strains to penicillin-sensitive pneumococcal strains is not tolerated, indicating that these MurM versions are toxic in a penicillin-sensitive background. It has been hypothesized that altered MurM variants only are tolerated in strains expressing low-affinity PBPs, and clinical isolates display a relatively conserved co-expression of certain mosaic PBP variants with specific MurM versions (del Campo et al., 2006). Therefore, we wanted to explore the toxicity of $MurM_{Uo5}$ in the sensitive laboratory strain *S. pneumoniae* R6 compared to a mutant expressing low-affinity PBPs. We also wanted to examine the fitness costs of the acquisition of different mosaic PBPs.

2 Materials

2.1 Strains

Table 2.1 *S. pneumoniae* and *S. oralis* strains used in this work, with a brief description of their relevant genotype and characteristics.

Strain	Genotype and characteristics	Reference
S. oralis		
GS850	GS820, but Δ*murM* + Δ*cbpd2*::*janus*, Kan^R	Dr. Gro Stamsås
Uo5	Wild-type, Sm^R	Prof. Mogens Kilian
S. pneumoniae		
DS665	Δ*pbp1a*::*janus*, Kan^R	Dr. Daniel Straume
KHB55	Δ*pbp2x*::*janus*, P_{comX}:*pbp2x*, Kan^R	Dr. Kari Helene Berg
KHB88	Δ*pbp2b*::*janus*, P_{comX}:*pbp2b*, Kan^R	Dr. Kari Helene Berg
KHB130	Wild-type RH4, but Δ*murMN*::*janus*, Kan^R	Dr. Kari Helene Berg
RH425	R704, but Sm^R	
SPH131	*comR* in the Ami locus, P_{comX}:*janus*, Kan^R	Dr. Kari Helene Berg
RH1	Δ*egb*::*spc*, Ery^R, Spc^R	

Table 2.2 Overview over the relevant *S. pneumoniae* mutants constructed in this work, with a brief description of their genotype and characteristics.

Strain	Genotype and characteristics	Reference
MH7	RH425, but $pbp2x_{mos}$, Sm^R	This work
MH10	RH425, but $pbp2x_{mos}$, Sm^R	This work
MH12	RH425, but $pbp2x_{mos}$, Sm^R	This work
MH17	RH425, but $pbp2x_{mos}$, Sm^R	This work
MH19	RH425, but $pbp2x_{mos}$, Sm^R	This work
MH53	MH10, but $pbp1a_{mos}$, Sm^R	This work
MH56	MH10, but $pbp1a_{mos}$, Sm^R	This work
MH65	MH10, but $pbp2b_{mos}$, Sm^R	This work
MH67	MH10, but $pbp2b_{mos}$, Sm^R	This work
MH68	MH10, but $pbp2b_{mos}$, Sm^R	This work
MH78	MH56, but $pbp2b_{mos}$, Sm^R	This work
MH80	MH56, but $pbp2b_{mos}$, Sm^R	This work
MH83	MH56, but $pbp2b_{mos}$, Sm^R	This work
MH90	MH10, but $pbp1a_{mos}$, Sm^R	This work
MH91	MH10, but $pbp1a_{mos}$, $pbp2b_{T446A}$ Sm^R	This work
MH105	SPH131, but P_{comX}:$murM_{Uo5}$, Sm^R	This work

Strain	Genotype and characteristics	Reference
MH108	MH83, but Δ*murMN*::*janus*, Kan^R	This work
MH110	RH425, but Δ*murMN*::*janus*, Kan^R	This work
MH122	MH10, but Δ*murMN*::*janus*, Kan^R	This work
MH124	MH91, but Δ*murMN*::*janus*, Kan^R	This work
MH126	MH56, but Δ*murMN*::*janus*, Kan^R	This work
MH128	MH68, but Δ*murMN*::*janus*, Kan^R	This work
MH130	MH83, but *janus* in the Ami locus, Kan^R	This work
MH132	MH130, but Δ*janus*::*comR*, Sm^R	This work
MH134	MH132, but P_{comX}:*janus*, Kan^R	This work
MH136	MH105, but Δ*murMN*::*janus*, Kan^R	This work
MH138	MH134, but Δ*janus*::$murM_{Uo5}$, Sm^R	This work
MH141	MH138, but Δ*murMN*::*janus*, Kan^R	This work
MH142	SPH131, but P_{comX}:$murM_{R6}$, Sm^R	This work
MH144	MH134, but P_{comX}:$murM_{R6}$, Sm^R	This work
MH146	MH142, but Δ*murMN*::*janus*, Kan^R	This work
MH147	MH144, but Δ*murMN*::*janus*, Kan^R	This work
MH149	MH105, but Δ*murN*::*janus*, Kan^R	This work
MH150	MH138, but Δ*murN*::*janus*, Kan^R	This work
MH151	MH105, but Δ*murM*::*janus*, Kan^R	This work
MH152	MH138, but Δ*murM*::*janus*, Kan^R	This work
MH153	MH83, but Δ*murM*::*janus*, Kan^R	This work
MH156	MH153, but Δ*janus*::$murM_{Uo5}$, Sm^R	This work

2.2 Primers

Table 2.3 List of primers used in this work, including a short description, and the 5'-3' nucleotide sequence.

Name	Description	Sequence 5'-3'	Reference
AmiF	*ami* F	CGGTGAAGGAAGTAAGAAGTTT	
CSS26	F seq P_{comX} R6	TAAAGTCGGTTTCACCTCTTC	
CSS29	R seq P_{comX} R6	CAACAATCAAGTGGTATACAG	Dr. Gro Stamsås
GS104	F seq in *comR*	TGCTATGTTTAGATGGTGCG	Dr. Gro Stamsås
GS105	F seq in *comR* 2	ATGGCTATTGCTGCTTTAAAGA	Dr. Gro Stamsås
GS428	F up *murN* R6	GATGAAAAAGTCAGTATTTAGATT	Dr. Gro Stamsås
GS429	R down *murM* R6	TTCCTACTCTCTTTCCTCCA	Dr. Gro Stamsås
GS430	F *murM* Uo5, overhang up *murM* R6	TGGAGGAAAGAGAGTAGGAAATGTTTACGTATAAA ATGAATGTTG	Dr. Gro Stamsås
GS431	R *murM* Uo5, overhang up murN R6	AATCTAAATACTGACTTTTTCATCCTAATTCCTACTT CGAAGTTTC	Dr. Gro Stamsås
GS439	R end *murM* Uo5	CTAATTCCTACTTCGAAGTTTC	Dr. Gro Stamsås

Name	Description	Sequence 5'-3'	Reference
Janus F	F *janus*	GTTTGATTTTTAATGGATAATGTG	
Janus R	R *janus*	CTTTCCTTATGCTTTTGGAC	
KHB31	*cpsO*.F	ATAACAAATCCAGTAGCTTTGG	Dr. Kari Helene Berg
KHB33	*cpsN*.F	TTTCTAATATGTAACTCTTCCCAAT	Dr. Kari Helene Berg
KHB34	*cpsN*.R	CATCGGAACCTATACTCTTTTAG	Dr. Kari Helene Berg
KHB36	P_{comX}.R	TGAACCTCCAATAATAAATATAAAT	Dr. Kari Helene Berg
KHB43	Stu0270.F-N	GCATTGCGCTTGATAAGTTTGAGGATAATCAAGATT TATCTTATAAA	Dr. Kari Helene Berg
KHB104	*mraW*.F	GAAGTGAAGCCGATTGAGAC	Dr. Kari Helene Berg
KHB107	*mraY*.R	ACACAATTCCGATAATCAAGAG	Dr. Kari Helene Berg
KHB111	sek *ftsL*.F	CAAGAGGTCAATGAACTATTAC	Dr. Kari Helene Berg
KHB112	sek *mraY*.R	GCCTGTAATTTGCGCCTTTC	Dr. Kari Helene Berg
KHB129	*pbp2b* up.F	CGATAAAGAAGAGCATAGGAAG	Dr. Kari Helene Berg
KHB132	*pbp2b* down.R	TCCCAATCAATGGTTTCATTGG	Dr. Kari Helene Berg
KHB198	*murN* down.F –RpsL overhang	CTAAACGTCCAAAAGCATAAGGAAAGGATGAAAAA GTCAGTATTTAGATT	Dr. Kari Helene Berg
KHB199	*murN* down.R	CACAATTTCAGACACCAGAGC	Dr. Kari Helene Berg
KHB374	*murM*(R6).F_P_{comX} overhang	ATTTATATTTATTATTGGAGGTTCAATGTACCGTTAT CAAATTGGCAT	Dr. Kari Helene Berg
KHB375	*murM*(R6).R_*cpsN* overhang	ATTGGGAAGAGTTACATATTAGAAATTACTTTCTAT GTTTTTTTCTTAATG	Dr. Kari Helene Berg
TreR	*tre* R	GTGACGGCAGTCACATTCTC	
VE47	*murM* F	ACCAGTAGTCATGGAAGCAAA	Dr. Vegard Eldholm
VE50	*murM kan* R	CACATTATCCATTAAAAATCAAACTTCCTACTCTCTT TCCTCCA	Dr. Vegard Eldholm

Table 2.4 List of primers designed for and used in this work, including a short description, and the 5'-3' nucleotide sequence.

Name	Description	Sequence 5'-3'
MVH1	F *pbp2b*Uo5	ATGAGAAAATTTAATAGCCATTCG
MVH2	R up *pbp2b*R6, overlap *pbp2b*Uo5	CGAATGGCTATTAAATTTTCTCATACAAATCAGTCTCA TTTCTAACTTAAAATC
MVH3	R *pbp2b*Uo5	CTAGTTCATTGGATGGTGTTGG
MVH4	F *pbp2b*R6, overlap *pbp2b*Uo5	CCAACACCATCCAATGAACTAGAAAGGAAATTATGCT TTATCCAAC
MVH5	F *pbp2x*Uo5	ATGAAAACCTGGAAAGAAAAAATAG
MVH6	R up *pbp2x*R6, overlap *pbp2x*Uo5	CTATTTTTTCTTTCCAGGTTTTCATATCTTACTCCGCTA TTCTAATATTTTC
MVH8	F down *pbp2x*R6, overlap *pbp2x*Uo5	CATTAAAAAAATTAAATTAACTTTAGGAGACTAATAT GTTTATTTCCATCAGTGCTG
MVH9	F ~1000 bp up *pbp1a*R6	CTTCCTGTAAACACAAGCCAAG
MVH10	R up *pbp1a*R6, overlap *pbp1a*Uo5	CTATTCGCAGAAAAGTTTGTTTGTTCATCTTGTTTTAC CACCTAATAAATG
MVH11	F *pbp1a*uo5	ATGAACAAACAAACTTTTCTGCG
MVH12	R *pbp1a*Uo5	TTATGGTTGTGCTGGTTGAGG
MVH13	F downstream *pbp1a*R6, overlap *pbp1a*Uo5	CCTCAACCAGCACAACCATAACATTTATCATCCAGATT TTTCTG
MVH14	R ~1000 up *pbp1a*R6	TGTAGGCAAGCCTGCAACC
MVH15	R *pbp2b*R6 tm chimera	CAACAAACGACCAATAATGGTC
MVH16	F *pbp2b*Uo5 tm chimera, overlap tm *pbp2b*R6	GACCATTATTGGTCGTTTGTTG TACATGCAGGTACTCAATAAAG
MVH17	R *pbp2x*R6 tm chimera	GCCTGTCCCAATAATGACCG

Name	Description	Sequence 5'-3'
MVH18	F *pbp2x*Uo5 tm chimera, overlap tm *pbp2x*R6	CGGTCATTATTGGGACAGGC AAAAAGTTTGGTGTTGACTTGGTC
MVH19	R *pbp1a*R6 tm chimera	GTAGTAGAAAAAAACTCCTCCG
MVH20	F *pbp1a*Uo5 tm chimera, overlap tm *pbp1a*R6	CGGAGGAGTTTTTTTCTACTACGTTAGCAAGGCTCCAG AACTTTC
MVH21	R *pbp2x* Uo5 (replaces MH7)	TTAGTCTCCTAAAGTTAATTTAATTTTTTTAATG
MVH22	F ~1000 up *pbp2x*Uo5	TGGTGTCCAGGAAATTGATGG
MVH23	R ~1000 bp down *pbp2x* Uo5	TGTAATCAAAAGTTAGTTTTACAG
MVH24	F ~1000 up *pbp2b*Uo5	AGGCATAAATCAAATCTATTAAAATG
MVH25	R ~1000 bp down *pbp2b* Uo5	TGATTTTGCTTCTTGCTCGTG
MVH26	F ~1000 up *pbp1a*Uo5	CCCTTGTGCTCATATTGTGG
MVH27	R ~1000 bp down *pbp1a* Uo5	TCTGAGCCAACTAATGCCAAC
MVH28	F *pbp2x*Uo5 tp chimera	ATGACCGCGACCTTGGTCAG
MVH29	R *pbp2x*R6 tp chimera, overlap tp *pbp2x*Uo5	CTGACCAAGGTCGCGGTCATGTACTTTCCTTTTACCTT CTCTTG
MVH30	F *pbp2b*Uo5 tp chimera	TATGCAGTAGCCCTCAATCC
MVH31	R *pbp2b*R6 tp chimera, overlap tp *pbp2b*Uo5	GGATTGAGGGCTACTGCATAGACACCTTCAGAATACT TGGC
MVH32	F *pbp1a*Uo5 tp chimera	ACGATTGTGGATGTGACAAAC
MVH33	R *pbp1a*R6 tp chimera, overlap tp *pbp1a*Uo5	GTTTGTCACATCCACAATCGTAGAAGCGACTTGCAATT CATC
MVH34	F *pbp2x*Uo5 ~500 bp in	GATGTCCATTAAACAAGAC
MVH35	F *pbp2x*Uo5 ~1000 bp in	GGATCAGGCATGAAGGTTATG
MVH36	F *pbp2x*Uo5 ~1500 bp in	CACATGATCTTAGTTGGGACG
MVH37	F *pbp2b*Uo5 ~500 bp in	CTATCTCTTTAGCCAGCTCAATG
MVH38	F *pbp2b*Uo5 ~1000 bp in	CTGAAGGTGTCTATGCAGTAG
MVH39	F *pbp2b*Uo5 ~1500 bp in	GCCAGTTTGATAACTACACACC
MVH40	F *pbp1a*Uo5 ~500 bp in	AGAGATCTTGACCTACTAC
MVH41	F *pbp1a*Uo5 ~1000 bp in	TCATTGCTCAGTTAGGTTCTCG
MVH42	F *pbp1a*Uo5 ~1500 bp in	GTATTTAGTGATGGTAGC
MVH43	F seq just up *murM*R6	CTTAGTTTGAACTTCAGCATAG
MVH44	R seq just down *murN*R6	GCCAGCGCATGTCTCTCC
MVH45	R seq just down *murM*R6	CTAGCAAATCCCCCATCTGG
MVH46	F *murM*Uo5 overlap KHB36	ATTTATATTTATTATTGGAGGTTCAATGTTTACGTATA AAATGAATGTTG
MVH47	R *murM*Uo5 overlap KHB33	ATTGGGAAGAGTTACATATTAGAAACTAATTCCTACTT CGAAGTTTC
MVH49	F up *murN*R6 overlap janus	CACATTATCCATTAAAAATCAAACCTTCTTTCGTGAGT GTTGTTAG

2.3 Peptides

Table 2.5 Peptides used in this work, and their amino acid sequence.

Peptide	Amino acid sequence	Stock solution	Supplier
CSP-1	N-EMRLSKFFRDFILQRKK-C	100 µg/ml	Research Genetics Inc
ComS*	N-LPYFAGCL-C	500 µM	Research Genetics Inc

2.4 Enzymes, molecular weight standards and nucleotides

Table 2.6 List of enzymes, molecular weight standard and nucleotides used in this work.

Name	Stock solution	Product number	Supplier
1 kb DNA ladder	500 µg/ml		New England BioLabs
dATP, dGTP, dCTP, dTTP	100 mM	4026/4027/2028/4029	TaKaRa
Phusion® High-Fidelity DNA polymerase	2 U/µl	M0530	New England BioLabs
One*Taq*® DNA polymerase	5 U/µl	M0273	New England BioLabs
RED*Taq*® Readymix™		R2523	Sigma-Aldrich
DNase			
RNase			
Trypsin	1.6 U/µg	93615	BioChemica
LytA	Isolated by Dr. Daniel Straume		
Proteinase K		BIO-37037	Bioline
Lysozyme			
Mutanolysin	4 U/µg	M9901	Sigma-Aldrich

2.5 Antibiotics

Table 2.7 List of antibiotics and antibiotic E-test® strips used in this work.

Antibiotic	Stock solution	Product number	Supplier
Kanamycin	100 mg/ml	K4000	Sigma-Aldrich
Streptomycin	100 mg/ml	S6501	Sigma-Aldrich
Benzylpenicillin (Penicillin G)	100 mg/ml	13752	Sigma-Aldrich
E-test® Benzylpenicillin	0.002-32 µg/ml	502618	Biomérieux
E-test® Oxacillin	0.016-256 µg/ml	520518	Biomérieux
E-test® Piperacillin	0.016-256 µg/ml	421166	Biomérieux
E-test® Ceftazidime	0.016-256 µg/ml	412293	Biomérieux
Bocillin-FL			

2.7 Kits

Table 2.8 List of kits used in this work.

Name	Purpose	Product number	Supplier
NucleoSpin® Gel and PCR Clean-up	DNA extraction from agarose gel	740609.250	Machnery-Nagel
Nucleobond® AXG columns & buffers	Isolation of genomic DNA from cells		Machnery-Nagel

2.8 Chemicals

Table 2.9 List of chemicals used in this work, including chemical formula, supplier and product number.

Chemical	Formula	Product number	Supplier
β-2-mercaptoethanol	C_2H_6OS		
Acetic acid 100%	CH_3COOH	1.00063.1011	Merck
Acetonitrile	HC_3CN	271004	Sigma-Aldrich
Active coal	C	1.020184.1000	Merck
Acrylamide 4x (40%) 37.5:1	C_3H_5NO	BIAC41	Saveen Wener
Adenosine	$C_{10}H_{13}N_5O_4$	A9251	Sigma-Aldrich
Agarose		15510-027	Invitrogen
Albumin		A7906	Sigma-Aldrich
Ammonium 28ersulfate	$(NH4)_2S_2O_8$	A3678	Sigma-Aldrich
BactoTM Brain Heart Infusion		237200	BD Diagnostics
BactoTM Todd Hewitt		249240	BD Diagnostic
Biotin	$C_{10}H_{16}N_2O_3S$	19606	Sigma-Aldrich
Bromophenol blue	$C_{19}H_9Br_4O_5Sna$	B-5525	Sigma-Aldrich
Casitone			
Calcium chlorine anhydride	CaCl	44970	Fluka
Choline chloride	$C_6H_{14}NO.Cl$	C1879	Sigma-Aldrich
Copper sulphate pentahydrate	$CuSO_4.5H_2O$	61240	Fluka
Di-calcium phosphate	KH2HPO4	1.05104.1000	Merck
Di-sodium hydrogen phosphate	Na_2HPO_4	1.06580.1000	Merck
EDTA	$C_{10}H_{16}N_2Na_2O_8.2H_20$	20 296.360	VWR

Chemical	Formula	Product number	Supplier
Glass beads		G4649	Sigma-Aldrich
Glass wool		1.04086.0250	Merck
Glucose 20%	$C_6H_{12}O_6$	10117gK	VWR
Glycerol 85%	$C_3H_8O_3$	1.04094.1000	Merck
Glycine	$C_2H_5NO_2$	1.0421.1000	Merck
Hydrochloric acid	HCl	30721	Riedel-De Haën
Iron(II)sulphate heptahydrate	$FeO_4S.7H_2O$	44970	Fluka
L-Aspargine monohydrate	$C_4H_8N_2O_3.H_2O$	A4284	Sigma-Aldrich
L-cysteine hydrochloride monohydrate	$C_3H_7NO_2S.HCl.H_2O$	30130	Fluka
Lithium chloride	LiCl	203637	Sigma-Aldrich
Magnesium chlorine hexahydrate	$ClMg.6H_2O$	63072	Fluka
Mangan(II)chloride tetrahydrate	$MnCl_2.4H_2O$	31422	Riedel-de Haën
Methanol	CH_2OH	603-001-00-x	Merck
Monosodium phosphate	NaH_2PO_4		
Nicotinic acid	$C_6H_5NO_2$	72309	Fluka
Phosphoric acid	H_3PO_4	749K02794373	Merck
peqGREEN		PEQL37-501	Saveen Werner
Pyrodoxine hydrochloride	$C_8H_{11}NO_3HCl$	95180	Fluka
Riboflavin	$C_{17}H_{20}N_4O_6$	R-7649	Sigma-Aldrich
Sodium acetate	$C_2H_3O_2Na$	S3272	Sigma-Aldrich
Sodium chloride	NaCl	1.06464.1000	Merck
Sodium dodecyl sulphate (SDS)	$NaC_{12}H_{25}SO_4$	05030	Fluka
Sodium hydroxide	NaOH	1.06469.1000	Merck
Sodium pyruvate	$C_3H_3NaO_3$	P8574	Sigma-Aldrich
Sucrose	$C_{12}H_{22}O_{11}$	102745C	BHD
N,N,N,N-tetramethyl ethylene diamine (TEMED)	$C_6H_{16}N_2$	T9281	Sigma-Aldrich
Thiamine hydrochloride	$C_{12}H_{17}ClN_4OS.HCl$	T4625	Sigma-Aldrich
Trifluoracetic acid	$C_2HF_3O_2$	302031	Sigma-Aldrich
Triton® X-100	$C_{14}H_{22}O(C_2H_4O)n$ (n = 9-10)	X-100	Sigma-Aldrich

Chemical	Formula	Product number	Supplier
Trizma® base	$NH_2C(CH_2OH)_3$	T1503	Sigma-Aldrich
Trizma® hydrochloride	$C_{12}H_{17}ClN_4OS.HCl$	T1503	Sigma-Aldrich
Uridine	$C_9H_{12}N_2O_6$	U6381	Sigma-Aldrich
Yeast extract		1.04086.0250	Merck
Zinc sulphate heptahydrate	$ZnSO_4.7H_2O$	96500	Fluka

2.9 Equipment

Table 2.10 List of equipment used in this work. Additional standard laboratory equipment was also used, but is not listed in this table.

Equipment	Model	Supplier
Fast prep	FastPrep® 24	MP™ Biomedicals
Gel imager	GelDoc-1000	BioRad
Gel imager II	Azure Imager c400	Azure Biosystems
HPLC machine	Dionex UltiMate 3000	Thermo-Fisher Scientific
HPLC column	Vydac 218TP C_{18}	Grace Davison Discovery Sciences
Microplate reader	Synergy H1 Hybrid Reader	BioTek®
Microscope	LSM700	Zeiss
Spectrophotometer	NanoDrop 2000	Thermo-Fisher Scientific
PCR machine	ProFlex PCR Systems	Applied Biodynamics
Vacuum pump and condensation trap	Gel pump GP100	Savant

2.10 Recipes for growth mediums and buffers

2.10.1 Solutions for C medium

Yeast extract solution

40 g yeast extract

360 ml dH_2O

37% HCl

16 g active coal

The solution was mixed for 10 minutes, and incubated 2 hours at 4°C, before it was filtered through a column packed with glass wool and celite overnight. The solution was adjusted to pH 7.8 with high-molarity NaOH, and the final volume adjusted to 400 ml with dH_2O. The final solution was sterile filtered, and stored in 4 ml aliquots at -80°C.

ADAMS I

150 µl 0.5 mg/ml Biotine

75 mg Nicotinic acid

87.5 mg Pyrodoxine hydrochloride (4°C)

80 mg Thiamine hydrochloride

35 mg Riboflavin

The solution was adjusted with dH_2O to a final volume of 0.5 L, and the pH adjusted to 7.0. The solution was sterile filtered, and stored at 4°C.

ADAMS II

500 mg Iron(II)sulphate heptahydrate

500 mg Copper sulphate pentahydrate

500 mg Zinc sulphate heptahydrate

200 mg Mangan(II)chloride tetrahydrate

10 ml HCl concentrate

The solution was adjusted with dH_2O to a final volume of 100 ml, sterile filtered and stored at 4°C.

ADAMS III

128 ml ADAMS I

3.2 ml 10X ADAMS II

1.6 g Asparagine monohydrate

160 mg Choline

0.4 g Calcium chlorine anhydride

16 g Magnesium chlorine hexahydrate

The solution was adjusted with dH_2O to a final volume of 800 ml, and the pH adjusted to 7.6. The solution was sterile filtered, and stored at 4°C.

Pre-C medium

22.5 mg L-cysteine HCl

4 g Sodium acetate

10 g Casitone

12 mg L-tryptophan

17 g Di-calcium phosphate

The solution was adjusted with dH_2O to a final volume of 2 L, and stored in sterile-filtered 150 ml aliquots at room temperature.

C medium

Added to 150 ml pre-C medium:

150 µl 0.4 mM Mangan(II)chloride

1.5 ml 20% Glucose

3.75 ml ADAMS III

110 µl 3% Glutamine

2.5 ml 2% Sodium pyruvate

95 µl 1.5 M Sucrose

1.5 ml 2 mg/ml Uridine adenosine

1.5 ml 8% Albumin/BSA

3.75 ml Yeast extract

The solution was sterile filtered before use. C medium was made the day of use, and stored at 4°C.

2.10.2 Todd Hewitt (TH) medium

Todd Hewitt-medium was made by dissolving 30 g TH broth in 1 L dH_2O, and sterilized by autoclavation.

2.10.3 Brain Heart Infusion (BHI) medium

Brain Heart Infusion-medium was made by dissolving 37 g BHI broth in 1 L dH_2O, and was sterilized by autoclavation.

2.10.4 Buffers and solutions for agarose gel electrophoresis

50x Tris-Acetate-EDTA (TAE)

424 g Tris base

57.1 ml Acetic acid

100 ml 0.5 M EDTA, pH 8.0

The solution as adjusted to 1 L with dH_2O.

6x Loading buffer

10 mM Tris-HCl, pH 8.0

1 mM EDTA

40 % Sucrose

0.01 % Bromophenol blue

1 kb DNA ladder (50 mg/ml)

50 µl 1 kb ladder (Invitrogen)

200 µl 10x loading buffer

750 µl dH_2O

1 % Agarose gel

0.5 g Agarose

50 ml TAE buffer

2 µl peqGREEN

The solution was boiled until the agarose was completely dissolved, before 2 µl peqGREEN dye was added.

2.10.5 Buffers and gels for SDS-PAGE

10x Tris-glycerine running buffer

30 g Tris base (0.25 M)

144 g Glycine (1.92 M)

40 ml 20% SDS

The solution was adjusted with dH_2O to a final volume of 1 L.

2x SDS sample buffer

0.125 M Tris-HCl, pH 6.8

4 % SDS

0.3 M 2% β-2-mercaptoethanol (0.2 M DTT)

20 % Glycerol

0.01 % Bromophenol blue

10 % polyacrylamide separation gel

3.86 ml 30% Acrylamide

2.1 ml 2% Bis-acrylamide

2.5 ml 1.5 M Tris-HCl buffer, pH 8.8

1.34 ml dH_2O

0.1 ml 10% SDS

5 µl TEMED

100 µl 10% APS (ammonium persulphate)

Final volume: 10 ml

The solution was degassed after mixing acrylamide, bis-acrylamide, Tris-HCl buffer and dH_2O, before the rest of the reactants were added. The APS-solution was made the day of use.

4 % polyacrylamide stacking gel

1 ml 30% Acrylamide

0.55 ml 2 % Bis-acrylamide

2.5 ml 0.5 M Tris-HCl buffer, pH 6.8

5.7 ml dH_2O

0.2 ml 10% SDS

5 µl TEMED

50 µl 10% APS (ammonium persulphate)

Final volume: 10 ml

The solution was degassed after mixing acrylamide, bis-acrylamide, Tris-HCl buffer and dH_2O, before the rest of the reactants were added. The APS-solution was made the day of use.

2.10.6 Buffers for HPLC

0.1 M Na-phosphate buffer pH 7.0

57.7 ml 1 M Na_2HPO_4

42.3 ml 1M NaH_2PO_4

Final volume: 100 ml

Buffer A: 0.05 % TFA (trifluoracetic acid)

250 µl TFA was diluted in dH_2O to a final concentration of 0.05 % TFA. Final volume: 0.5 l.

Buffer B: 15% Acetonitrile in 0.05 % TFA

250 µl TFA and 75 ml acetonitrile was diluted in dH_2O to a final concentration of 15% acetonitrile and 0.05 % TFA. Final volume: 0.5 L

2.10.7 Other buffers and solutions

1 M Tris-HCl buffers

Tris-HCl buffers were made by dissolving 15.15 g Tris base in 100 ml dH_2O. The Tris-HCl buffers were adjusted to the desired pH by either NaOH or HCl.

1 M Ethylenediaminetetraacetic acid (EDTA) pH 8.0

18.6 g EDTA was dissolved in 100 ml dH_2O, and the solution adjusted to pH 8.0 by NaOH.

3 Methods

3.1 Growth and storage of *S. pneumonia* and *S. oralis*

All strains of *S. pneumoniae* and *S. oralis* were grown under anaerobic conditions at 37°C. They were grown either in liquid C-medium in airtight tubes, or on Todd Hewitt (TH) agar plates in airtight containers. When grown on plates, AnaeroGen™ sachets (Oxoid) were added to the containers. The AnaeroGen™ sachets react with atmospheric oxygen, and reduce the level of O_2 to <1% within 30 minutes, with the simultaneous production of CO_2 (Oxoid, 2019).

Frozen stocks and starter cultures were both made by adding glycerol to a final concentration of 15% to cultures in the exponential growth phase, at $OD_{550} \approx 0.3$. Both were stored at -80°C.

3.2 The Polymerase Chain Reaction (PCR)

The Polymerase Chain Reaction (PCR) is a method used to amplify large numbers of specific DNA-fragments from a sample. PCR consists of three temperature-specific reactions repeated in cycles 25-30 times. Theoretically, for every cycle, the number of DNA-fragments (or amplicons) are doubled. This makes it possible to generate large amounts of DNA-fragments even from very small samples. The main components of PCR are template DNA (which includes the target sequence), primers annealing to each end of the target DNA, a thermostable DNA polymerase, and the four deoxynucleotide triphosphates (dNTPs) dATP, dCTP, dGTP and dTTP (Saiki et al., 1985).

The three steps of PCR are denaturation, annealing and elongation, each of which are carried out at different temperatures (Garibyan and Avashia, 2013). The first step of PCR, denaturation, occurs when the temperature is increased to 94-98°C. The two strands in the double stranded DNA (dsDNA) are separated into single stranded DNA (ssDNA). This makes it possible for the primers to anneal to the complementary sequences of the ssDNA in the second step of the reaction – annealing. The annealing temperature is based on the melting temperature (T_m) of the primers, which is dependent on their length and GC content. Annealing is typically carried out at between 40-65°C. The primers used in this work was designed to have a T_m of approximately 55-60°C. The third step is elongation. In this step, the DNA polymerase attaches to and elongates the DNA from the free 3'OH end of the primers, by incorporating the dNTPs present in the reaction mix. This generates new dsDNA, which is subsequently used as a new DNA template in the next cycle of the reaction. Most commercially used DNA polymerases are thermostable, and have an optimum temperature of ~72°C .

In this work, three different DNA polymerases were used: Phusion® High-Fidelity (HF), One*Taq*® and Red*Taq*®. The Phusion® HF DNA polymerase is a high-speed polymerase, working at approximately 30 seconds per kilobase when using genomic DNA (gDNA) as a template (BioLabs, 2019b). This was the chosen polymerase when the PCR end-product was to be used for sequencing or in transformation experiments. When the accuracy of the end-product was of less importance, such as in PCR-screening, either One*Taq*® or Red*Taq*® DNA polymerase was used.

The following protocol was used for PCR with the Phusion® HF DNA polymerase: a reaction mix containing the polymerase, DNA template, primers, dNTPs, and a 5x Phusion® HF buffer was prepared on ice. The volumes and concentration of each reagent is listed in Table 3.1. The reaction buffer contained Mg^{2+}, which was crucial or the enzymatic activity of the polymerase. For difficult PCR reactions, additional Mg^{2+} were added, by substituting 1 µl dH_2O with 1 µl 50 mM $MgCl_2$. However, excessive amounts of Mg^{2+} were avoided, as it can cause incomplete denaturation of the dsDNA and incorrect primer annealing (BioLabs, 2019b).

Table 3.1 Reaction mix per PCR reaction with the Phusion® High-Fidelity DNA polymerase.

Reagent	**Final concentration/volume**
10 µl 5x Phusion® High-Fidelity buffer	1x
1 µl template DNA	~20-100 ng
1 µl 10 mM dNTP	0.2 mM
2.5 µl 10 µM forward primer	0.5 µM
2.5 µl 10 µM reverse primer	0.5 µM
0.5 µl 2 U/µl Phusion® High-Fidelity DNA Polymerase	0.02 U/µl
32.5 µl dH_2O	to a final volume of 50 µl
Final volume: 50 µl	

The thermocycler program was adjusted based on the length and quality of the DNA template, the efficiency of the DNA polymerase, and the T_m of the primers. The standard Phusion® PCR program used is presented in Table 3.2.

Table 3.2 Basic PCR program for amplification of DNA-fragments using Phusion® High-Fidelity DNA polymerase.

Step	Temperature	Time	Repeats
Initial denaturation	98°C [a)]	5-10 min	1x
Denaturation	98°C [a)]	30 sec	
Annealing	58°C [b)]	30 sec	25-30x
Elongation	72°C	X sec [c)]	
Final extension	72°C	5-10 min	1x
Storage	4°C	∞	

a) When amplicons were used as template DNA, the denaturation temperature was set to 94°C. When using either the One*Taq*® or Red*Taq*® DNA polymerase, the denaturation temperature was always set to 94°C.

b) The annealing temperature was adjusted based on T_m of the primers. The primers used in this work was designed to have a T_m of approximately 58-60°C.

c) The elongation time was based on the length of the DNA template, with 30 seconds added for every 1000 bp when using the Phusion® HF DNA polymerase, and 1 minute per kilobase when using One*Taq*® or Red*Taq*® DNA polymerase.

3.2.1 PCR-screening of potential transformants

PCR using One*Taq*® or Red*Taq*® DNA polymerase was used to screen potential transformants. By using primers targeting a DNA sequence that would only be present in the transformant, a positive PCR reaction would strongly indicate a successful transformation.

The following protocol was used for PCR using One*Taq*®: the reaction solution was prepared by mixing the reagents listed in Table 3.3 on ice, before the samples were applied to the thermocycler. The standard program presented in Table 3.2 was adjusted for the properties of the One*Taq*® DNA polymerase. This polymerase is slower than the Phusion® HF DNA polymerase, working at a speed of approximately 1 kilobase per minute (BioLabs, 2019a). The One*Taq*® polymerase is also slightly less thermostable, so the initial denaturation and denaturation temperature was set to 94°C.

Table 3.3 Reaction mix per PCR reaction with the One*Taq*® DNA Polymerase.

Reagent	Final concentration/volume
4 µl 5x One*Taq*® Standard reaction buffer	1x
1 µl template DNA	~20-100 ng
0.5 µl 10 mM dNTP	0.25 mM
1 µl 10 µM forward primer	0.5 µM
1 µl 10 µM reverse primer	0.5 µM
0.125 µl 5 U/µl One*Taq*® DNA polymerase	0.03 U/µl
12.375 µl dH_2O	To a final volume of 20 µl
Final volume: 20 µl	

For PCR-screening using Red*Taq*®, a ReadyMix™ PCR reaction mix was used. This contains buffer, dNTPs, the *Taq* DNA polymerase and an inert loading dye (Sigma-Aldrich, 2019). One ice, the Readymix was mixed with the primers, DNA template and dH_2O as presented in Table 3.4, before the sample was applied on the thermocycler, following the same procedure as for the One*Taq*® DNA polymerase.

Table 3.4 Reaction mix per PCR reaction with the Red*Taq*® ReadyMix™ PCR reaction mix.

Reagent	Final concentration/volume
5 µl Red*Taq*® ReadyMix™ PCR reaction mix [a)]	
0.2 µl 10 µM forward primer	0.2 µM
0.2 µl 10 µM reverse primer	0.2 µM
1 µl DNA template	~20-100 ng
3.6 µl dH_2O	To a final volume of 10 µl
Final volume: 10 µl	

a) The Readymix™ contains buffer, dNTPs, *Taq* DNA polymerase, as well as an inert loading dye.

3.2.2 Overlap extension PCR

Overlap extension PCR is a method based on standard PCR (section 3.2.1), in which two or more DNA-sequences are spliced into larger fragments. This enables the design of novel DNA constructs. In this work, overlap extension PCR was used to make constructs for deleting genes, for gene replacements via the Janus cassette, and for inserting genes behind a titratable promoter. One prerequisite for overlap extension PCR is that the fragments that are to be spliced have overlapping 3' ends. This is achieved by using primers that have a 5' overhang which is complementary to the 3' end of the second fragment. For example, overlap extension PCR was used to make a construct for knocking out the *murMN* operon in *S. pneumoniae* R6. To enable

the selection of successful transformants, the operon was replaced with the Janus cassette, which encodes an antibiotic selection marker (section 3.6.1). The construct was made by combining the flanking regions of the R6 *murMN* operon with the Janus cassette, as illustrated in Figure 3.1.

In the first step over overlap extension PCR, the DNA-fragments that are to be combined are amplified, using primers that introduces the complementary overhangs. In the case of the Δ*murMN*::*janus* construct, the reverse primer of the upstream fragment, VE50, had a 5' overhang complementary to one end of the Janus cassette, and the forward primer of the upstream fragment, KHB198, had a 5' overhang complementary to the other end of the Janus cassette (Figure 3.1A). In the second step, the amplicons from the first step are combined in a PCR reaction using the flanking primers. For the Δ*murMN*::*janus* construct, this included the splicing of the upstream fragment with the Janus cassette using the VE47 and Janus R flanking primers, and combining the downstream fragment with the Janus cassette using the Janus F and KHB199 flanking primers (Figure 3.1B). The overlapping sequences introduced in the first step hybridize, and are extended from the free 3'OH ends. In this way, the overlapping sequences function as primers. In combination with the elongation from the flanking primers, this generates the spliced DNA-fragments. If more than two fragments are to be spliced, the flanking primers are designed to have a 5' overhang that introduces an overlap complementary to the end of the third DNA-fragment. In the case of the Δ*murMN*::*janus* construct, the Janus cassette functioned as the overlapping sequence, and the two amplicons from the second step were combined using the flanking primers VE47 and KHB199 (Figure 3.1C). The final construct was isolated using gel electrophoresis (see section 3.3) and subsequently used to replace the *murMN* operon with the Janus cassette (see section 3.6).

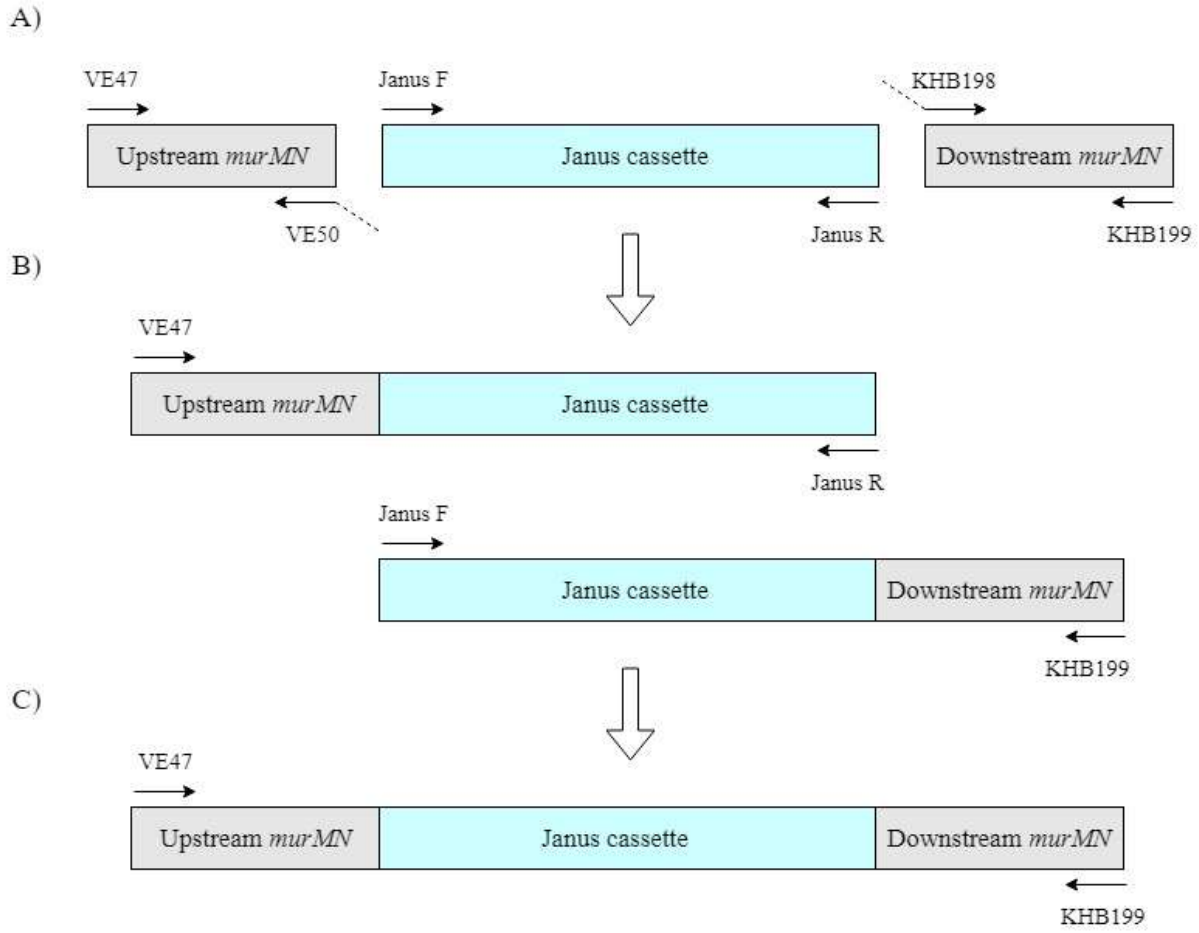

Figure 3.1 The construction of the Δ*murMN::janus* construct using overlap extension PCR. The boxes illustrate the DNA sequences, while the arrows (pointing in a 5'-3' direction) indicate the primers used. A) The first step includes the amplification of the fragments that are to be spliced, in separate reactions. In the case of the Δ*murMN::janus* construct, this includes the ~1000 bp upstream and downstream fragments of the *murMN* operon and the ~1.3 kb Janus cassette. Two of the primers, VE50 and KHB198, have 5' overhangs (illustrated with dotted lines) complementary to the ends of the Janus cassette, which introduce overlapping sequences that enable the splicing of the fragments in the second PCR reaction. B) The second step includes two separate PCR reactions; the splicing of the upstream fragment with the Janus cassette, and the splicing of the downstream fragment with the Janus cassette, using the flanking primers VE47 + Janus R, and Janus F + KHB199, respectively. C) In the last step, the amplicons from step 2 are combined in a final PCR reaction, using the flanking primers VE47 and KHB199.

3.3 Gel electrophoresis

Gel electrophoresis is a method used to separate macromolecules such as proteins or DNA based on size or charge. The molecules are separated by pushing the molecules through a gel matrix, driven by an electric current. The molecules will move through the gel at different rates, depending on their size or charge. In this work, agarose gel electrophoresis was used to separate DNA-fragments, while SDS-PAGE was used to separate proteins.

3.3.1 Agarose gel electrophoresis

Agarose gel electrophoresis was used to separate DNA-fragments. The agarose gel electrophoresis setup includes the agarose gel, which is placed in an electrophoresis chamber; a container connected to a power supply. The gel is covered with a conductive buffer. The agarose gel consists of a matrix of agarose polymers stabilized by hydrogen bonds, containing small pores that allow the movement of the DNA-molecules through the matrix. The size of the pores is dependent on the agarose concentration (Lee et al., 2012). The samples are applied in small wells at the top of the gel. DNA has a negative charge at neutral pH, due to the presence of negatively charged phosphate groups, enabling it to move through the matrix in the gel when an electric field is applied. The negatively charged DNA moves towards the positively charged anode. Smaller molecules move faster through the gel matrix than large ones, allowing the separation of fragments based on size (Lee et al., 2012). To visualize the DNA, a fluorescent dye is added to the gel, such as peqGREEN, which fluoresces under UV light upon binding DNA.

In this work, agarose gel electrophoresis was used to separate and analyse both PCR fragments and genomic DNA. The following protocol was used: first, a 1% agarose gel was made by mixing 0.5 g agarose with 50 µl TAE (40 mM Tris-Acetate, 1 mM EDTA) buffer. The solution was boiled until the agarose was completely dissolved. After rapid cooling to approximately 60°C, 2 µl peqGREEN was added to the gel solution. The solution was poured into a cast, and a comb used to create the wells into which the samples were to be loaded. The gel was allowed to set, before it was transferred to the electrophoresis chamber and covered with TAE buffer. The samples were mixed with a 6x loading buffer to a final concentration of 1x, to make it easier to apply the samples to the wells in the gel. The loading buffer contains glycerol, which makes the solution more viscous, and the dye bromophenol blue. In the case of amplicons made using Red*Taq*®, the loading buffer was already present in the reaction mix. A 1 kb DNA ladder was applied to the first well. The ladder contains DNA-fragments of known sizes, which makes it possible to determine the approximate size of the fragments in the samples. The gel electrophoresis was run on 90 V until the DNA-fragments were sufficiently separated, between 20 and 45 minutes. The fragments were visualized under UV light in a Gel Doc-1000 (BioRad).

3.3.2 Extraction of DNA from agarose gels

After separation of DNA using agarose gel electrophoresis, the fragments were isolated from the gel and cleaned using the Nucleospin® Gel and PCR Clean-up kit from Macherey-Nagel.

The piece containing the desired DNA-fragment was cut from the gel and dissolved in the binding buffer Buffer NTI (approximately 200 µl NTI per 100 mg gel) at 55°C. The dissolved gel was transferred to a Nucleospin® Gel and PCR Clean-up column, placed in a 2 ml collection tube, and was centrifuged for 30 seconds at 13 000 x *g*. In this step, the DNA present in the sample binds to the silica membrane in the column, aided by the chaotropic salts present in Buffer NTI. In the second step, the column was washed with 700 µl Buffer NT3, for 30 seconds at 13 000 x *g*, to remove salts and other contaminants. A second centrifugation, 1 minute at 13 000 x g, was performed to remove any residual NT3. The flow-through was discarded, and the column placed in a clean 1.5 ml Eppendorf tube. The DNA was then eluted from the column with 15-40 µl Buffer NE, depending on the relative concentration of DNA in the sample. Buffer NE is slightly alkaline, with a pH = 8.5. Under these conditions, the DNA is released from the silica membrane in the column. The column was incubated for 1 minute at room temperature, before the DNA was eluted by centrifugation at 13 000 x *g* for 1 minute. The eluate was stored at -20°C. The DNA concentration and purity of the eluate was determined by spectrophotometry in a NanoDrop 2000 (Thermo-Fisher Scientific), by measuring absorbance at 260 nm. Buffer NE was used as blanking solution. The purity of the DNA was determined by analysing the 260/280 nm ratio. A 260/280 >> 1.8 indicates RNA contamination, while a 260/280 << 1.8 indicates contamination of proteins or compounds with a strong 280 nm absorbance, such as phenols (Scientific, 2009).

3.3.3 SDS-PAGE

SDS-PAGE (sodium dodecyl sulphate - polyacrylamide gel electrophoresis) is a method commonly used to separate proteins based on molecular mass. SDS is a potent detergent that binds and denatures the proteins in a sample, and gives a negative charge along the entire denatured protein, which provides a uniform charge-to-mass ratio. This makes it possible to separate the proteins solely based on molecular mass, using polyacrylamide gel electrophoresis (PAGE) (Brunelle and Green, 2014). Compared to the agarose gel, the polyacrylamide gel matrix has pores of a highly uniform size, which enables a precise separation of small molecules. The pore size is dependent on the concentration of acrylamide and bis-acrylamide. In this work, SDS-PAGE was used to separate Bocillin FL-labelled PBPs (section 3.10), using a discontinuous gel system which included a stacking gel and a separation gel. The samples are applied to the stacking gel, which has a lower polyacrylamide concentration, and a lower pH, than the separation gel. When the samples are applied to the stacking gel wells, it spans approximately 2-5 mm, which means the proteins will not enter the gel at the same time. The

function of the stacking gel is to stack the proteins closer together, so that they enter the separation gel at the same time – this way, the separation of the proteins according to size will not be disrupted by the time they enter the gel (Brunelle and Green, 2014). In the separation gel, the proteins are separated by size according to the principle described for agarose gel electrophoresis in section 3.3.1.

The following protocol was used: First, the samples were prepared by mixing the labelled proteins with a 2x SDS sample buffer in a 1:1 ratio, and the proteins denatured by boiling the solution for 10 minutes. The sample buffer contains both SDS and β-mercaptoethanol. β-mercaptoethanol is a reducing agent, and cleaves the disulphide bridges within the protein structures. Together with the SDS and the heat treatment, this results in full denaturation of the proteins, and the distribution of a uniform negative charge-to-mass ratio, enabling the separation of the proteins based on molecular mass using gel electrophoresis.

Second, the stacking and separation gels were made. As non-polymerized acrylamide is a potent neurotoxin that can be absorbed through the skin, gloves was worn when preparing the gels. A casting chamber setup (BioRad) was assembled, consisting of two glass plates vertically placed in a casting stand. The 10% separation gel was made by mixing the reagents listed in section 2.10.5. After mixing the acrylamide, bis-acrylamide, Tris-HCl buffer pH 8.8 and dH_2O, the solution was degassed, before adding the rest of the reactants. The APS and TEMED were added last, as they initiate the polymerization of the gel. 3.2 ml of the gel solution was quickly transferred into the cast, and topped with dH_2O to ensure a level gel surface. After polymerization of the separation gel, the overlaying dH_2O was removed, and the 4% stacking gel made by mixing the reagents listed in section 2.10.5, by the same procedure as the separation gel. 1 ml of the gel solution was applied on top of the polymerized separation gel in the cast. A 10-welled comb was inserted into the gel solution before it was allowed to polymerize. After polymerization, the casting chamber was transferred into the gel electrophoresis chamber, which was subsequently filled with the running buffer. The comb was removed, and the wells gently washed with running buffer, before the samples were applied together with a loading buffer containing the dye bromomethyl blue. The dye is added to follow the migration of the samples through the gel. Each well was loaded with 10 µl of sample. The electrophoresis was run at 200 V for ~45 minutes after the bromomethyl blue dye had reached the bottom of the gel. The proteins were visualized in an Azure Imager c400 (Azure Biosystems).

3.4 Isolation of genomic DNA (gDNA)

Isolation of gDNA from cells was performed by using Nucleobond® AXG columns and buffers (Macherey Nagel). The following protocol was used: first, the relevant culture was grown to an OD_{550} of between 0.3 and 0.5. 10 ml of the culture was centrifuged at 4000 x *g* for 10 minutes to collect the cells. The pellet was resuspended in 5 ml cold buffer G3. To lyse the cells, the culture was treated with 20 µl 40 mg/ml lysozyme, 25 µl proteinase K and 20 µl 1000 µg/ml mutanolysin, and incubated at a 37°C water bath for 40 minutes, or until the lysate was clear. To rid the lysate of any residual cell material that might clog and obstruct the column, it was briefly centrifuged at 4000 x *g* for 5 minutes. The lysate was mixed with 1.2 ml buffer G4, before being further incubated at a 50°C water bath for 30 minutes. After incubation, the sample was mixed with 5 ml buffer N2, before being added to the AXG 100 column, which that had been equilibrated with 2 ml of buffer N2. After binding the DNA, the column was washed three times with 4 ml buffer N3. The gDNA was then eluted from the column with 5 ml buffer N5. To precipitate the gDNA from the eluate, 3.5 ml (0.7 x volume) of isopropanol was added. The solution was mixed well, and incubated for 30-60 minutes at room temperature, before the DNA was collected by centrifugation at 13 000 x *g* for 25 minutes. The pellet was washed with 4 ml ice cold 70% ethanol (13 000 x *g* for 15 minutes), before it was carefully resuspended in 100-150 µl dH_2O. Isolated gDNA was stored at -20°C.

3.5 DNA sequencing

DNA sequencing involves the determination of the order of the bases in DNA. The most common sequencing methods today are based on Sanger sequencing.

The original Sanger sequencing setup includes a DNA polymerase, an ssDNA template, a sequencing primer, regular dNTPs, and ddNTPs (di-deoxynucleotidetriphosphates) (Sanger et al., 1977). The four ddNTPs (ddATP, ddGTP, ddCTP and ddTTP) are labelled with different fluorochromes. During the sequencing reaction, the primer anneals to the ssDNA template, and the DNA polymerase synthesize the complementary strand by the incorporation of the dNTPs or ddNTPs. ddNTPs lack the 3'OH-group from which the DNA polymerase extend the DNA sequence. Thus, when the polymerase incorporates a ddNTP, the extension is terminated. The ddNTPs are present in a much lower concentration than dNTPs, which ensures a random incorporation of the ddNTP in the sequence, and the generation of a collection of fragments terminated at different positions. The fragments are then separated by size by gel electrophoresis, and the fluorochrome detected by a laser, enabling the determination of the

DNA sequence (Sanger et al., 1977). Since the dawn of sequencing technologies, several new and improved methods have seen the light of day, such as Illumina high-throughput sequencing allowing for massive parallel sequencing of thousands of samples. This has revolutionized the field of molecular biology and enabled the sequencing of whole genomes at a fraction of the cost and time of Sanger sequencing (van Dijk et al., 2014).

3.5.1 Targeted gene sequencing

Targeted gene sequencing was performed to verify transformants and to determine the sequence of mosaic genes. The target gene with approximately 1000 bp flanking regions was amplified using PCR, as described in section 3.2. The PCR product was verified by agarose gel electrophoresis, and the fragment extracted from gel as described in section 3.3.1 and 3.3.2. Depending on the size of the gene or fragment to be sequenced, between 50-200 ng PCR product was mixed with dH_2O to a final volume of 10 µl, including 1 µl 10 µM sequencing primer. The sequencing mix was stored at -20°C. Targeted gene sequencing was performed by GATC, Eurofins Genomics.

3.5.2 Whole genome sequencing

In this work, whole genome sequencing (WGS) was performed on certain pneumococcal mutants in the search for potential suppressor mutations. For whole genome sequencing, genomic DNA was isolated from the relevant cultures as described in section 3.4. The integrity of the isolated gDNA was determined by agarose gel electrophoresis, as described in section 3.3.1. The samples were normalized to a concentration of 50 ng/µl in dH_2O, and stored at -20°C. WGS was performed by Microbes NG at the University of Birmingham, UK, using Illumina sequencing technology. *S. pneumoniae* R6 was used as a reference genome.

3.6 Natural transformation of *S. pneumoniae*

As described in section 1.2, the pneumococci, and other streptococci in the mitis phylogenetic group, are competent for natural genetic transformation, in which they are able to incorporate free DNA from the environment into their own genome through homologous recombination. Competence is transiently induced by a quorum sensing-like mechanism; when the extracellular concentration of the competence stimulating peptide (CSP) reaches a threshold value, the genes required for transformation are activated (Håvarstein et al., 1995). This ability was exploited to transform strains of *S. pneumoniae,* by utilizing a synthetic CSP (CSP-1) to selectively induce the competent state. To achieve maximum control of the transformation mechanism during experiments, spontaneous induction of competence should be avoided. Therefore, all *S.*

pneumoniae mutants used in this work had the native CSP transporter, comA, deleted. The Δ*comA* mutants are unable to secrete CSP, and thus unable to self-induce competence.

Transformation of *S. pneumoniae* was performed using the following protocol: The cultures were grown to an OD_{550} = 0.05 - 0.1. 1 ml of culture was incubated at 37°C for 2 hours with ~100-200 ng of transforming DNA, and 250 ng/ml CSP-1. Negative controls without the transforming DNA were included. Competence induced by CSP-1 lasts for approximately 40 minutes, after which the cells returns to a non-competent condition (Håvarstein et al., 1995). After incubation, 30 µl of the cultures were plated on TH agar plates with the appropriate selective antibiotic. The plates were incubated anaerobically overnight at 37°C. Potential transformants were verified using PCR-screening (section 3.2.1) and/or sequencing (section 3.5.1).

3.6.1 The Janus cassette

A common method for selection of bacterial transformants that do not provide a readily selectable phenotype, is the incorporation of a gene encoding antibiotic resistance as a reference marker, along with the intended gene change. An especially helpful tool is the use of bicistronic cassettes, such as the Janus cassette developed for *S. pneumoniae* (Sung 2001). The Janus cassette encodes both resistance to kanamycin (Kan^R) and a dominant sensitivity for streptomycin (Sm^S), enabling it to be used as a selective agent for both is acquisition and deletion (negative selection) in a streptomycin resistant background. The cassette was constructed based on a common recessive mutation in the *rpsL* gene in *S. pneumoniae*, which results in streptomycin resistance. The dominant *rpsL+* gene encoded on the Janus cassette overrides the recessive mutation, which causes loss of resistance (Sung et al., 2001).

The Janus cassette can be used for both gene knockouts and gene replacements. Gene knockouts are made by replacing the target gene with the Janus cassette. First, constructs are made of the Janus cassette with the flanking regions of the target gene. This enables the construct to be inserted over the target gene by homologous recombination. Gene replacement using Janus is a two-step process, in which the first step is the replacement of the target gene with the Janus cassette, and the second step is the replacement of the cassette with the intended gene. After the first step, successful transformants are Kan^R and can be selected on plates containing kanamycin. After the second step, the original resistance to streptomycin is restored (and the resistance to kanamycin lost), and transformants can be selected on plates containing streptomycin.

In this work, the Janus cassette was used to make a series of mutants. To make gene knockouts, overlap extension PCR (section 3.2.2) was used to make constructs of the Janus cassette with ~1000 bp flanking regions upstream and downstream of the target gene. The constructs were then used in transformation, as described in section 3.6, and the Janus cassette incorporated over the target genes. Transformants were selected on TH plates containing 400 μg/ml kanamycin. Correspondingly, gene replacements were made by making a construct of the replacement gene with flanking regions from the target gene, and used to replace the Janus cassette. Transformants were selected on TH plates containing 200 μg/ml streptomycin.

3.6.2 Selection on a gradient of penicillin G

In addition to negative selection using the Janus cassette, selection on a gradient of penicillin G was performed when selecting for transformants that had acquired genes conferring an increased resistance against penicillin. As presented in the introduction, resistance against β-lactams in *S. pneumoniae* is in large mediated by the presence of low-affinity versions of the Penicillin-Binding Proteins (PBPs). In this work, the low-affinity *pbp1a*, *pbp2b* and *pbp2x* from the highly resistant isolate *S. oralis* Uo5 were transferred to the sensitive laboratory strain *S. pneumoniae* R6. Amplicons of the Uo5 *pbps*, including the native Uo5 flanking regions (~1000 bp), were used to transform the streptomycin resistant *S. pneumoniae* R6 derivate RH425. TH plates with a 1.5x gradient of penicillin G, just above and below the minimal inhibitory concentration (MIC) of *S. pneumoniae* R6 was used to select for transformants which had acquired mosaic, low-affinity versions of the *pbps*. A negative control was included. In the cases where colonies grew on a higher concentration on the positive plates than the negative plates, as illustrated in Figure 3.2, the colonies were picked and the relevant *pbp* sequenced.

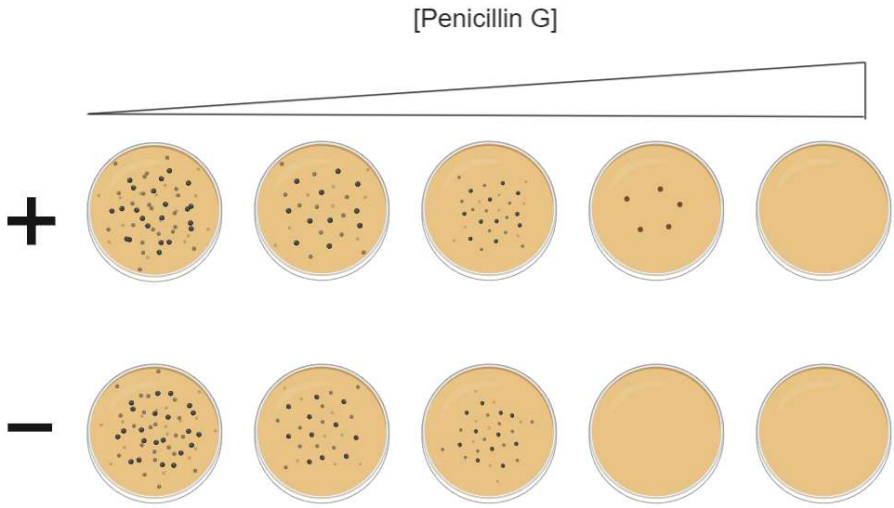

Figure 3.2 Selection on a gradient of penicillin G was used to select for transformants which had acquired low-affinity versions of the Penicillin-Binding Proteins. When colonies grew on a higher concentration of penicillin G on the positive plates, these colonies were picked and analysed for changes in the relevant *pbp*.

3.7 Phase contrast microscopy

Phase contrast microscopy was used to study potential morphological changes in some of the pneumococcal mutant strains, compared to the wild type *S. pneumoniae* R6. Additionally, the morphological effects of overexpressing the *murM* gene from *S. oralis* Uo5 in *S. pneumoniae* cells was examined under the microscope.

The following protocol was used: First, the cell cultures were grown to an OD_{550} = 0.3. If relevant, ComS* was added to the growth medium to induce gene expression from the P_{comX} promoter (section 3.11). For the mutant strains unable to reach this OD_{550}, the cells from 1 ml of culture at maximum OD_{550} were harvested by centrifugation (1 minute at 13 000 x *g*), and resuspended in 100 µl PBS. To fix the cells on the glass slide, a thin layer of a 1.2% agarose/PBS gel was cast on the slide and allowed to set. 0.5 µl of sample was applied on the slide, and then covered with a cover glass. The cells were viewed in a Zeiss LM700 microscope using a 100x phase contrast objective. Images were taken with an ORCA-Flash 4.0 V2 Digital CMOS camera (Hamamatsu Phonetics) connected to the microscope, using a 100x phase contrast objective.

3.8 Cell wall analysis

The fine structure of the peptidoglycan composition can differ between strains of the same species, as a result of environmental conditions or minor genetic differences. For example, the presence of branched muropeptides in *S. pneumoniae* is completely lost upon the deletion or inactivation of the *murMN* operon (Filipe et al., 2001). Differences in the level of branching

can also occur between pneumococcal strains harbouring the *murMN* operon, in large caused by differences in the *murM* sequence. It has been found that resistant pneumococcal isolates often have a higher degree of branched muropeptides in their cell wall than sensitive strains (Fiser et al., 2003).

In this work, reverse phase high performance liquid chromatography (RP-HPLC) was used to analyse the muropeptide composition of a selection of pneumococcal transformants. First, the cell wall was isolated from cells of the relevant cultures. Then, the cell walls were fragmented, and the stem peptides enzymatically cleaved from the glycan chains. The peptide composition was subsequently analysed by RP-HPLC.

3.8.1 Isolation of bacterial cell wall

The cell wall was isolated as previously described by Vollmer (2008), with some minor modifications: First, cells were collected from 0.5 litres of culture with an OD_{550} = 0.5 by centrifugation (5 minutes at 7000 x *g*), and the pellet resuspended in 40 ml cold 50 mM Tris-HCl buffer pH 7.4. To lyse the cells and break down membranes and proteins, the suspension was then drop-wise added to 120 ml boiling 5% SDS, with stirring. The suspension was boiled for 5-10 minutes, and then cooled to room temperature. To collect the cell walls, the solution was centrifuged for 10 minutes at 12 000 x *g*, at room temperature to avoid the precipitation of the SDS molecules. To remove residual SDS, the pellet was washed repeatedly; first twice with 20 ml 1 M NaCl, and then four times with 20 ml dH_2O, by successive resuspension and centrifugation steps (12 000 x *g*, 10 minutes, room temperature). The cell wall was then mechanically fragmented using acid washed glass beads in a FastPrep® 24 machine (MP BioMedicals): first, the pellet was resuspended in 2 ml dH_2O, and approximately 1 ml acid-washed glass beads (diameter of ≤106 µm, Sigma-Aldrich) was added. The sample was treated with 6 pulses of 20 seconds at maximum speed, with a 1-minute pause between each pulse. To remove the glass beads they were allowed to sediment, before the supernatant containing the fragmented cell wall was carefully transferred to a clean tube. Any remaining glass beads, whole cells, and unfragmented cell wall was removed by centrifugation at low speed: 2000 x *g* for 5 minutes. The supernatant containing the fragmented cell wall material was carefully transferred to a new tube, which was centrifuged for 15 minutes at 25 000 x *g* (room temperature) to collect the cell wall fragments. The pellet was resuspended in 2 ml 100 mM Tris-HCl buffer pH 7.4 with 20 mM $MgSO_4$, 50 µg/ml RNase and 10 µg/ml DNase. The RNase and DNase were added to break down any residual RNA and DNA present in the sample. The

suspension was then incubated 2 hours at 37°C, with shaking, before adding 100 µg/ml trypsin and 10 mM $CaCl_2$. Trypsin was added to hydrolyse any residual proteins in the solution. The solution was incubated overnight at 37°C, with shaking.

To inactivate the enzymes (RNase, DNase and trypsin), SDS was added to a final concentration of 1%, followed by 15 minutes incubation at 80°C. The volume was adjusted to 20 ml with dH_2O, before the cell walls were collected by centrifugation (30 minutes at 13 000 x *g*, room temperature). The pellet was resuspended in 10 ml 8 M LiCl and incubated 15 minutes at 37°C, before the sample was centrifuged (30 minutes at 13 000 x *g*, room temperature). Then, the pellet was resuspended in 10 ml 100 mM EDTA pH 7.4, before a new round of incubation (15 minutes at 37°C) and sedimentation by centrifugation (30 minutes at 13 000 x *g*, room temperature) followed. The pellet was then washed, first with 20 ml dH_2O, then 20 ml acetone, followed by a final wash with 20 ml dH_2O, by repeated resuspensions and centrifugations (30 minutes at 13 000 x *g*, room temperature). The final pellet, containing the purified cell walls, was resuspended in approximately 1 ml dH_2O. The purified cell walls were then vacuum dried, and the weight of the dry product determined, before dH_2O was added to give a final concentration of 25 mg/ml. The samples were stored at -80°C.

3.8.2 Analysis of the muropeptide composition using HPLC

High performance liquid chromatography (HPLC) is a method used to separate and analyse the different compounds present in a sample. The sample is dissolved in a solvent (mobile phase), which is pushed by high pressure through a column filled with a porous packing material (stationary phase) (Desmarais et al., 2013). Based on the strength of the interactions between the compounds in the mobile phase and the column packing material, the compounds flow through the column at different rates. The rate of which a specific compound elute from the column is known as retention time, and this is used to separate the compounds. Retention time can vary based on the composition and gradient of the buffers used to elute the compounds. In reverse phase HPLC, the stationary phase is non-polar and the mobile phase mildly polar, and the retention time of the compounds is based on the strength of hydrophobic interactions between the compounds in the mobile phase and the stationary phase. The compounds are detected by UV-light as they elute from the column. A chromatogram showing the UV absorbance as a function of time is produced, where each peak of the chromatogram represents one specific compound, as illustrated for muropeptide composition of *S. pneumoniae* R6 in

Figure 3.3. The magnitude of the peak is proportional to the quantity of the given compound (Desmarais et al., 2013).

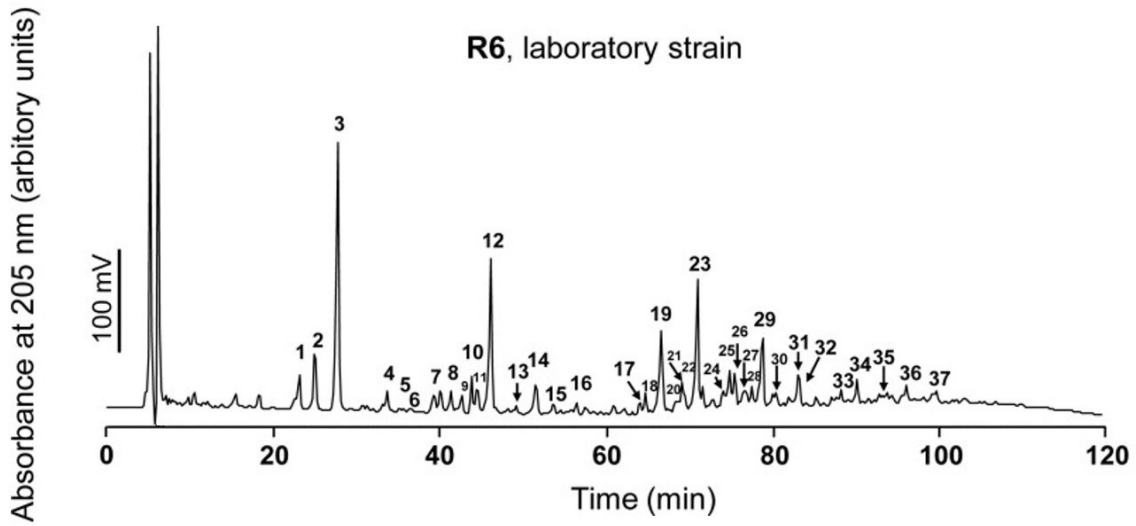

Figure 3.3 Chromatogram of the peptide composition from *S. pneumoniae* R6, acquired by reverse phase HPLC. The chromatogram shows the UV absorbance at 205 nm as a function of time. The different muropeptides (such as tri-, tetra-, and pentapeptides, monomers, dimers, trimers, branched etc) have different retention times and will elute from the column at different time points. Modified figure from (Vollmer, 2008).

In this study, reverse phase HPLC was used to determine the composition of peptidoglycan stem peptides of a selection of *S. pneumoniae* transformants that had acquired one or more mosaic low-affinity PBPs, and a Δ*murMN* mutant.

To prepare for the HPLC analysis, the stem peptides were cleaved from the glycan chains. The purified cell walls (section 3.8.1) were treated with the pneumococcal autolysin LytA amidase, which cleaves the lactyl-amide bond between MurNAc and the first amino acid of the stem peptide (Mellroth et al., 2012). Between 0.4 - 0.5 mg of cell wall was treated with 2.5 µg LytA in 100 µl 20 mM Na-phosphate buffer pH 7.0. The solution was incubated at 37°C overnight, with shaking. Then, to remove residual LytA, the solution was incubated 20 minutes at 95°C, which denatures and precipitates the enzyme. This was followed by centrifugation (20 000 x *g* for 20 minutes) to remove any undigested cell wall material. The supernatant was collected, and adjusted with 20% phosphoric acid to a pH = 2-3. The cell wall digest was stored at -20°C.

The isolated stem peptides were separated by HPLC using a reverse phase C_{18} column (Vydac 218TP C_{18} 5 µm, Grace Davison Discovery Sciences), on a HPLC system (Gibson). The column was equilibrated with a 0.05% trifluoracetic acid (TFA) buffer (buffer A). Between 40-100 µl

25 mg/ml cell wall digest was injected into the C_{18} column, and the peptides eluted by a linear gradient of 0-15% acetonitrile; starting with buffer A (0.05% TFA), through an increasing amount of buffer B (15% acetonitrile in 0.035% TFA). The flow rate was kept at 500 µl per minute for 120 minutes, and the peptides were detected (at 206 nm) as they exited the column.

3.9 Antibiotic sensitivity analysis using E-test® strips

The resistance level of the transformants obtained in this work were analysed by determining the minimal inhibitory concentration (MIC) of penicillin G (benzylpenicillin), oxacillin, ceftazidime and piperacillin, using E-test® strips.

The cultures were grown to an $OD_{550} \approx 0.3$, before 100 µl of the culture was mixed into 5 ml TH soft agar (which held 47°C). This overlay was poured over TH plates, and after the soft agar had cooled, the E-test® strips with a gradient of the appropriate antibiotic was placed on the surface. The plates were incubated overnight, anaerobically at 37°C. The MIC (in µg/ml) was determined the following day, by reading the concentration from the E-test® strip scale where the inhibition zone ended.

3.10 Visualization of PBPs with Bocillin FL

Bocillin FL is a fluorescent Penicillin V derivate that can be used to visualize and study PBPs (Zhao et al., 1999). Bocillin FL binds covalently to the penicillin-binding domain of the PBPs. The Bocillin-labelled PBPs can be separated using SDS-PAGE, and subsequently observed under UV light. In this work, Bocillin FL was used to determine the relative affinity for penicillin of the mosaic PBPs in one of the pneumococcal transformants expressing mosaic PBPs, compared to the wild type *S. pneumoniae* R6.

The relevant cultures were grown to an $OD_{550} = 0.21$, before the cells were harvested by centrifugation (10 minutes at 4000 x *g*). To lyse the cells, the pellet was resuspended in 100 µl 20 mM sodium phosphate buffer (pH 7.2) with 0.2% Triton X-100, and incubated 5 minutes at 37°C. The lysate was stored at -80°C. To label the PBPs, 15 µl of each sample was mixed with a 2-fold dilution series of Bocillin FL, from 2.5 µM to 0.16 µM, and incubated for 30 minutes at 37°C. After labelling, the proteins were separated by SDS-PAGE (section 3.3.3), and the proteins visualized using an Azure Imager c400.

3.11 Overexpression of genes using the ComRS system

As described in section 1.2.1, competence for genetic transformation in *S. pneumoniae* is regulated by the ComCDE system. While ComX and the core competence genes regulated by ComX are present in the genomes of all streptococci known to be naturally transformable, there exists different systems for competence regulation within the genus (Berg et al., 2011). In *Streptococcus thermophilus* of the salivarius phylogenetic group, competence is regulated by the ComRS system (Fontaine et al., 2010). The main components of the ComRS system include the inducer peptide ComS, which activates the transcriptional regulator ComR, which again actives expression from the ComX promoter P_{comX}. In 2011, Berg *et al.* introduced components of the ComRS system in *S. pneumoniae* R6, as a tool to study essential genes. Because the deletion of essential genes is lethal, the study of these genes is especially challenging. A common approach is to control the expression of essential genes ectopically, behind a titratable promoter. This makes it possible to delete the native gene and then, by manipulating the concentration of the synthetic inducer peptide ComS*, the expression of the ectopic gene can be either depleted or overexpressed. The effects of gene depletion, or overexpression, can provide valuable information about the function of a gene (Berg et al., 2011). *comR* and P_{comX} from *S. thermophilus* were placed within neutral locations in the pneumococcal genome. None of the components in the ComRS system have any close homologues in pneumococci. Thus, Berg *et al.* (2011) were able to utilize the ComRS system for genetic studies in pneumococci, without causing any unintended effects on other cellular functions.

In this work, the ComRS system was used to ectopically express the essential genes *pbp2b* and *pbp2x* during *pbp* transformation experiments. The inducer peptide ComS* was added to a final concentration of 0.2 or 2 μM, both in the liquid growth medium and on the plates. Furthermore, the ComRS system was used to study the cellular effect of overexpressing the *S. oralis* Uo5 *murM* gene ($murM_{Uo5}$) in a *S. pneumoniae* R6 background. The effects of overexpressing $murM_{Uo5}$ on cellular growth was analysed using a growth assay, and the effects on morphology was studied under the microscope, as described in section 3.12 and 3.7, respectively.

3.12 Growth assay

Growth assays were conducted to study the effects of a given mutation on growth and viability, and to determine the growth effects of cells overexpressing the *murM* gene from *S. oralis* Uo5 in different *S. pneumoniae* backgrounds. This was achieved by monitoring the growth from

early exponential phase (OD_{550} = 0.05-0.1) until stationary phase, by automatic detection of optical density in a Synergy H1 Hybrid Reader (BioTek®).

The relevant cultures were grown to an OD_{550} = 0.05-1, before 300 µl aliquots were added to the wells in a 96 well microtest plate. In cultures overexpressing *murM*, the inducer peptide ComS* was added to the growth medium in a final concentration of between 0.05 to 2 µM. The plate was incubated in the Synergy H1 microplate reader at 37°C, in which the growth was monitored for 18-20 hours by the automatic detection of the OD_{550} every 5-10 minutes. *S. pneumoniae* R6 (RH425) was used as the wild type control for normal growth.

3.13 Temperature sensitivity analysis

A temperature sensitivity analysis was conducted on one of the pneumococcal mutants that displayed an uncharacteristic sensitivity to the soft-agar overlay assay used during MIC determination (section 3.9). To determine whether this phenotype was a result of increased temperature sensitivity, as the overlay agar held a temperature of 47°C, a temperature sensitivity analysis was performed.

The temperature sensitivity analysis was conducted by monitoring cellular growth under different temperature conditions. The relevant cultures were grown to an OD_{550} = 0.05, before each culture was split into four tubes. These were incubated under different temperatures on heating blocks: 37°C, 40°C, 43°C, and 46°C. The OD_{550} was manually monitored every 20 minutes for approximately 3 hours, until the cultures reached stationary phase. To test the survivability of the cells under the different temperature conditions, a sample was taken from each tube after 60 minutes of growth. A 10-fold dilution series ranging from 10^{-1} to 10^{-5} was made from each sample, before 3 µl from every dilution was spotted on a TH agar plate, as illustrated in Figure 3.4. The plates were incubated anaerobically overnight at 37°C, before the number of colonies in each spot analysed.

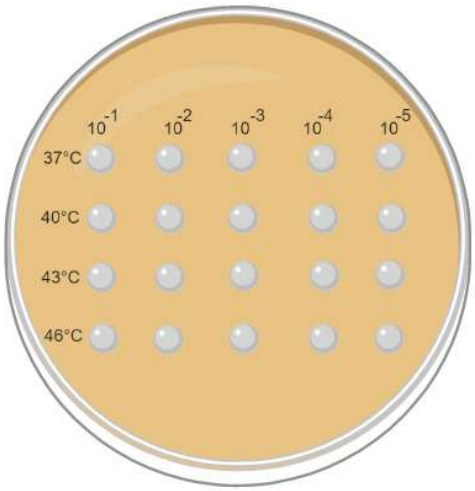

Figure 3.4 Temperature sensitivity analysis. Each culture was incubated at four different temperatures: 37°C, 40°C, 43°C and 46°C. After 60 minutes, a sample was taken from each temperature, and a 10-fold dilution series was made, from 10^{-1} to 10^{-5}. 3 µl from each dilution was subsequently spotted on a TH-agar plate, in the manner illustrated here. After overnight incubation, the number of colonies in each spot was analysed.

4 Results

4.1 Transferring low-affinity PBPs from *S. oralis* Uo5 to *S. pneumoniae* R6

Resistance to penicillin in *S. pneumoniae* is caused by the expression of mutated PBPs that have lowered affinity for these antibiotics. In addition, the activity of an altered MurM version (involved in branching of stem peptides in the cell wall) is important for resistance. Deletion of *murM* often results in a dramatic drop in resistance (Filipe et al., 2001). Curiously, attempts to transfer such altered MurM versions into sensitive *S. pneumoniae* strains have proved to be lethal to the cells. Why these MurM versions are not tolerated is not clear, but it has been speculated that they are only tolerated if the cells also have a set of low-affinity PBPs, which might have higher preference for branched stem peptides. In this work, we wanted to explore this hypothesis by looking at the functional relationship between low-affinity PBPs and their associated MurM version using a penicillin sensitive strain as a host. The idea was that the penicillin sensitive *S. pneumoniae* R6 strain would accept the altered MurM from the highly penicillin resistant isolate *S. oralis* Uo5 if also the associated low-affinity PBPs were transferred. *S. oralis* Uo5 expresses three low-affinity PBPs ($PBP2x_{Uo5}/1a_{Uo5}/2b_{Uo5}$) and a MurM protein, which is highly divergent from $MurM_{R6}$ (50% identity and 72% similarity) (Todorova et al., 2015). To test this, we first needed to transfer the low-affinity PBPs into the penicillin sensitive *S. pneumoniae* R6 strain. Since it is not completely clear whether several low-affinity PBPs can be transferred simultaneously in one transformation event, or if they must be acquired successively in a specific order, two different approaches were used to transfer low-affinity PBPs from *S. oralis* Uo5 to *S. pneumoniae* R6. The first approach involved replacing the given PBP_{R6} with PBP_{Uo5} in the native locus, through gene replacements via the Janus cassette. The second approach involved amplifying the PBP genes from Uo5, and using one or more PCR products to transform *S. pneumoniae* R6 and selecting for transformants using a gradient of penicillin G. The resulting mutants could also be used as a tool to understand which low-affinity PBP variants that contribute to resistance to different types of β-lactams.

4.1.1 *pbp* replacements using the Janus cassette

Gene replacements via the Janus cassette were used to transfer whole *S. oralis* Uo5 *pbp* genes (pbp_{Uo5}), or specific parts of the genes, into the native position in *S. pneumoniae* R6. Three different constructs combining Uo5 and R6 sequences were made for each of the three main resistance determining PBPs: PBP1a, PBP2b and PBP2x, using overlap extension PCR as described in section 3.2.2. Construct 1 included the whole *pbp* gene from Uo5, combined with

pbp-flanking regions from R6. The ~1000 bp flanking regions were included to ensure the presence of the homologous sections required for the integration of the DNA through homologous recombination. The cytoplasmic and transmembrane regions of PBP2b and PBP2x have been identified to be of importance for molecular interactions, and cannot readily be replaced in a wild-type background (Berg et al., 2014). Construct 2 was therefore designed to include the transmembrane encoding region as well as the flanking regions from R6, with the remaining part of the *pbp* gene from Uo5. Construct 3 was designed to only include the transpeptidase domain encoding sequence from Uo5, while the remaining part of the gene and flanking regions were from R6. An overview of the construct design is illustrated in Figure 4.1. The precise sequence blocks included from each species differ between each *pbp*.

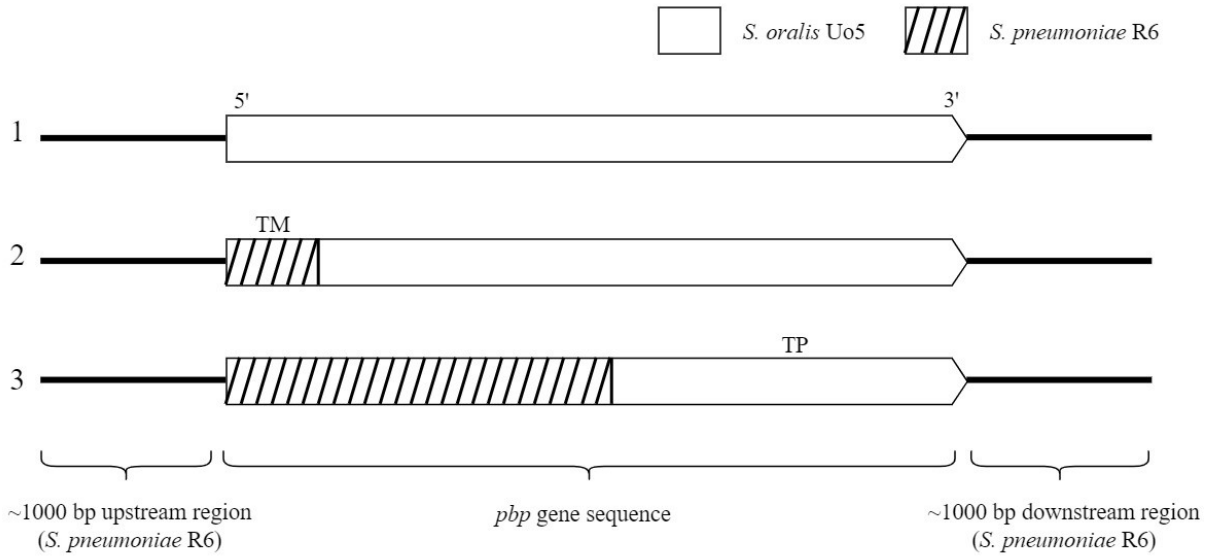

Figure 4.1 Overview of the *pbp* gene construct designs used for the transformation of low-affinity PBPs from the highly β-lactam-resistant *S. oralis* Uo5 to the sensitive *S. pneumoniae* R6. Black lines = flanking regions, white blocks = *pbp* gene sequence. Blank = sequence from Uo5, hatched = R6 sequence. Each construct was made for the three *pbps pbp1a*, *pbp2b* and *pbp2x*. TM = transmembrane encoding sequence, TP = transpeptidase encoding region.

The constructs were used to transform *S. pneumoniae* strains R6 in which the native *pbp* gene had been replaced by the Janus cassette. Transformations were executed as described in section 3.6. The *pbp1a* constructs were transformed into strain DS665 (Δ*pbp1a*::*janus*), while the *pbp2b* and *pbp2x* constructs were used to transform KHB88 (Δ*pbp2b*::janus) and KHB55 (Δ*pbp2x*::janus), respectively. In the case of *pbp2b* and *pbp2x*, which are both essential, the native genes were ectopically expressed from the inducible P_{comX} promoter (section 3.11) throughout the experiments, by adding the inducer peptide ComS to the growth medium to a final concentration of 0.2 – 2 µM.

None of the transformations were successful. In most cases, zero colonies were obtained on the selective plates. In the few cases where colonies grew on the positive plates, they were present in approximately equal numbers on the negative control plates as well, and PCR-screening (section 3.2.1) showed that none of the colonies were correct. These colonies were thus most likely false positives resulting from spontaneous regeneration of streptomycin resistance, which is known to occur with the Janus system (Sung et al., 2001). Parallel control transformations were conducted to confirm that the negative results were not caused by faulty experimental conditions.

4.1.2 Selection for transformants using a gradient of penicillin G

As the *pbp* gene replacements using the Janus cassette did not yield any viable transformants, a second approach was conducted. The successful integration of pbp_{Uo5} sequences in *S. pneumoniae* R6 has been achieved by using Uo5 gDNA and PCR-fragments as transformative DNA, and selecting for transformants on plates containing either cefotaxime, piperacillin or oxacillin (Todorova et al., 2015). Therefore, we chose to use PCR fragments of the Uo5 *pbps* to transform *S. pneumoniae* R6, and select for transformants on plates having increasing concentrations of penicillin G.

Amplicons containing the Uo5 *pbps*, including the native Uo5 flanking regions (~1000 bp) were used to transform RH425, a streptomycin resistant derivate of *S. pneumoniae* R6. TH agar plates with a 1.5x gradient of penicillin G covering just above and below the minimal inhibitory concentration (MIC) of R6 was used to select for transformants that had acquired low-affinity versions of the PBPs. As it was not possible to accurately predict which part of the *pbp* genes that would be changed, it was difficult to design potential PCR screening primers. Therefore, transformants growing on higher concentrations of penicillin G compared to the wild-type were identified by sequencing the relevant *pbp.*

In the first step, $pbp2x_{Uo5}$ was used to transform RH425. It resulted in growth of more than 45 colonies on plates having 1.5x more penicillin G than the plate where the wild-type was completely inhibited. Sequencing of five colonies from this plate revealed that four of them had acquired different mosaic PBP2x variants ($PBP2x_{mos}$) constituting different parts of the R6 and Uo5 PBP2x (Figure 4.2). As Figure 4.2 shows, the Uo5 fragments covered the three catalytic motifs of *pbp2x*.

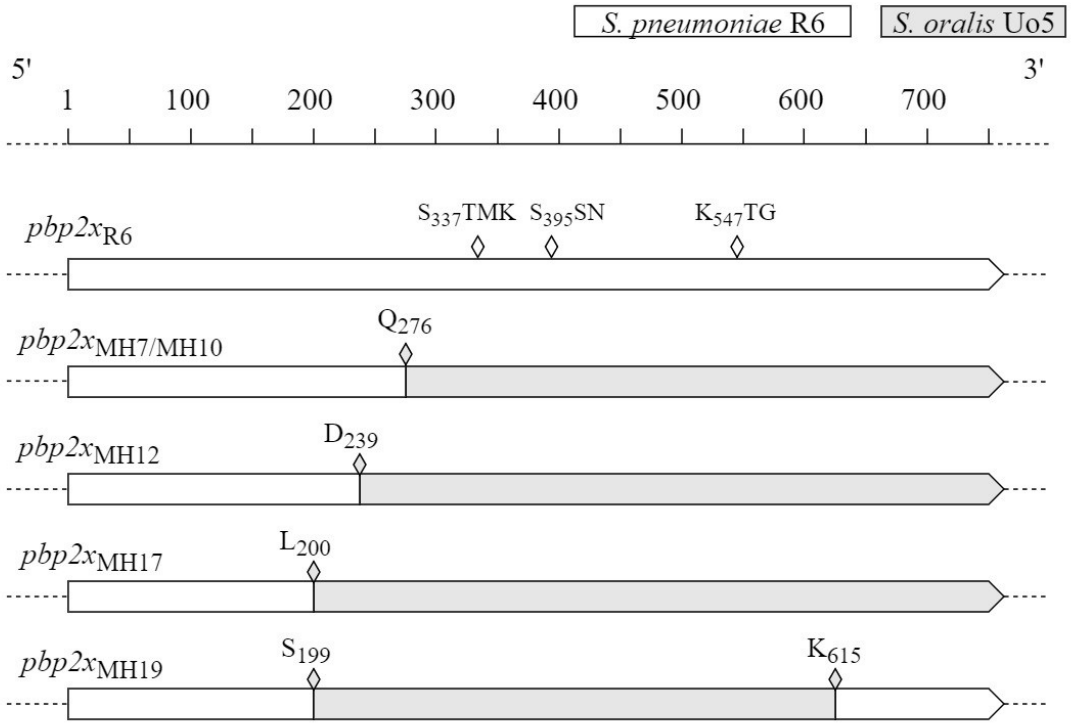

Figure 4.2 The four mosaic *pbp2x* sequences (5'-3') obtained through transformation of *S. pneumoniae* R6 with $pbp2x_{Uo5}$. The three catalytic motifs in *S. pneumoniae* R6 are marked with white diamonds. The Uo5 fragments are marked in grey, and the first and last Uo5 residues are marked with grey diamonds.

The same procedure was repeated for both $pbp1a_{Uo5}$ and $pbp2b_{Uo5}$, but even after 72 hours, no apparent differences between the positive and negative plates could be observed. In a subsequent transformation, all three Uo5 *pbps* were used to transform RH425 simultaneously. Notably, in all the transformants that were sequenced, mosaic structures were only found in *pbp2x*, while no changes were observed in either *pbp1a* or *pbp2b*.

Next, $pbp1a_{Uo5}$ and $pbp2b_{Uo5}$ were separately used to transform the $pbp2x_{mos}$ strain MH10. Transformants containing a mosaic *pbp1a* in strain MH10 (expressing $pbp2x_{mos}$) were readily obtained (Figure 4.3), while transformants having a mosaic *pbp2b* proved more difficult to acquire. However, after repeated attempts, three clones were obtained, harbouring three distinct mosaic *pbp2b* sequences in the MH10 strain (Figure 4.4).

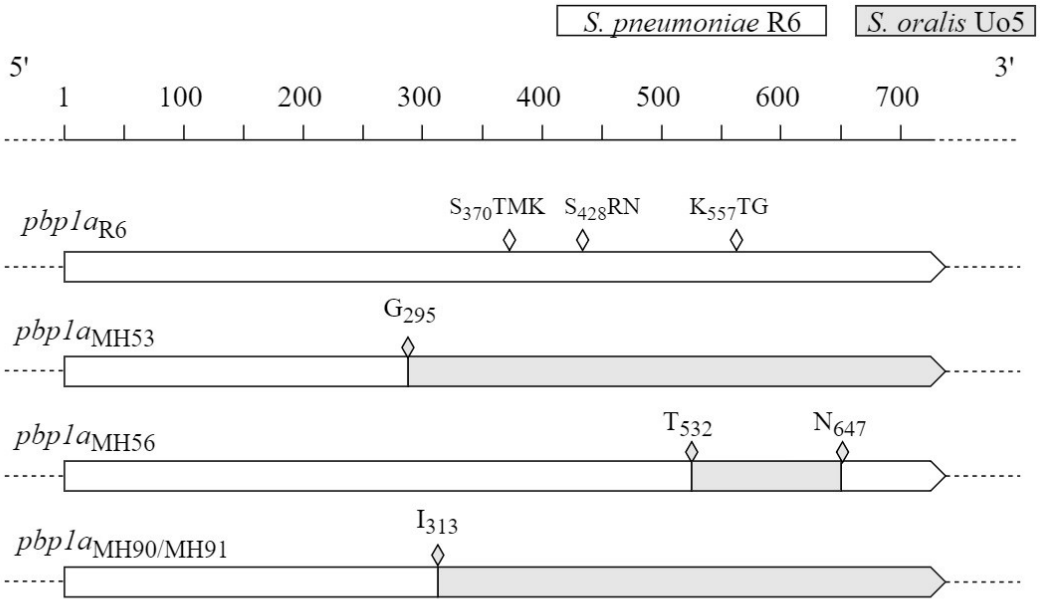

Figure 4.3 The three mosaic *pbp1a* sequences (5'-3') obtained through transformation of MH10 ($pbp2x_{mos}$) with $pbp1a_{Uo5}$. The three catalytic motifs in *S. pneumoniae* R6 are marked with white diamonds. The Uo5 fragments are marked in grey, and the first and last Uo5 residues are marked with grey diamonds.

In the third and final step, $pbp2b_{Uo5}$ was used to transform the $pbp1a_{mos}$,$pbp2x_{mos}$ double mutant MH56, generating clones with three mosaic PBPs. Only three transformants were obtained, and sequencing identified three different mosaic *pbp2b* versions (Figure 4.4).

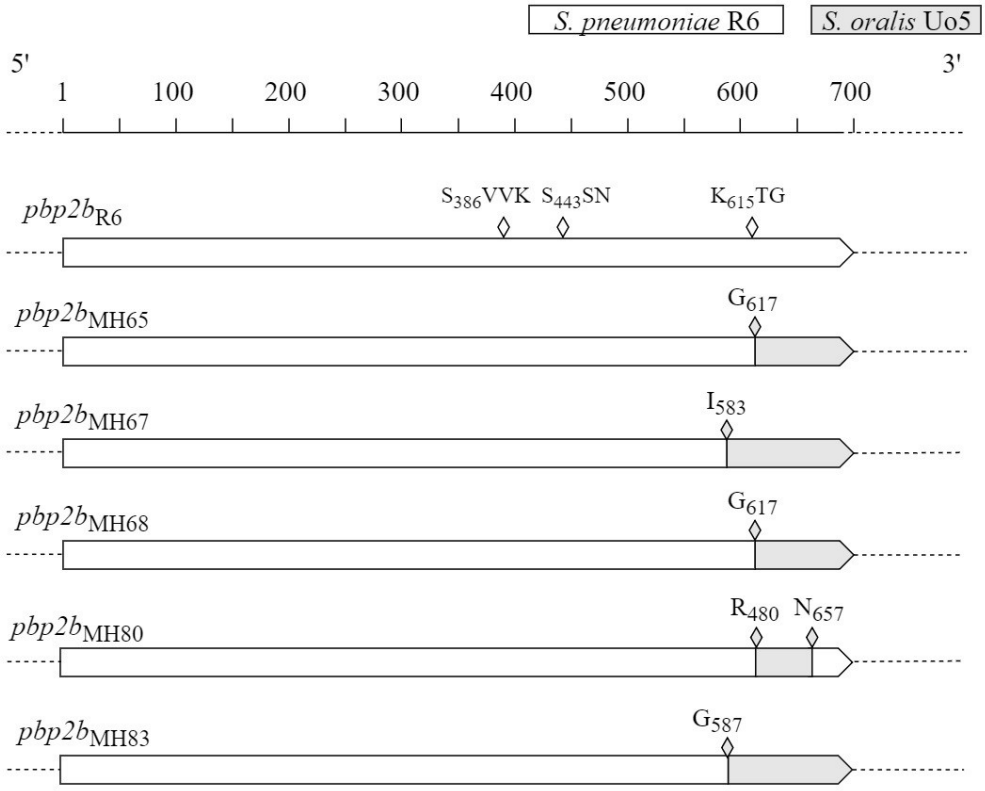

Figure 4.4 The different mosaic *pbp2b* sequences (5'-3') obtained through transformation of MH10 ($pbp2x_{mos}$) and MH56 ($pbp2x_{mos}$/$pbp1a_{mos}$) with $pbp2b_{Uo5}$. The three catalytic motifs in *S. pneumoniae* R6 are marked with white diamonds. The Uo5 fragments are marked in grey, and the first and last Uo5 residues are marked with grey diamonds.

Interestingly, sequences from Uo5 *pbp* genes that have recombined with the R6 genes did not involve the parts encoding the cytoplasmic or transmembrane regions for any of the sequenced mosaic PBPs. A flow-scheme illustrating the construction pathway of the PBP_{mos} clones made in this work is illustrated in Figure 4.5.

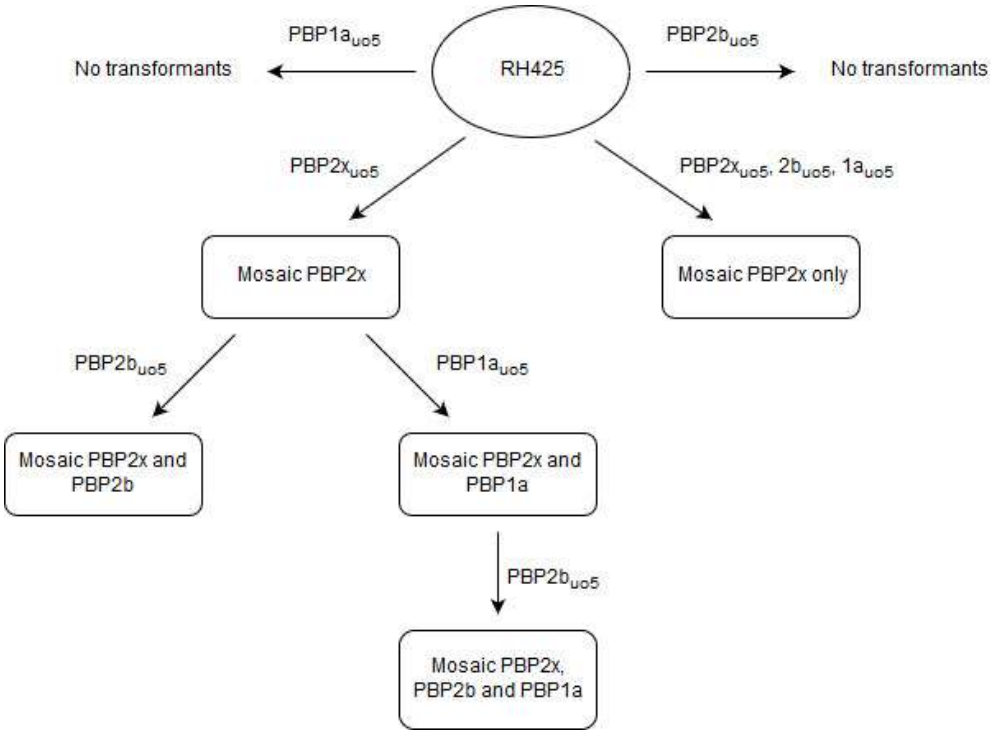

Figure 4.5 The construction of *S. pneumoniae* expressing different mosaic versions of PBP2x, PBP1a and PBP2b. In separate transformations, PBP1a$_{Uo5}$, PBP2b$_{Uo5}$ and PBP2*x*$_{Uo5}$ were transformed into RH425, a derivate of *S. pneumoniae* R6, and transformants were selected on a gradient of penicillin G. Only mosaic PBP2x clones were obtained. A subsequent transformation including all three PBPs simultaneously only gave clones harbouring mosaic *pbp2x* sequences. Second, PBP1a$_{Uo5}$ and PBP2b$_{Uo5}$ were transformed into a PBP2x$_{mos}$ clone (MH10). Third, PBP2b$_{Uo5}$ was transformed into a PBP1a$_{mos}$,PBP2x$_{mos}$ strain (MH56), providing clones expressing three mosaic, low-affinity PBPs.

4.2 Characterization of pneumococcal strains expressing mosaic PBPs

It has previously been shown that introduction of low-affinity PBPs into sensitive pneumococcal strains gives them higher resistance to penicillin (Todorova et al., 2015). To confirm that this also was the case for the pneumococcal strains with mosaic PBPs generated in this work, their minimal inhibitory concentration (MIC) values to different β-lactams were determined, and compared to that of the R6 parental strain, RH425, and of the PBP donor strain, *S. oralis* Uo5. The purpose of this experiments was also to determine how different combinations of low-affinity PBPs influence the resistance to various β-lactams, and to use the strains as a tool to study the role of MurM in resistance.

The strains were also examined for changes in cellular growth and morphology. Furthermore, as a higher level of β-lactam resistance in clinical pneumococcal isolates are associated with a

higher level of branching, the muropeptide composition was analysed for a selection of the strains.

4.2.1 Minimal inhibitory concentration of PBP_{mos} mutants

The minimal inhibitory concentrations (MIC) of the β-lactams penicillin G, oxacillin, piperacillin and ceftazidime were determined for a selection of the PBP_{mos} mutants (Table 4.1), using E-test® strips (section 3.9). Between three and four transformants from each mosaic PBP background were tested, including MH7, MH10 and MH19 ($PBP2x_{mos}$), MH53, MH56, MH90 and MH91 ($PBP2x_{mos}$ and $PBP1a_{mos}$), MH65, MH67 and MH68 ($PBP2x_{mos}$ and $PBP2b_{mos}$) and MH78, MH80 and MH83 ($PBP2x_{mos}$, $PBP1a_{mos}$ and $PBP2b_{mos}$).

Table 4.1 Minimal inhibitory concentration (MIC) of penicillin G, oxacillin, piperacillin and ceftazidime for a selection of the transformants with mosaic *pbps*, given in µg/ml.

		Minimal inhibitory concentration (MIC) in µg/ml			
Strain	**Mosaic *pbp***	**Penicillin G**	**Oxacillin**	**Piperacillin**	**Ceftazidime**
***S. pneumoniae* R6**		0,004	0,016	0,016	0,064
***S. oralis* Uo5**		6	16	24	16
MH7	***pbp2x***	0,012	0,25	0,016	4
MH10		0,012	0,25	0,016	4
MH19		0,012	0,25	0,016	4
MH53	***pbp2x, pbp1a***	0,016	0,38	0,016	4
MH56		0,012	0,38	0,016	4
MH90		0,016	0,38	0,016	4
MH91		0,19	3	0,125	4
MH65	***pbp2x, pbp2b***	0,032	1	0,19	4
MH67		0,012	0,38	0,19	4
MH68		0,032	1	0,19	4
MH78	***pbp2x, pbp1a* and *pbp2b***	0,094	2	0,5	4
MH80		0,125	3	0,5	3
MH83		0,094	2	0,25	4

For penicillin G, oxacillin and piperacillin, a slight but steady increase in MIC was observed with the acquisition of each additional mosaic PBP (Table 4.1). However, even in the mutants harbouring three mosaic PBPs, the MIC came nowhere close to that of the PBP donor strain *S. oralis* Uo5. Generally, the mutants with $pbp2x_{mos}$ and $pbp2b_{mos}$ achieved slightly higher MIC values compared to the mutants with $pbp2x_{mos}$ and $pbp1a_{mos}$.

The highest penicillin G MIC achieved by any of the strains were 0.19 µg/ml for MH91 and 0.125 µg/ml for MH80. While this represents an approximately 30-fold increase in resistance

compared to the parental strain RH425 (0.004 µg/ml), it is far below the 6.0 µg/ml MIC of *S. oralis* Uo5. The MIC values for piperacillin follows the same pattern: the highest level of piperacillin resistance was observed in MH78 and MH80 (*pbp2x*$_{mos}$,*1a*$_{mos}$,*2b*$_{mos}$), which obtained MIC values ~30 times higher than RH425 (0.5 and 0.016 µg/ml, respectively). The piperacillin MIC value of *S. oralis* Uo5 is still approximately 50 times higher (24 µg/ml). For oxacillin, the MIC of MH80 is nearly 200 times higher than for RH425 (3.0 and 0.016 µg/ml, respectively), which is only ~5 times lower than that of *S. oralis* Uo5 (16 µg/ml). For ceftazidime, an over 60-fold increase in resistance was observed with the acquisition of a *pbp2x*$_{mos}$, but no additional increase in resistance was achieved with the subsequent addition of *pbp1a*$_{mos}$ and/or *pbp2b*$_{mos}$. Ceftazidime is a third-generation cephalosporin, and does not inhibit PBP2b (Hakenbeck et al., 1987). However, the lack of increased MIC values with the addition of the low-affinity PBP1a is noteworthy.

One strain stands out: MH91, which was obtained when introducing PBP1a$_{Uo5}$ into strain MH10 (PBP2x$_{mos}$). It displayed a significantly higher MIC value for both penicillin G, oxacillin and piperacillin than the other clones containing PBP2x$_{mos}$ and PBP1a$_{mos}$. This could potentially be the result of either the acquisition of different *pbp1a*$_{Uo5}$ sequences that confers a higher resistance level than those present in the other PBP2x$_{mos}$/1a$_{mos}$ double mutants, or from spontaneous mutations in the PBPs or other resistance-determining genes driven by the penicillin G selection pressure during transformation. As the *pbp2x*$_{mos}$ and *pbp1a*$_{mos}$ sequences were identical between the MH90 and MH91 strains, which had diverging MIC values, the latter explanation seemed more likely. To identify potential additional resistance-determining mutations, MH91 was subjected to whole-genome sequencing (see section 4.3). The genome sequencing revealed alterations in a few genes, including a T$_{446}$A substitution in the PBP2b protein sequence, most likely a spontaneous mutation caused by the penicillin selection pressure during the transformations. This substitution has been well-characterized, and is known to confer a reduced affinity for penicillins in PBP2b (Calvez et al., 2017, Pagliero et al., 2004).

4.2.2 Detection of PBPs in RH425 (wild-type) and MH83 (PBP2x$_{mos}$/1a$_{mos}$/2b$_{mos}$)

To confirm that the observed increase in resistance described above was a result of reduced β-lactam affinity of the new, mosaic PBPs, a Bocillin FL assay (section 3.10) was used. The assay was used to determine the relative β-lactam affinity of the mosaic PBPs in MH83 in comparison to the wild-type RH425 PBPs. The PBPs were labelled with a 2-fold dilution series (from 2.5

to 0.16 µM) of the fluorescent penicillin V derivate Bocillin FL, and subsequently separated by SDS-PAGE. The labelled PBPs were visualized in an Azure c400 imaging system (Figure 4.5).

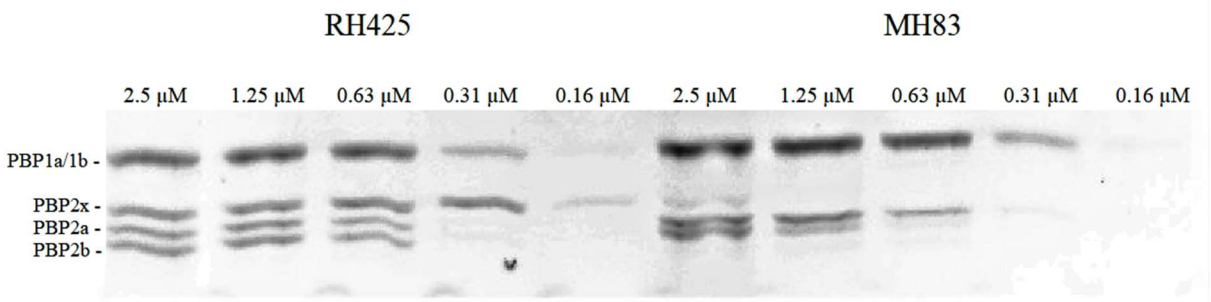

Figure 4.5 PBP profiles of RH425 and MH83. MH83 contains mosaic PBP2x, PBP1a and PBP2b. RH425 was used as the wild-type control for high-affinity PBPs. The PBPs were labelled with a 2-fold dilution series of Bocillin FL (from 2.5 to 0.16 µM indicated on top) and separated by SDS-PAGE.

PBP1a and PBP1b were not successfully separated, so a potential reduction in penicillin affinity of the mosaic PBP1a was not possible to verify based on this experiment. However, PBP2a, PBP2b and PBP2x separated well, and by comparing the band profiles between MH83 and RH425, a reduced penicillin affinity is evident in both $PBP2b_{MH83}$ and $PBP2x_{MH83}$. The PBP2a bands are, as expected, highly comparable between MH83 and RH425. The PBP2x and PBP2b bonds, however, deviate between the two isolates: while $PBP2b_{RH425}$ is detected as a strong band at 0.63 µM Bocillin FL, $PBP2b_{MH83}$ is almost undetectable at this concentration. The affinity of $PBP2x_{MH83}$ is significantly reduced: only a weak band is detected at the highest concentration of Bocillin FL (2.5 µM), in stark contrast to $PBP2x_{RH425}$, which is bound by Bocillin FL even at the lowest concentration (0.16 µM). These results confirm that at least the mosaic PBP2x and PBP2b in MH83 encode proteins with a reduced affinity for penicillin.

4.2.2 Expression of low-affinity PBPs does not inhibit growth, but results in abnormal cell morphologies in *S. pneumoniae* R6.

As the PBPs are instrumental enzymes in the cell wall synthesis machinery, any changes to the active site of the proteins might confer adverse effects on their enzymatic function, and thus potentially disturb normal cell division. As we have confirmed that the mosaic PBPs have an altered level of interaction with β-lactams (Figure 4.6), and that the sequence blocks acquired from *S. oralis* Uo5 in most of the cases overlapped the transpeptidase catalytic site motifs, we wanted to examine the isolates with low-affinity PBPs for potential effects on growth and morphology.

The growth curves of the mutants with altered PBPs (MH10 (low-affinity PBP2x), MH56 (low-affinity PBP2x and 1a), MH68 (low-affinity PBP2x and 2b), MH83 (low-affinity PBP2x, 1a and 2b) show that they had growth rates similar to the wild type and reached cell densities comparable to the wild type. The exception was strain MH91, which displayed a slight decrease in doubling time, and reached stationary phase at a lower OD_{550} compared to the other strains. The other strains with corresponding mosaic PBPs combinations (see Table 4.1) displayed growth similar to the strains in Figure 4.6 (data not shown).

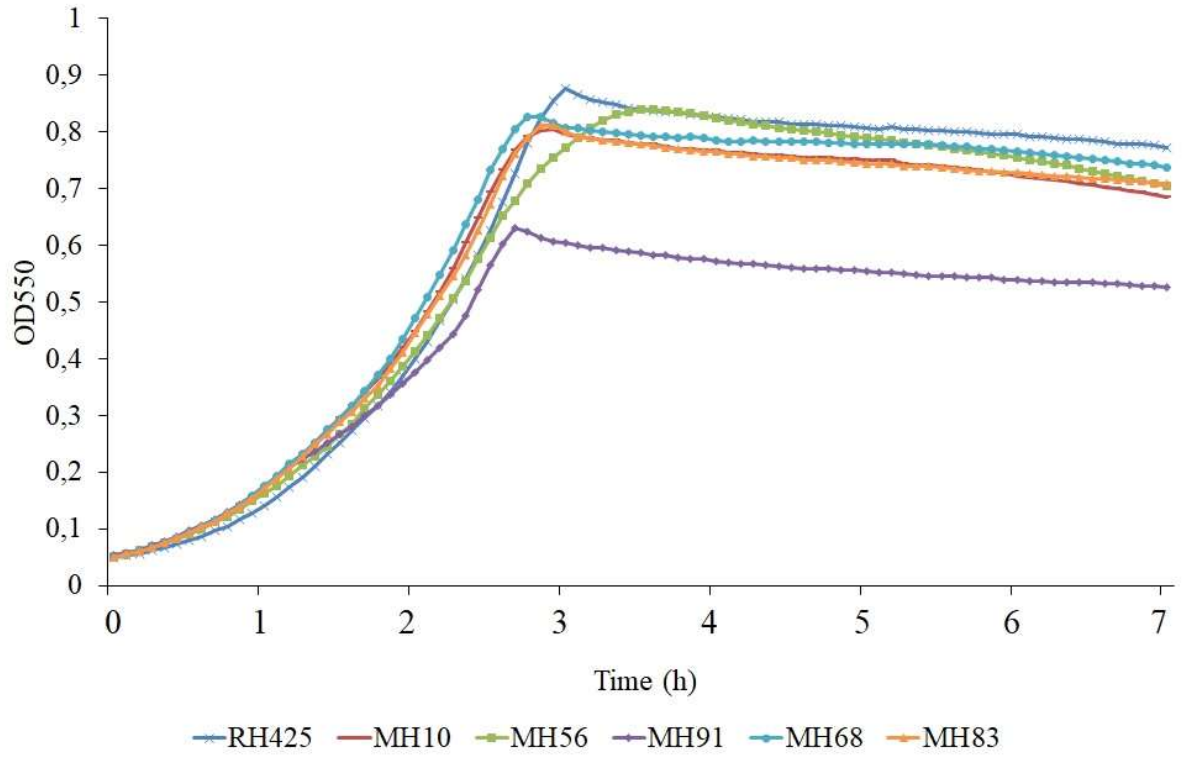

Figure 4.6. Growth of strains with low-affinity PBPs. The cultures were incubated at 37°C in C-medium, and growth was monitored from early exponential phase until stationary phase by automatic detection of the OD_{550} at 5-minute intervals. RH425 = wild-type *S. pneumoniae* R6. MH10 ($PBP2x_{mos}$), MH56 ($PBP2x_{mos}/1a_{mos}$), MH68 ($PBP2x_{mos}/2b_{mos}$), MH83 ($PBP2x_{mos}/1a_{mos}/2b_{mos}$) and MH91 ($PBP2x_{mos}/1a_{mos}$ and $PBP2b_{T446A}$). Similar results were obtained in repeated experiment.

The morphology of the isolates was examined using phase-contrast microscopy, as described in section 3.7 (Figure 4.7). *S. pneumoniae* has an ellipsoid shape, and generally grow in pairs or in short chains (Zapun et al., 2008b). Microscopic examination of the cells expressing different low-affinity PBPs (Figure 4.7) reveal that the morphology of the cells expressing a

low-affinity PBP2x (MH10) and both a low-affinity PBP2x and PBP1a (MH56) do not significantly deviate from the wild-type cells (Figure 4.7A-C). However, both the MH68 (low-affinity PBP2x and 2b) and MH91 (low-affinity PBP2x, 1a and 2b) (Figure 4.7D and E, respectively) cells grew in short chains, suggesting a disturbance in the cell division balance between elongation and septal division. This phenotype has previously been observed in pneumococcal cells in which the expression of PBP2b was depleted (Berg et al., 2013). The PBP2b-depleted cells also displayed a compressed, "lentil-like" morphology. While the cellular shape of MH68 appear normal at this resolution, the MH91 cells appear slightly more rounded. Thus, the abnormal morphology of the MH68 and MH91 cells might be a result of reduced activity of the low-affinity PBP2b. This would also explain the reduction in growth observed for MH91. As described above, genome sequencing revealed a point mutation in the MH91 *pbp2b* gene: a $T_{446}A$ substitution. Indeed, previous studies have identified a reduced catalytic activity of $PBP2b_{T446A}$ (Calvez et al., 2017). The morphology of the MH83 cells, which express low-affinity PBP2x, PBP1a and PBP2b, appear normal, indicating that the possible negative effects of expressing a low-affinity PBP2b is restored in a strain expressing all three low-affinity PBPs.

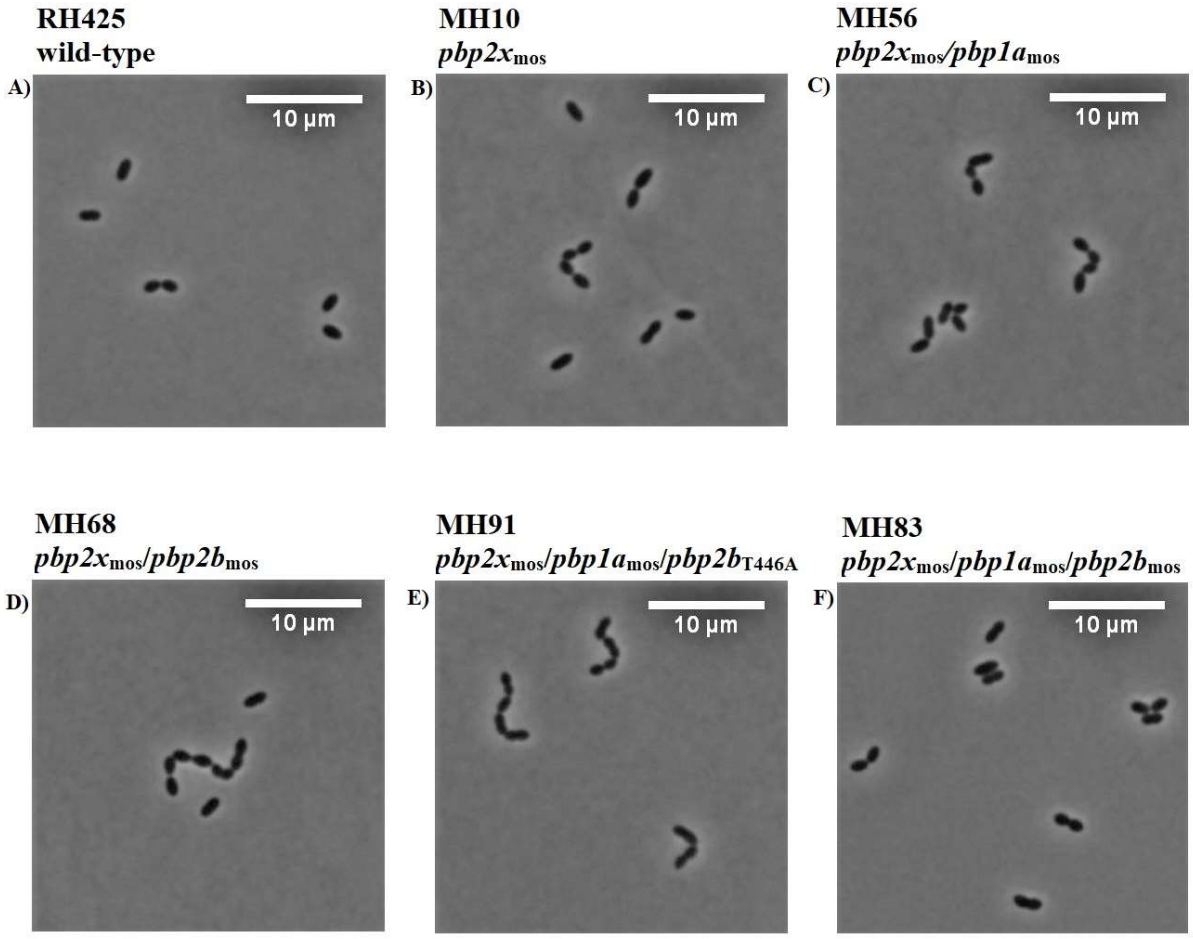

Figure 4.7 Phase contrast microscopy images of strains expressing low-affinity PBPs and the wild-type control. The *pbp* genotype is listed under the strain name. A) Wild-type S. pneumoniae R6. B) MH10 (low-affinity PBP2x). C) MH56 (low-affinity PBP2x and 1a). D) MH68 (low-affinity PBP2x and 2b). E) MH91 (low-affinity PBP2x, 2b and 1a). F) MH83 (low-affinity PBP2x, 2b and 1a). The images were analysed using Microbe J.

4.2.3 The low-affinity PBP2b is important for building a cell wall with higher content of branched stem peptides in *S. pneumoniae* R6.

Cell wall analyses of β-lactam resistant isolates of *S. pneumoniae* have, as discussed in section 1.6.3, revealed a higher level of branched stem peptides than in their sensitive relatives (Filipe and Tomasz, 2000). This is highly correlated with the presence of a mosaic *murM* gene, which, in addition to *murN*, encodes the proteins responsible for the synthesis of the interpeptide bridge of branched stem peptides. It has been hypothesized that branched peptides are better substrates for certain low-affinity PBPs due to alterations in the accessibility of the active site, and that this contributes to the increased level of branching in some resistant isolates (Zapun et al., 2008a). However, the large complexity of the protein complexes involved in cell wall biosynthesis, and how they are regulated makes this especially difficult to study. In the present work, we have created penicillin resistant strains by letting the pneumococci only have access

to the low-affinity *pbp* gene of interest during transformation. Except for possible suppressor mutations, we have full control of which low-affinity PBP that results in the resistance observed. We reasoned that these strains also might be used to determine which of the low-affinity PBP2x/1a/2b that are important for the increased branching of stem peptides in the peptidoglycan of resistant isolates. First, to rule out that any differences in stem peptide branching was a result from alterations in the *murM* gene, this gene was verified to be intact in all strains having mosaic PBPs. Then, the cell wall was isolated from strain MH56 (low-affinity PBP2x and 1a) and MH83 (low-affinity PBP2x, 1a and 2b), as described in section 3.8.1. Purified cell wall from the *S. pneumoniae* R6 strain RH1 (wild type) was used as control. The purified cell wall (0.5 mg) was treated with the amidase LytA to release the stem peptides from the peptidoglycan. LytA cleaves the amide bond between the lactyl group in MurNAc and the first amino acid (L-Ala) in the stem peptide (Mellroth et al., 2012). The stem peptides were subsequently separated using reverse-phase HPLC (using a linear gradient from 0 to 15% acetonitrile over 120 minutes), as described in section 3.8.2. The HPLC chromatograms for MH56, MH83 and RH1 are presented in Figure 4.8A, with the proposed structure of selected stem peptides in Figure 4.8B. These proposed structures are based on previous mass spectrometry analyses of pneumococcal muropeptide profiles isolated and analysed under comparable conditions (Berg et al., 2013).

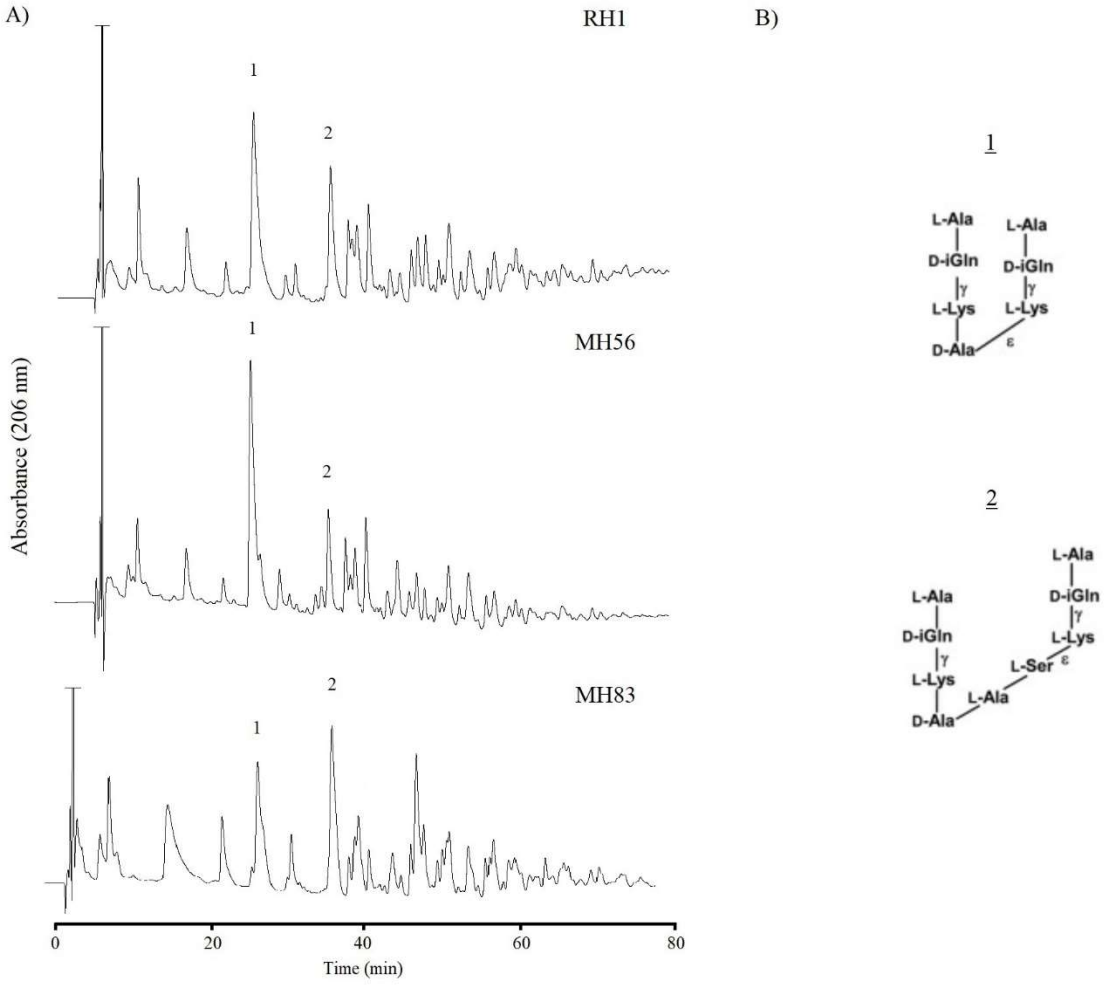

Figure 4.8 Stem peptide profile of pneumococcal strains with different mosaic PBPs. A) Reverse-phase HPLC chromatograms of the stem peptide profiles of RH1 (wild-type), MH56 (PBP2x$_{mos}$/1a$_{mos}$) and MH83 (PBP2x$_{mos}$/ 1a$_{mos}$/2b$_{mos}$). B) Proposed structures of peak 1 and 2, based on previously conduced mass spectrometry analysis by (Berg et al., 2013).

The HPLC analysis revealed that no significant difference could be observed between the stem peptide composition in the cell wall of the PBP2x$_{mos}$/1a$_{mos}$ double mutant MH56 and the wild-type R6. However, MH83, which also has the PBP2b$_{mos}$ was found to have a higher degree of branched stem peptides than both the wild-type and the MH56. While the ratio of linear vs. branched peptides (peak 1/peak 2) in RH1 was 1.78, this ratio was only 0.90 in MH83. This constitutes a significant shift in the stem peptide composition in MH83. This strongly indicates that the low-affinity PBP2b is the main determinant for incorporating branched stem peptides in the cell wall of penicillin resistant pneumococci. However, whether PBP2b requires a low-affinity PBP2x and PBP1a to do this cannot be excluded here. It would be desirable to examine the stem peptide composition in cell wall from a strain only expressing the low-affinity PBP2b. Unfortunately, construction of this strain was not successful in this work. Furthermore, since

the MH83 *murM* gene does not diverge from that of the parental strain, RH425, this strongly suggest that the increased level of branching in this strain did not results from the increased activity of MurM.

4.2.4 Will deletion of the native *murMN* genes affect penicillin resistance in *S. pneumoniae* R6 harbouring low-affinity PBPs?

The central role of branched muropeptides in β-lactam resistance in *S. pneumoniae* is evident from the loss of resistance observed upon the deletion of *murM* in clinical isolates (Filipe and Tomasz, 2000). To determine whether the same loss in resistance would occur in the R6 mutants with low-affinity PBPs selected under the laboratory conditions in this work, Δ*murMN* knockouts were constructed by replacing the *murMN* operon with the Janus cassette in a selection of the strains; MH10 (low-affinity PBP2x), MH56 (low-affinity PBP2x and 1a), MH68 (low-affinity PBP2x and 2b) and MH83 (low-affinity PBP2x, 1a and 2b). The transformants were subsequently examined for a potential reduction in MIC values. Even though the loss of branching is associated with a reduced antibiotic resistance, as well as increased sensitivity to certain cell wall inhibitors, such as fosfomycin, vancomycin and nisin (Filipe et al., 2002), the loss of *murMN* is generally not associated with adverse effects on growth under standard laboratory conditions (Zapun et al., 2008a). No significant differences in growth was observed between the Δ*murMN* mutants and their parental strains under standard growth conditions (data not shown).

4.2.4.1 Deletion of *murMN* increases sensitivity to penicillin in strains having low-affinity PBPs

The MIC values of the Δ*murMN* mutants were determined using E-test® strips, as described above. However, repeated attempts to determine the MIC of the MH83 Δ*murMN* mutant, MH108, failed, as the cells surprisingly did not survive the soft-agar overlay process used when determining the MIC values. Repeated attempts, including the use of an alternative overlay medium (BHI soft agar), increasing the volume of cells (from 100 µl cell culture (OD_{550} = 0.3) in 5 ml agar, to 300 µl in 5 ml agar), as well as lowering the temperature of the overlay agar (from 47°C to 45°C), still did not yield any viable cells in the plate. The MIC of MH108 was therefore determined using a simplified approach: the culture was grown to an OD_{550} = 0.1, before 100 µl were plated out on a plain TH agar plate. The relevant E-test® strip was placed on top of the agar, and the plates were incubated as normal. To provide a basis of comparison between MH108 and its parental strain MH83, as some deviations from the standard method might occur, the MIC of MH83 was also determined using this simplified approach. The

penicillin G and oxacillin MIC of the mosaic PBP clones and their Δ*murMN* derivates, are presented in Figure 4.9A and 4.9B. The strains in which the MIC values was determined using the simplified method are marked with an asterisk.

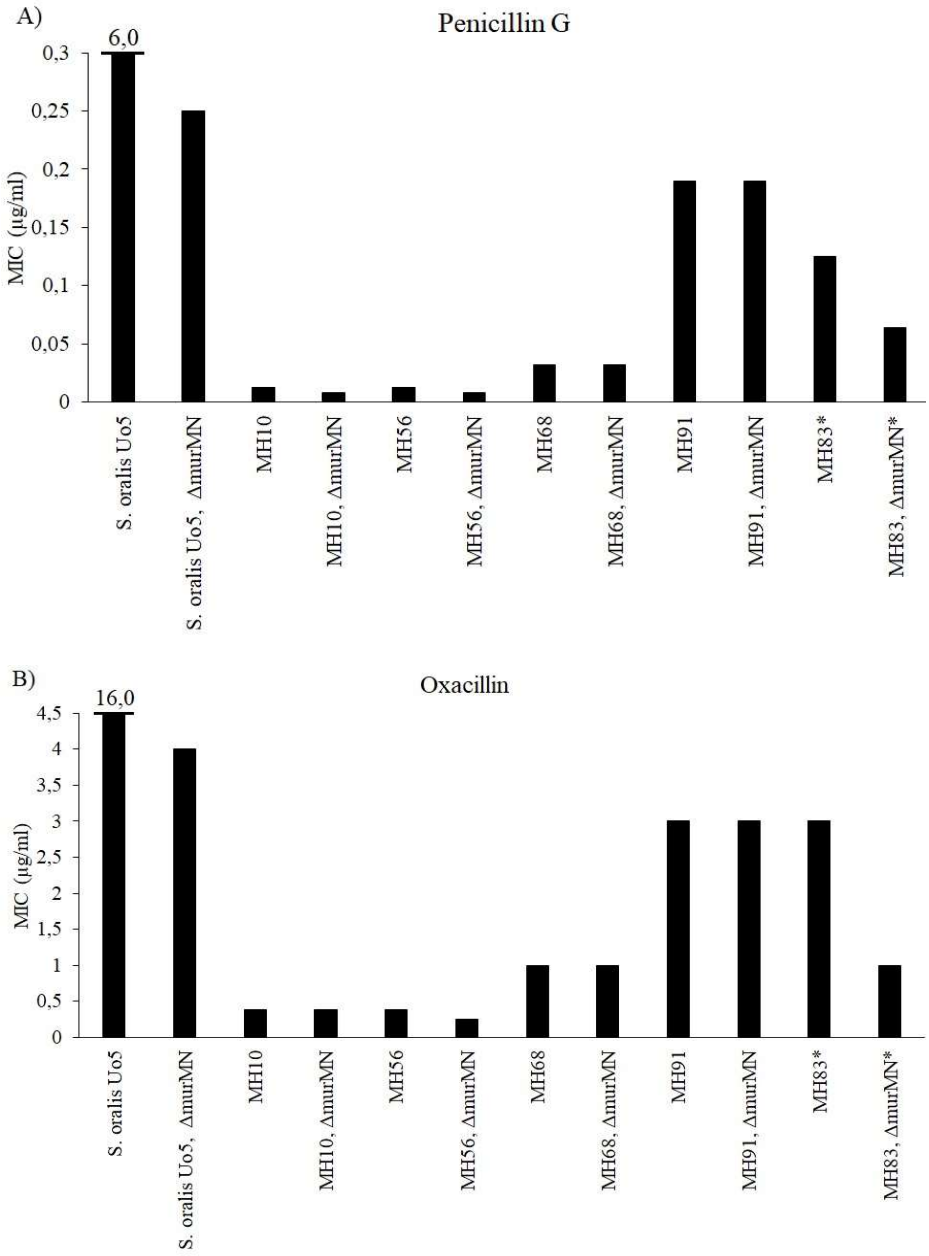

Figure 4.9 The minimal inhibitory concentration (MIC) of A) penicillin G and (B) oxacillin of strains with low-affinity PBPs and their Δ*murMN* derivates. MH10 (low-affinity PBP2x), MH56 (low-affinity PBP2x and 1a), MH68 (low-affinity PBP2x and 2b) and MH83 (low-affinity PBP2x, 1a and 2b). Additionally, the MIC of *S. oralis* Uo5 and its Δ*murM* derivate strain GS850 was determined. Note the higher MIC value of *S. oralis* Uo5 indicated at the top of the bar.

* MIC values were estimated using the simplified approach (described in the main text), and are therefore not entirely comparable with the MIC values of the other isolates.

Surprisingly, the loss of penicillin resistance upon deletion or inactivation of *murM* or *murMN* was not as evident for strain MH10, MH56, MH68 and MH83 as what has been observed for resistant clinical isolates of *S. pneumoniae*. Generally, no significant reduction of MIC was observed in any of the transformants, except for the MH83 Δ*murMN* isolate, MH108. For both penicillin G and oxacillin, the MIC decreased upon the deletion of *murMN*, from 0.125 to 0.064 µg/ml, and 3.0 to 1.0 µg/ml, respectively. This modest reduction still represents a far higher MIC than that of the RH425 parental strain, which is 0.004 µg/ml for penicillin G and 0.016 for oxacillin. Notably, the effect of *murMN* deletion was most dramatic in strain MH83, which displayed a high level of branched stem peptides in the cell wall.

4.2.4.2 Temperature sensitivity analysis of MH108

In addition to the loss of branched stem peptides and reduced β-lactam resistance, deletion of the *murMN* operon has been shown to result in hypersensitivity against a number of cell wall synthesis inhibitors, such as fosfomycin, nisin and vancomycin (Filipe et al., 2002). Because the deletion of *murMN* did not appear to have any impact on growth under standard laboratory conditions, in agreement with previous studies, it was surprising that MH108 was unable to grow in soft-agar overlay assays. Possibly, lack of *murMN* might be related to an increased sensitivity to cell wall stress, e.g. that a cell wall not containing branched stem peptides is weakened compared to a normal cell wall, giving it less strength to withstand the higher temperature used in soft-agar overlays. To determine whether MH108 did not survive the overlay procedure due to the high temperature of the overlay soft agar, which held 47°C, a temperature sensitivity analysis was conducted as described in section 3.13. In addition to MH108, its parental strain MH83 was included in the analysis. RH425 and its Δ*murMN* mutant strain MH110 were included as wild-type controls. Briefly, each culture was split into four glass tubes, which were incubated under different temperature conditions: 37°C, 40°C, 43°C and 46°C. The growth was monitored over approximately 3 hours, from early exponential phase until the cultures reached stationary phase. The growth curves for each temperature are presented in Figure 4.10.

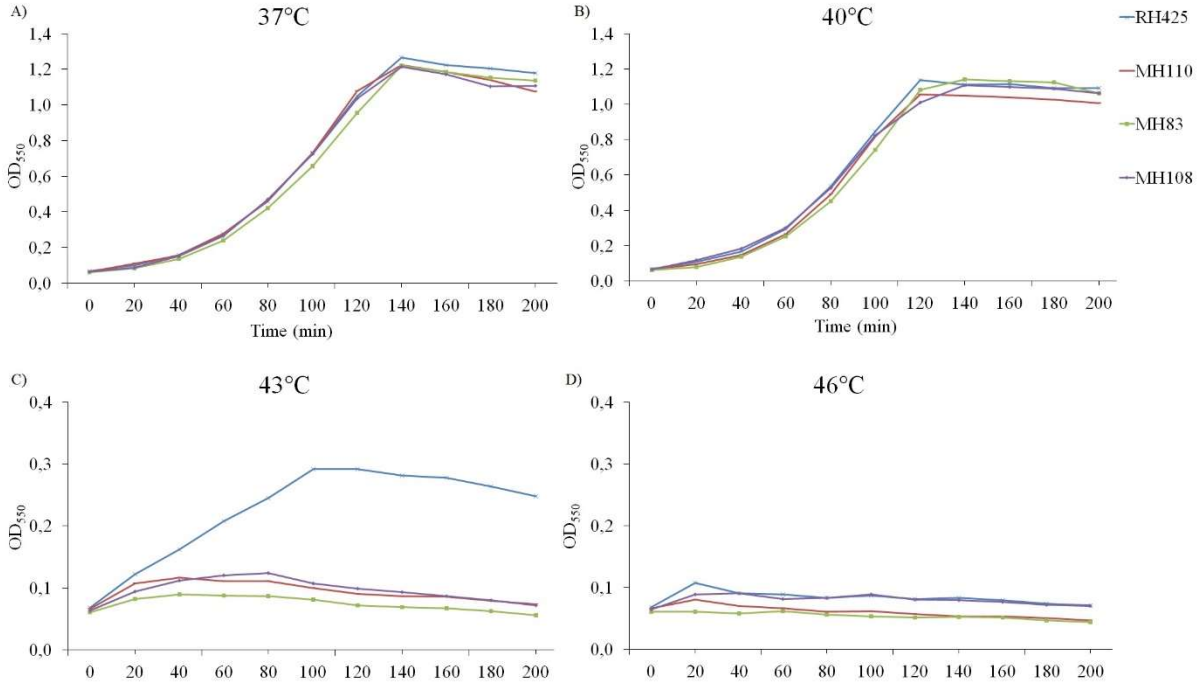

Figure 4.10 Temperature sensitivity analysis. Growth curves for MH83 and its Δ*murMN* derivate MH108, and the wild-type controls RH425 and MH110 (RH425, but Δ*murMN*), during incubation at different temperatures. A) 37°C, B) 40°C, C) 43°C and D) 46°C. Note the different OD_{550} values of the Y-axis between A+B and C+D. Similar results were obtained in repeated experiment.

In this experiment, MH108 did not significantly differ from neither its parental strain, MH83, nor the Δ*murMN* control cells (MH110). At 37°C and 40°C, all four cultures grew equally well (Figure 4.10A and B). At 43°C, all cultures exhibited retarded growth (Figure 4.10C), although the wild type cells grew to a significantly higher OD_{550} (~ 0.3) than the other strains. There was, however, a clear difference between the growth of RH425 and the three other mutants. While RH425 reached an OD_{550} of approximately 0.3 before reaching stationary phase, neither of the three other mutants exceeded an $OD_{550} \approx 0.1$. No significant difference in growth could be determined between MH110, MH83 or MH108. At 46°C (Fig. 4.10D), the growth of all four cultures was severely retarded.

To test the survival of cells under these conditions, a sample was taken from each culture after 1 hour of growth. A 10-fold dilution series was made from each sample (from 10^{-1} to 10^{-5}), and spotted on TH plates, as described in section 3.13. After overnight incubation, the number of colonies in each spot was analysed. Pictures of the plates are presented in Figure 4.11. The results showed that there was no significant difference in survival between the four strains when grown at increasing temperatures. The RH425 and MH83 colonies appear more opaque than their Δ*murMN* counterparts, MH110 and MH108, possibly due to the integrity provided by the

branched cell wall. Based on these experiments, the observation that MH108 did not survive in soft-agar overlay assays cannot be explained by higher temperature sensitivity in Δ*murMN* mutants, To further explore the abnormal phenotype in MH108, the stem peptide composition of the cell wall was analysed and compared to that of a wild-type Δ*murMN* control. Additionally, to examine whether changes in other genes had occurred that might explain this phenotype, MH108 was subjected to whole genome sequencing. The results are presented in section 4.3 and 4.2.4.3, respectively. Additionally, to clarify the role of the absence of *murMN* in this context, a complement strain was made, by replacing the Janus cassette in the *murMN* locus with *murMN*. This strain restored both the resistance level and temperature stress tolerance of the MH108 parental strain, MH83, which strongly suggest that the detrimental effects observed for MH108 was a direct result of the loss of *murMN*.

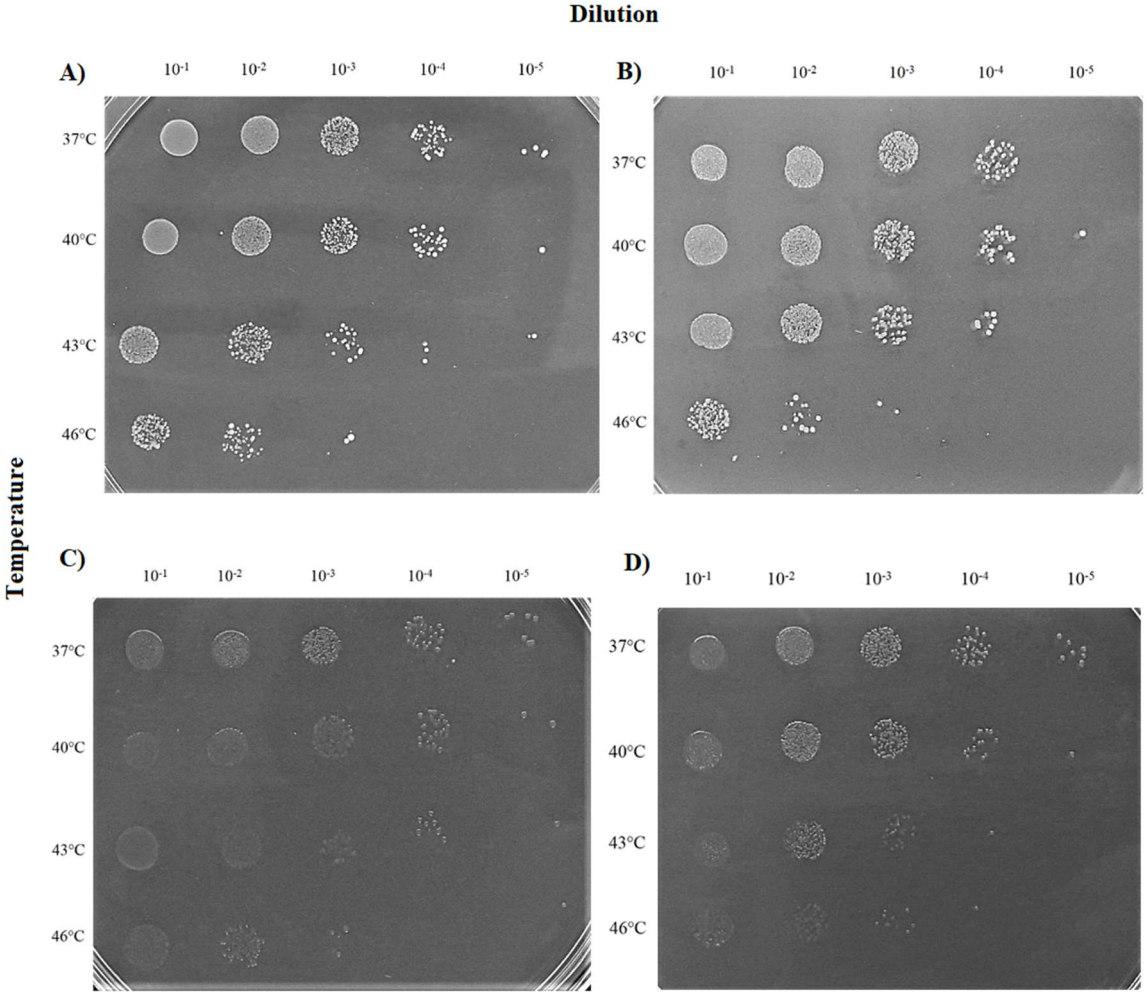

Figure 4.11 Temperature sensitivity analysis. To test the survival of cells incubated at different temperatures, a 10-fold dilution series of cells incubated at 37°C, 40°C, 43°C and 46°C were spotted on TH agar plates. A) MH83 (PBP2x$_{mos}$/1a$_{mos}$/2b$_{mos}$), B) Wild-type RH425, C) MH108 (MH83, but Δ*murMN*) and D) Wild-type, but Δ*murMN* (MH110).

4.2.4.3 The stem peptide composition of the Δ*murMN* mutants

The cell wall of MH108 was isolated, and the stem peptide composition analysed (as described in section 3.8) and compared to that of a Δ*murMN* wild-type control (KHB130). As expected, the branching of the cell walls was lost upon the deletion of *murMN*. No significant difference could be observed between the stem peptide composition of the cell wall in MH108 and the wild-type control KHB130 (Figure 4.12). Thus, the abnormal phenotype of MH108 could not be explained by effects on the stem peptide composition.

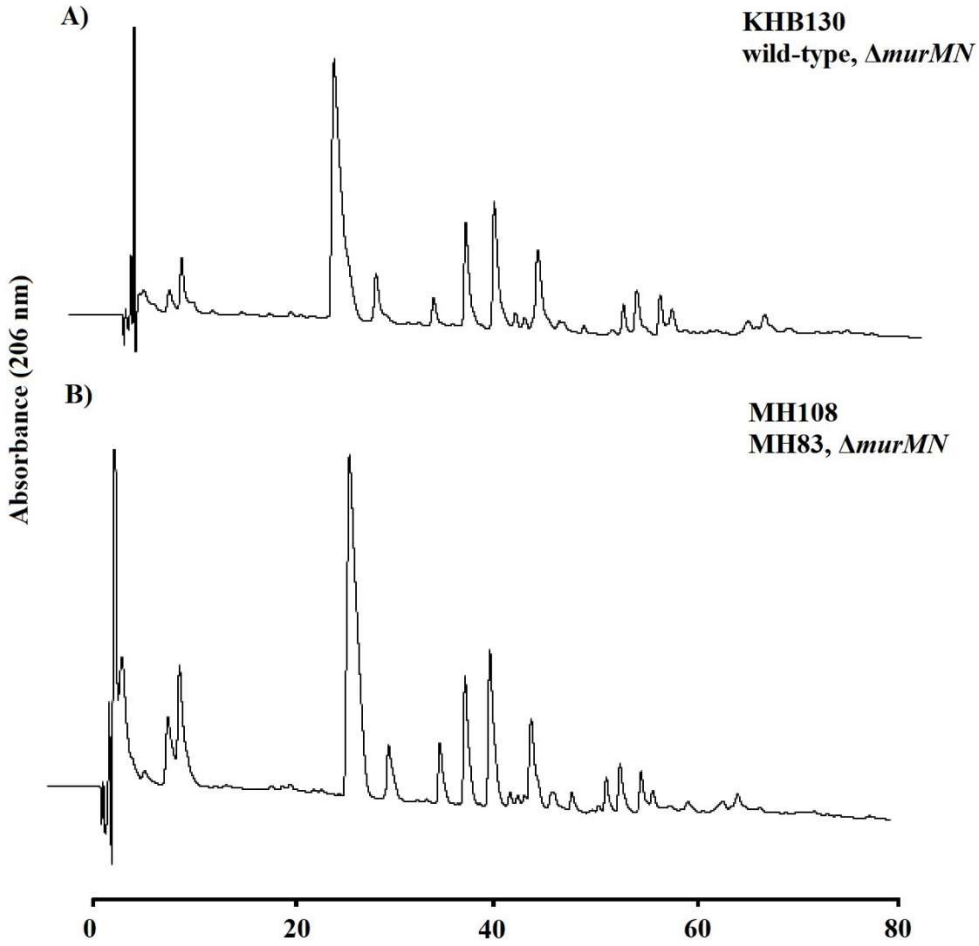

Figure 4.12 Stem peptide profile of Δ*murMN* derivates of MH83 (MH108) and the wild-type (KHB130), acquired by reverse-phase HPLC.

4.3 Whole genome sequencing

Two strains were selected for whole genome sequencing: MH91 and MH108. The genome sequencing revealed alterations in several genes in both MH91 and MH108. The main findings, which is limited to include mutations that led to changes at the amino acid level of protein encoding genes, are presented in Table 4.2.

Table 4.2 Mutated genes in MH91 and MH108, identified through whole genome sequencing, using *S. pneumoniae* R6 as the reference genome.

Gene	Gene name	MH91	MH108
dltA	*Spr1982*	$A_{280}T$	-
xerD	*Spr0447*	Extension	Extension
pbp2b	*Spr1517*	$T_{446}A$	Mosaic
pbp2x	*Spr0304*	Mosaic	Mosaic
pbp1a	*Spr0329*	Mosaic	Mosaic
murM	*Spr0540*	-	Deletion*
murN	*Spr0541*	-	Deletion*
recR	*Spr1516*	-	Several substitutions
pstB	*Spr1253*	-	$G_{71}V$

* Replaced with the Janus cassette.

MH91 displayed a significantly higher penicillin resistance level than the other mutants obtained after transferring $pbp1a_{Uo5}$ into MH10 ($pbp2x_{mos}$). As described in section 4.2.1, the genome sequencing revealed a spontaneous mutations in *pbp2b* leading to a $T_{446}A$ substitution in the protein, a well-characterized mutation known to confer a reduced penicillin-affinity in PBP2b (Calvez et al., 2017). In addition to the $pbp2b_{T446A}$ substitution, the only other gene affected in MH91, which was not also mutated in MH108, included an $A_{280}T$ substitution in *dltA*. This gene is found within the *dltABCD* operon, which encode proteins involved in the D-alanylation of teichoic acids. Addition of D-alanine to teichoic acids reduces the negative charge of the cell envelope, and it has been shown to have an impact on resistance to antimicrobial agents such as antimicrobial peptides and vancomycin in both pneumococci and staphylococci ((Peschel et al., 1999, Peschel et al., 2000, Kovács et al., 2006). Whether the $A_{280}T$ change in DltA affects this enzyme's activity and thus the level of D-alanylation of teichoic acids was not explored in this thesis. It would be interesting, though, to check if replacement of $DltA_{A280T}$ in MH91 with the wild-type DltA would affect the penicillin resistance.

MH108 displayed a curious sensitivity to the inoculation in high-temperature soft-agar, which was not observed in any of the other Δ*murMN* strains expressing different low-affinity PBPs. The genome sequencing confirmed the presence of mosaic variants of *pbp2x*, *pbp1a* and *pbp2b* in MH108, as well as the deletion of the *murMN* operon. In addition to these, the mutations present only in MH108 included a few substitutions in *recR*, which lies just downstream of *pbp2b* in the genome, and a $G_{17}V$ substitution in *pstB*. PstB is an ATP-binding phosphate transporter, and mutated versions of this gene have been found to reduce or retard the uptake of inorganic phosphate from the environment. This has been shown to be detrimental for cell survival in saliva (Verhagen et al., 2014). Whether or not this specific substitution would confer this phenotype is not clear, but the substitution of two small, non-polar amino acids do not immediately suggest such an effect. However, further analysis of this gene in MH108 is needed to clarify its potential function in this context.

An extension of the *xerD* gene was present in both MH91 and MH108. In *Escherichia coli*, XerD and CerX have been identified as tyrosine recombinases important for the resolution of chromosome dimers during cell division (Le Bourgeois et al., 2007). While this system appears to be highly conserved among bacteria, a different, analogous system have been identified in *S. pneumoniae*, involving only one tyrosine recombinase: XerS (Le Bourgeois et al., 2007). As this mutation was present in both MH91 and MH108, it was most likely introduced with or prior to the transformation of $pbp1a_{mos}$, and are probably not related to either phenotype. Further analysis of the effect of the mutations observed in MH91 and MH108 is needed to substantiate this claim.

4.4 Why is $murM_{Uo5}$ not tolerated in *S. pneumoniae*?

Specific versions of MurM have been shown to be essential for penicillin resistance in many pneumococcal isolates. An obvious question is whether substitution of the native MurM in sensitive *S. pneumoniae* with the MurM version found in resistant isolates would result in increased resistance. However, repeated attempts to replace the full *murMN* operon with $murM_{Uo5}$ were unsuccessful, both through gene replacement via the Janus cassette, and when selecting for transformants on a gradient of penicillin G. The $murM_{Uo5}$ gene differs greatly from $murM_{R6}$. They are located in different positions in the genome and oriented in different directions, and the genes only display a 50% identity at the amino acid level (Todorova et al., 2015). Additionally, attempts to replace *murM* in *S. pneumoniae* R6 with *murM* from the penicillin resistant *S. mitis* B6 (unpublished data from Håvarstein's group) or the *S. oralis* Uo5

murM gene via the Janus cassette have been unsuccessful (Todorova et al., 2015). Todorova *et al*. obtained only a single transformant when replacing $murM_{R6}$ with $murM_{Uo5}$, while maintaining $murN_{R6}$ in its native position, into a strain containing mosaic (R6xUo5) *pbp2x*, *pbp2b* (and *murE*) genes. The authors reasoned that suppressor mutations most likely had occurred, and postulated that $murM_{Uo5}$ is not tolerated in *S. pneumoniae* R6.

To avoid the toxicity of $MurM_{Uo5}$ in *S. pneumoniae* R6, we first chose to study the effects of $murM_{Uo5}$ in an R6 background using the ComRS gene expression system (section 3.11) The $murM_{Uo5}$ gene was placed behind the inducible P_{comX} promoter in a wild-type R6 background (SPH131), and in the penicillin resistant MH83 strain. The idea was that $murM_{uo5}$ might be better tolerated in the MH83 strain, which has all three low-affinity PBPs: $PBP2x_{mos}/1a_{mos}/2b_{mos}$. The ComRS system was introduced into MH83 by transferring the P_{comX}::janus and P_1::P_{comR}::*comR* gene fragments from SPH131 (Berg et al., 2011), giving rise to strain MH134. The Janus cassette behind P_{comX} was subsequently replaced by $murM_{Uo5}$, both in MH134 and SPH131, giving rise to strains MH138 and MH105, respectively. To test if the presence of native $MurM_{R6}$ and/or $MurN_{R6}$ would affect the tolerance of $MurM_{Uo5}$, ectopic expression of $murM_{Uo5}$ was also studied in $\Delta murMN_{R6}$, $\Delta murN_{R6}$ and a $\Delta murM_{R6}$ backgrounds. As a control, the *S. pneumoniae* R6 native *murM* gene ($murM_{R6}$) was placed behind the P_{comX} promoter in both MH134 and SPH131, giving rise to MH144 and MH142, respectively. Overexpression of $murM_{R6}$ was studied both in a wild type and a $\Delta murMN_{R6}$ background.

If $murM_{Uo5}$ was not tolerated in the R6 strain, the overexpression of $murM_{Uo5}$ in these cells would result in severe growth inhibition and morphological defects. Therefore, cells overexpressing $murM_{Uo5}$ were examined for effects on growth and morphology.

4.4.1 The absence of MurN makes overexpression of MurM toxic in *S. pneumoniae*.

The possible toxic effects of overexpressing $murM_{Uo5}$ and $murM_{R6}$ in *S. pneumoniae* R6 were analysed using a growth assay, as described in section 3.12. Ectopic expression of $murM_{Uo5}$ and $murM_{R6}$ was induced with 0, 0.05, and 0.2 μM ComS*, and the growth was monitored by measuring the OD_{550} every 5-10 minutes for 20 hours. Negative effects on growth would be observed as a reduction in doubling time, and might also result in transition to stationary phase at a lower cell density compared to the wild-type. The growth curves for the overexpression of $murM_{Uo5}$ and $murM_{R6}$ in both an R6 wild-type (SPH131) and a penicillin resistant (MH83) background are presented in Figure 4.13.

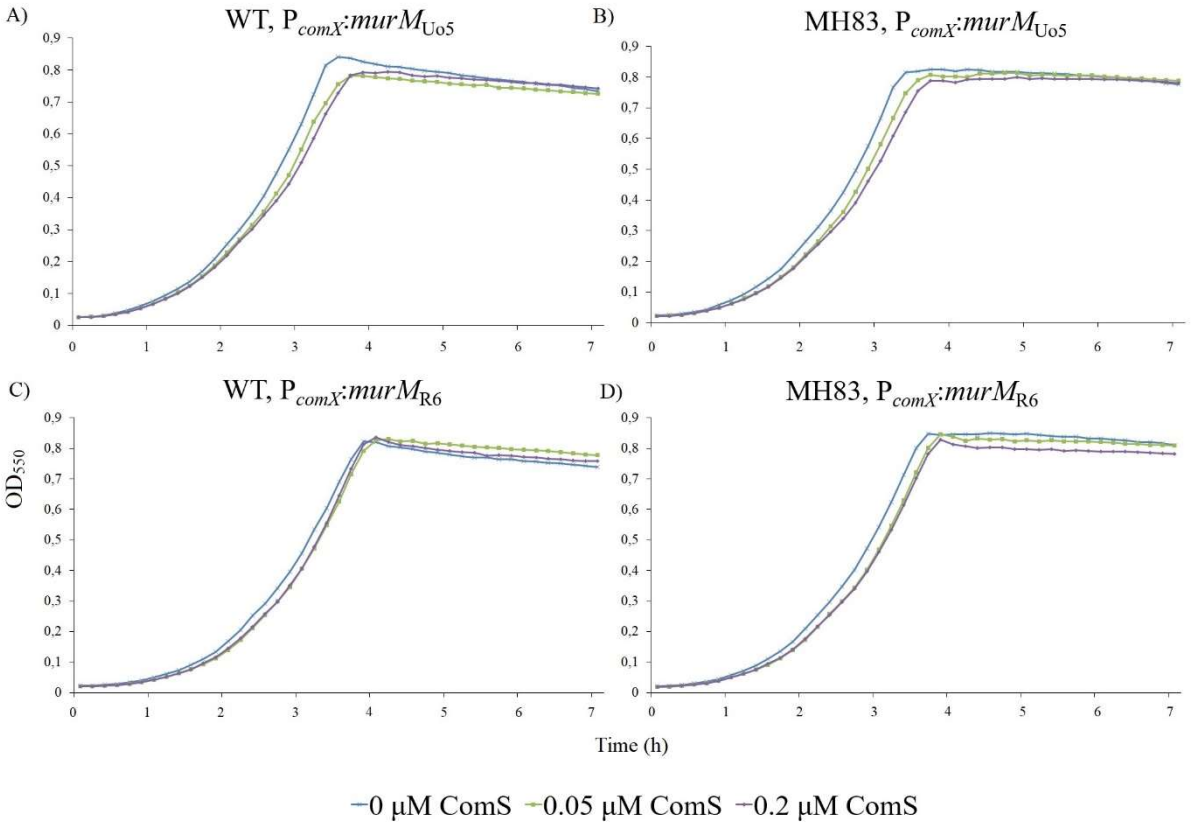

Figure 4.13 Growth curves for pneumococci overexpressing the *murM*$_{Uo5}$ (A and B) and *murM*$_{R6}$ (C and D) genes. A) MH105 = SPH131, but P$_{comX}$:*murM*$_{Uo5}$. B) MH138 = MH83, but P$_{comX}$:*murM*$_{Uo5.}$ C) MH142 = SPH131, but P$_{comX}$:*murM*$_{R6}$. D) MH144 = MH83, but P$_{ComX}$:*murM*$_{R6}$. The expression of *murM*$_{Uo5}$ and *murM*$_{R6}$ were induced with 0, 0.05 and 0.2 µM ComS*. Similar results were obtained in repeated experiment.

Surprisingly, overexpression of *murM*$_{Uo5}$ (0.2 µM ComS) appeared to have little impact on the growth of wild type *S. pneumoniae* R6 (MH110). The same result was also obtained when overexpressing *murM*$_{Uo5}$ in the R6 strain harbouring PBP2x$_{mos}$/1a$_{mos}$/2b$_{mos}$ (MH138). The growth curves of cells overexpressing *murM*$_{Uo5}$ or *murM*$_{R6}$ are highly comparable, i.e. the ComS* induced cultures did not deviate significantly from the non-induced cultures Additionally, no notable difference could be observed between the wild-type and PBP2x$_{mos}$/1a$_{mos}$/2b$_{mos}$ backgrounds.

To test if the natively expressed *murMN*$_{R6}$ locus was rescuing the cells from the reported toxic effects of MurM$_{uo5}$, the experiment was repeated in Δ*murMN*$_{R6}$ backgrounds.

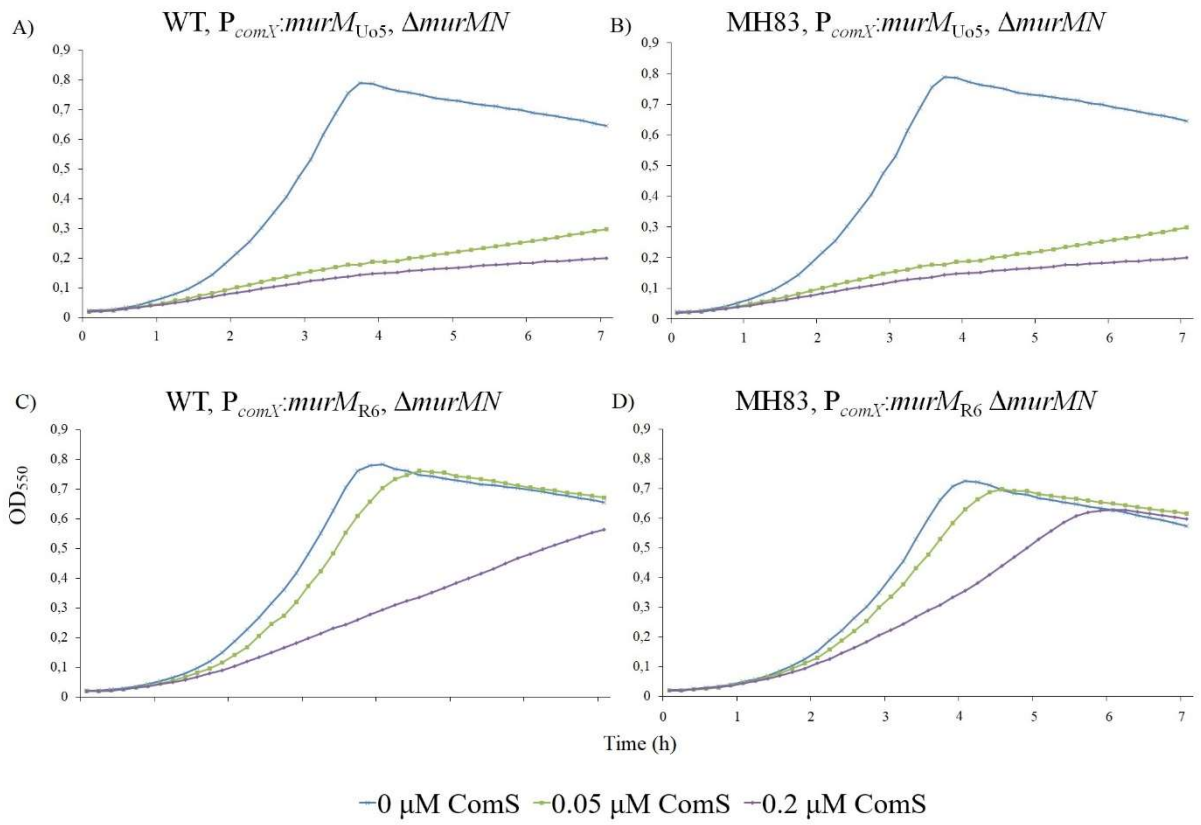

Figure 4.14 Growth curves for strains overexpressing the *murM*$_{Uo5}$ (A and B) and *murM*$_{R6}$ (C and D) genes in Δ*murMN*$_{R6}$ backgrounds. A) MH136 = SPH131, but P$_{comX}$:*murM*$_{Uo5}$, Δ*murMN*. B) MH141 = MH83, P$_{comX}$:*murM*$_{Uo5}$, Δ*murMN*. C) MH146 = SPH131, but P$_{comX}$:*murM*$_{R6}$, Δ*murMN*. D) MH147 = MH83, but P$_{comX}$:*murM*$_{R6}$, Δ*murMN*. The expression of *murM*$_{Uo5}$ and *murM*$_{R6}$ were induced with a gradient of 0, 0.05 and 0.2 µM ComS. Similar results were obtained in repeated experiment.

As shown in Figure 4.14A and B, the cells overexpressing *murM*$_{Uo5}$ were strongly affected in a Δ*murMN* background, and displayed significantly reduced growth. The overexpression of *murM*$_{R6}$ also somewhat negatively affected growth (Figure XC and D), but in a notably lesser degree than for *murM*$_{Uo5}$: the cells were only mildly affected when induced with 0.05 µM ComS*, which is in stark contrast to the strong inhibition by the cells overexpressing *murM*$_{Uo5}$. Both were affected at 0.2 µM ComS*, but again, the *murM*$_{Uo5}$ overexpression resulted in significantly stronger adverse effects.

Together, this strongly suggest that *murM*$_{Uo5}$ is tolerated in an R6 background, as long as the *murMN*$_{R6}$ operon is present. The results also indicate that while the cells are generally negatively impacted by the overexpression of *murM* in a Δ*murMN*$_{R6}$ background, overexpressing *murM*$_{Uo5}$ has a stronger inhibitory effect on growth than *murM*$_{R6}$.

The requirement of MurMN$_{R6}$ for the tolerance of *murM*$_{Uo5}$ expression in an R6 background, explains why the *murMN*$_{R6}$ operon could not be readily replaced by the *murM*$_{Uo5}$ or *murM*$_{B6}$ genes. To study whether this requirement included the presence of the whole *murMN*$_{R6}$ operon, or either just *murM*$_{R6}$ or *murN*$_{R6}$, the overexpression of *murM*$_{Uo5}$ was repeated both in a Δ*murN* (Figure 4.15A and B) and Δ*murM* background (Figue 4.15C and D).

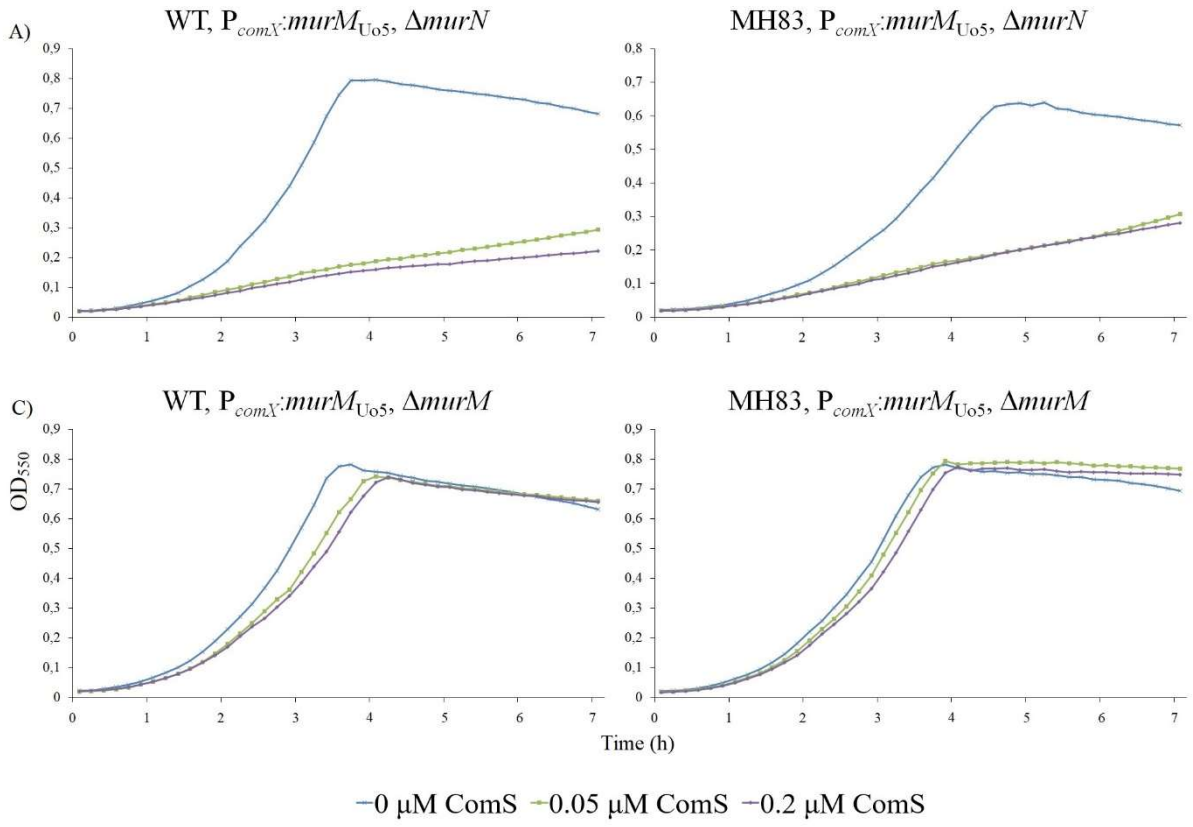

Figure 4.15 Overexpressing *murM*$_{Uo5}$ in a Δ*murN*$_{R6}$ background. A) MH149 = SPH131, but P$_{ComX}$:*murM*$_{Uo5}$, Δ*murN*. B) MH150 = MH83, but P$_{comX}$:*murM*$_{Uo5}$, Δ*murN*. C) MH152 = SPH131, but P$_{ComX}$:*murM*$_{Uo5}$, Δ*murM*. D) MH153 = MH83, but P$_{ComX}$:*murM*$_{Uo5}$, Δ*murM*. Similar results were obtained in repeated experiment.

The cells overexpressing *murM*$_{Uo5}$ in a Δ*murN*$_{R6}$ background behaved similarly to cells overexpressing *murM*$_{Uo5}$ in the absence of the entire *murMN*$_{R6}$ operon (Figure 4.15 A and B). Growth were severely inhibited both at 0.05 and 0.2 µM ComS*.However, as evident from Figure 4.15 C and D, the cells appeared to tolerate the overexpression of *murM*$_{Uo5}$ in a Δ*murM*$_{R6}$ background.

Based on these results, the overexpression of *murM*$_{Uo5}$ appears to be tolerated in an R6 background as long as *murN*$_{R6}$ is present, but have severe adverse effects in a Δ*murN*$_{R6}$ background. No significant difference could be observed between the wild-type R6 and the resistant strain harbouring low-affinity PBP2x$_{mos}$/1a$_{mos}$/2b$_{mos}$.

4.4.2 Cells overexpressing *murM*$_{Uo5}$ develop gross morphological abnormalities

The morphological effects of overexpressing *murM*$_{Uo5}$ in *S. pneumoniae* R6 was studied using phase contrast microscopy. The cells were prepared for phase contrast microscopy as described in section 3.7. The cultures were grown to an OD_{550} = 0.3, and induced with 0 and 2 µM ComS*. Some cultures, including MH136 and MH141, were not able to reach an OD_{550} = 0.3 when induced with 2 µM ComS*. These were prepared for microscopy by harvesting cells from 1 ml culture at maximum OD_{550}, and resuspending the pellet in 100 µl PBS. The morphological effects on cells overexpressing MurM$_{Uo5}$ were examined in both the wild-type background, as well as in MH83 (low-affinity PBP2x, 2b and 1a) (Figure 4.16).

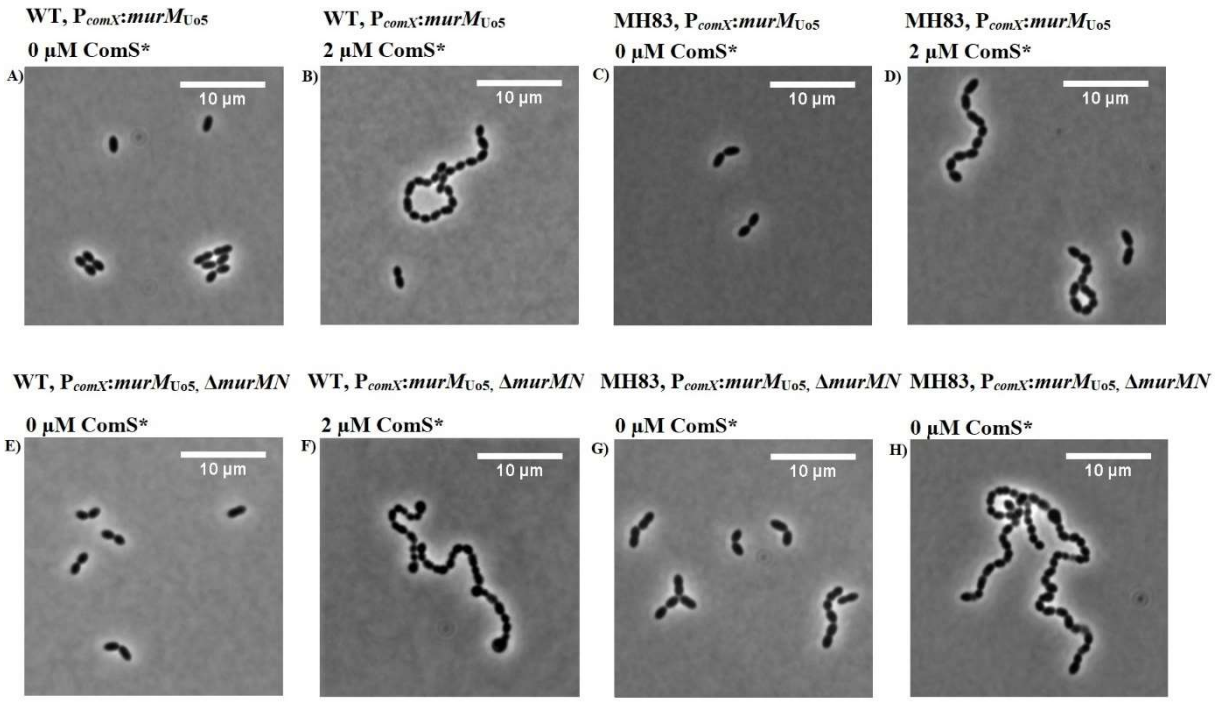

Figure 4.16 Microscopic analysis of cells overexpressing *murM*$_{Uo5}$ from the inducible promoter P*comX*. Uninduced cells are compared to cells induced with 2 µM ComS*. A) MH105 (wild-type, 0 µM ComS*), B) MH105 (wild-type, 2 µM ComS*), C) MH138 (MH83, 0 µM ComS*), D) MH138 (MH83, 2 µM ComS*), E) MH136 (wild-type, 0 µM ComS*), F) MH136 (wild-type, 2 µM ComS*), G) MH141 (MH83, 0 µM ComS*), H) MH141 (MH83, 2 µM ComS*).

The cells overexpressing MurM$_{Uo5}$ displayed severe growth defects, especially in a Δ*murMN* background. When induced with 2 µM ComS*, the cells with an intact *murMN* operon grew in long chains, and displayed slightly uneven cellular shape (Figure 4.16B and D). The cells lacking *murMN*, however, displayed a grossly abnormal morphology. The cells grew in very long chains, and were severely uneven in shape. Some of the cells grew abnormally large and rounded, suggesting a major disturbance of normal cell division. Due to time limitations, cells

overexpressing MurM$_{Uo5}$ in Δ*murM* and Δ*murN* backgrounds, and cells overexpressing MurM$_{R6}$, were not examined in the microscope. It would be interesting to see whether the morphological defects are as severe in cells overexpressing the native MurM$_{R6}$, as for MurM$_{Uo5}$. As with the growth assay, no significant difference could be observed between the wild-type cells and MH83 cells, indicating that the presence of low-affinity PBPs do not rescue the toxic effect of MurM$_{Uo5}$ in an *S. pneumoniae* Δ*murN* background.

4.4.3 The presence of MurM$_{Uo5}$ do not further increase penicillin resistance in *S. pneumoniae*

Based on the results from overexpressing MurM$_{Uo5}$ in *S. pneumoniae* R6 cells, the transfer of MurM$_{Uo5}$ into the native locus of *S. pneumoniae* R6 should be possible as long as *murN*$_{R6}$ remains unaltered. Therefore, we attempted to transfer *murM*$_{Uo5}$ to MH83 (low-affinity PBP2x, 1a and 2b) through gene replacement via the Janus cassette. This resulted in a successful transformation, and sequencing confirmed that the *murM*$_{Uo5}$ sequence was unaltered. Due to time limitations, this mutant (MH156) was only examined for effects on growth, morphology and penicillin resistance level. The presence of MurM$_{Uo5}$ did not appear to affect neither growth or morphology (data not shown). Interestingly, the presence of MurM$_{Uo5}$, which is an important resistance factor in *S. oralis* Uo5, did not further increase the resistance level of *S. pneumoniae* R6, even in the presence of low-affinity PBPs. This could indicate that MurM$_{Uo5}$ it not able to fully substitute for MurM$_{R6}$ in *S. pneumoniae*. However, the mutant did not display any sensitivity to the elevated temperature during MIC determination using the soft-agar overlay assay, as its MH83 Δ*murM* parental strain did, which indicate that MurM$_{Uo5}$ could substitute at least some of the functions of MurM$_{R6}$ *S. pneumoniae*.

The fact that this important resistance factor in *S. oralis* Uo5 did not further increase the resistance level in *S. pneumoniae* R6 expressing low-affinity PBPs, could explain why transformation with *S. oralis* Uo5 DNA do not yield pneumococcal transformants that reach the resistance level of this donor strain.

5 Discussion

5.1 Transfer of low-affinity PBPs from *S. oralis* Uo5 to *S. pneumoniae* R6

One of the main goals of the present work was to systematically transfer low-affinity PBPs from the highly penicillin resistant isolate *S. oralis* Uo5 into the sensitive *S. pneumoniae* R6 strain. We wanted to exploit these mutants to further characterise the impact individual low-affinity PBPs and combinations of them have on resistance in the pneumococcus. Single pbp_{Uo5} gene transfers were used instead of genomic Uo5 DNA as transforming DNA. This approach was chosen to have full control over the order of which PBP that was transferred and that no other genetic elements from the Uo5 genome would concomitantly recombined into the R6 receiver genome. The results presented in this work is in accordance with previous studies that have shown that the transfer of *pbp* sequence blocks from *S. oralis* Uo5 to *S. pneumoniae* R6 is possible under the selection pressure of different β-lactams (Todorova et al., 2015, Reichmann et al., 1997).

Using penicillin G as the selective antibiotic, transformants containing a low-affinity PBP2x were obtained. However, repeated attempts to produce transformants containing a low-affinity PBP2b or a low-affinity PBP1a failed unless a low-affinity PBP2x was already present in the cells. This is in agreement with previous studies, that have identified low-affinity PBP2x as the primary determinant of penicillin resistance (Zerfass et al., 2009). A study by Kocaoglu O., et al(2015), estimated MIC values of all six PBPs in the R6 derivate *S. pneumoniae* D39, and showed that the MIC of PBP2x is lower than that of PBP1a (3-4 fold) and PBP2b (~20 fold) . This explains why it was not possible to obtain mutants only having low-affinity PBP1a or PBP2b when selecting for transformants on penicillin G. Introduction of low-affinity PBP1a or PBP2b would not increase the MIC of the transformants since PBP2x still will be inhibited like for wild type cells. However, subsequent introduction of low-affinity PBP2b and PBP1a into MH10 ($pbp2x_{mos}$) produced double mutants containing low-affinity PBP2x and PBP1a as well as mutants having low-affinity PBP2x and PBP2b. When selecting for the double mutant $PBP2x_{mos}/2b_{mos}$, transformants appeared on plates having a penicillin G concentration that most probably would inhibit PBP1a (which has approximately five-fold lower MIC than PBP2b (Kocaoglu et al., 2015)). However, since PBP1a is a non-essential PBP when grown under laboratory conditions, colonies having $PBP2x_{mos}/2b_{mos}$ could grow on higher penicillin G concentrations than the parental MH10 strain. Although being a non-essential PBP, PBP1a's

contribution to β-lactam resistance is known to be significant (Hakenbeck et al., 2012), making it possible to select for triple mutants containing low-affinity PBP2x, PBP1a and PBP2b.

We were unable to obtain any transformants containing the full *pbp* genes from *S. oralis* Uo5; all the low-affinity PBPs obtained in this work were mosaic versions in which the Uo5 sequence blocks were found within or overlapping the transpeptidase domain. Furthermore, none of the low-affinity PBPs contained Uo5 sequences, which overlapped the cytoplasmic or transmembrane segment. Similar results were obtained in a previous study, when using Uo5 *pbp* amplicons to transform *S. pneumoniae* R6 using piperacillin, cefotaxime and oxacillin as the selective antibiotics (Todorova et al., 2015). This suggest that the cytoplasmic and/or transmembrane domains of the Uo5 PBPs cannot readily substitute the corresponding R6 domains, or that mutations in these domains would not confer a significant increase in resistance, and is therefore not a selectable phenotype under a β-lactam selection pressure. The importance of the functions of the cytoplasmic and transmembrane domains of PBP2x and PBP2b in *S. pneumoniae* have previously been addressed by Berg et al.,(2014), who found that they were important for either sub-cellular localisation or yet unidentified molecular interactions, most likely with other members of the cell wall synthesis machinery such as their cognate transglycosylases. Interestingly, Todorova *et al*. (2015) did obtain transformants in which the Uo5 sequence blocks overlapped the cytoplasmic and transmembrane domains in *pbp2x*, *pbp2b* and *pbp1a*, but only when using *S. oralis* Uo5 gDNA to transform R6. This strongly suggest that some compensatory gene transfer events or substitutions had occurred, which allowed for the replacement of these domains. In fact, genome sequencing of these mutants revealed several mutation throughout the genomes of which transfer of *murE* from Uo5 to R6 was an important factor for resistance. In addition, several consecutive transformations of gDNA from the penicillin resistant *S. mitis* B6 strain to *S. pneumoniae* R6 showed multiple recombination events throughout the R6 genome including the PBPs (with the exception of PBP3) (Sauerbier et al., 2012) (Sauerbier et al 2012). Further studies on the non-PBP genes affected during these transformations could potentially identify novel proteins being involved in penicillin resistance and/or interactions with PBPs.

Surprisingly, given that R6 readily accepted Uo5 *pbp* fragments when selecting with penicillin G, replacement of the R6 *pbps* with Uo5 *pbps* through negative selection (see section 3.6.1 in methods) when removing the Janus cassette was unsuccessful, even when using constructs in which the native R6 cytoplasmic and transmembrane domains were preserved. The amino acid

sequence of the PBP2x$_{mos}$ acquired in MH10 only differed from the sequence of *pbp2x* construct nr. 3 by a single residue, in position 281. In *S. pneumoniae* R6 (and pbp2x construct nr. 3), this residue is a glutamine (Q), while it is a leucine (L) in *S. oralis* Uo5 (and *PBP2x*$_{MH10}$). This residue is located within an α-helix of the transpeptidase domain, and while the $Q_{281}L$ substitution has been identified in resistant isolates previously, it has not been implicated as a resistance-determining substitution (Carapito et al., 2006). However, as the substitution results in the loss of a polar residue within an α-helix, it might be of some significance. Of note, all the mosaic *pbp2x* versions obtained in this work contained the $Q_{281}L$ substitution. To test whether this single substitution was sufficiently important to allow successful replacement with Janus in the R6 strain we attempted to transform KHB55 (Δ*pbp2x*$_{R6}$::janus, P$_{comX}$:*pbp2x*$_{R6}$) with *pbp2x*$_{MH10}$. However, this transformation only resulted in two transformants, strongly indicating that the presence of a leucine in position 281 is not the reason for the difficulties experienced when trying to introduce a low-affinity PBP2x into the R6 strain using the Janus system. In previous work conducted at the Molecular Microbiology research group the same difficulties were faced when transferring low-affinity PBPs from the highly penicillin resistant *S. mitis* B6 to *S. pneumoniae* R6 using the Janus protocol. However, after numerous attempts and large colony screens, mosaic PBPs containing a combination of B6 and R6 sequences were obtained using this method, for *pbp2x*, *pbp2b* and *pbp1a* (unpublished data). Of note, none of these mosaic PBPs contained B6 sequences overlapping the cytoplasmic or transmembrane domains.

We know that the presence of *pbp2x*$_{MH10}$ is tolerated in *S. pneumoniae* R6, so the poor transformation efficiency achieved when transforming KHB55 with *pbp2x*$_{MH10}$ via Janus, with the concurrent expression of the native *pbp2x*, highlights the challenges of using this protocol for interspecies replacement of PBPs to *S. pneumoniae* R6. This is supported by the fact that the problems of using this method spanned different PBPs and included separate studies. The reasons why are not clear, but we can speculate that the integration of the *S. mitis* and *S. oralis* PBPs in R6 might require additional mutations in non-PBP genes, and that these compensatory mutations might be more easily selected for under a β-lactam selection pressure. The results of the whole genome sequencing of MH91 and MH108 did not reveal alterations in any clear candidate genes, but further analysis is needed to clarify their potential roles. One can also speculate that *S. pneumoniae* R6 does not tolerate the concurrent expression of two different versions of the same PBP, which would complicate the need for ectopic expression of the native PBP during transformation when working with the essential genes *pbp2b* and *pbp2x*. However,

this would not explain the difficulties in transferring *pbp1a*, as this non-essential gene was not ectopically expressed during the transformations (personal communication, Dr. Daniel Straume).

5.2 Increased β-lactam resistance in *S. pneumoniae* R6 mutants with mosaic *pbps*

The β-lactam resistance level of the transformants harbouring the different low-affinity PBPs was determined by measuring their MIC values for penicillin G, oxacillin, piperacillin and ceftazidime. As expected, a steady increase in resistance against penicillin G, oxacillin and piperacillin was observed with the acquisition of each additional low-affinity PBP. For ceftazidime, a significant increase in resistance was achieved upon the acquisition of a low-affinity PBP2x, but subsequent addition of a low-affinity PBP1a and/or PBP2b did not further reduce the susceptibility for this β-lactam. This was expected for the addition of a low-affinity PBP2b, as this enzyme is not inhibited by ceftazidime (Hakenbeck et al., 1987) , but the lack of increase in resistance with the addition of a low-affinity PBP1a was more unexpected, although it could be related to the fact that PBP1a is not essential in *S. pneumoniae*. Furthermore, it is well-known that mutations that confer reduced affinity for one β-lactam is not always transferrable to all β-lactams (Hakenbeck et al., 2012). It might be that the low-affinity PBP1a versions obtained in this work, do not provide a significant reduction in affinity for ceftazidime.

None of the transformants obtained the high penicillin resistance level observed for the *S. oralis* Uo5 donor strain, which also has been reported in a previous study (Todorova et al., 2015). The reasons for this are most likely multifactorial. First, we were unable to obtain pneumococcal transformants containing the entire Uo5 *pbps*. While substitutions in the cytoplasmic and transmembrane domains in *S. pneumoniae* alone are not known to confer resistance, these domains could potentially be of importance for the functionality of the low-affinity PBPs and for their interaction with other cell division proteins relevant for the high level of penicillin resistance of *S. oralis* Uo5. However, as previously described, Todorova et al. (2015) were able to obtain pneumococcal transformants containing entire *S. oralis* Uo5 *pbp* gene sequences (for *pbp2x* and *pbp1a*) when transforming with gDNA. These mutants displayed higher MIC values than the transformants obtained by transforming *S. pneumoniae* R6 with *pbp* PCR fragments, but as alterations in non-*pbp* resistance genes (*murE*) were discovered in these transformants as well, we cannot conclude anything about the effects of these domains on resistance.

Additionally, non-PBP genes contribute to resistance in *S. oralis* Uo5, such as *murM* and *murE* (Todorova et al., 2015, Chesnel et al., 2005). Todorova *et al*. found that alterations in *murE* in *S. pneumonia* R6 resulted in a higher level of resistance, especially in combination with low-affinity PBP2x and PBP2b, and that recombination between $murE_{Uo5}$ and $murE_{R6}$ was selectable using piperacillin. However, a strain harbouring $pbp2b_{mos}$, $pbp2x_{mos}$ and $murE_{mos}$ still did not reach the resistance level of *S. oralis* Uo5, suggesting that there are other genes and/or physiological clues involved, which are not easily transferred to *S. pneumoniae* R6 (Todorova et al., 2015). The complexity of the resistant-determining PBP substitutions, and the largely unmapped complementary mutations that allow a simultaneous reduction of affinity for β-lactams, while maintaining the transpeptidase function of the enzyme, further complicates the study of penicillin resistance in *S. pneumoniae*. It might be that some of the substitutions important for resistance in *S. oralis* Uo5 do not confer resistance in an R6 background.

The consistently higher resistance level of MH91 relative to the other mutants obtained after transformation of a low-affinity PBP1a into MH10 ($pbp2x_{mos}$) was most likely caused by a spontaneous $T_{446}A$ mutation in *pbp2b*, identified through whole genome sequencing. This $T_{446}A$ substitution is a well-characterized substitution, known to confer reduced affinity for penicillin (Zapun et al., 2008a, Contreras-Martel et al., 2009). Mutations in a few other genes were also identified through whole genome sequencing, but none that were found likely to be involved in resistance. These additional mutations (not the $PBP2b_{T446A}$ mutation) were also identified in the MH108 ($pbp2x_{mos}$, $pbp1a_{mos}$ and $pbp2b_{mos}$, Δ*murMN*) strain, and were therefore probably introduced with or prior to the acquisition of low-affinity PBP2x or PBP1a, and most likely present in the other double PBP2x/PBP1a mutants as well. However, further analysis of the mutated genes identified through whole genome sequencing is needed to substantiate this claim.

5.3 Cell fitness cost of acquiring mosaic *pbps*

MH91 was the sole transformant that displayed a reduction in growth under standard conditions. This might be due to decreased enzymatic activity of one of the low-affinity PBPs. As previously described, the $T_{446}A$ mutation in PBP2b has been associated with a reduction in growth. A study comparing the relative activity of different versions of pneumococcal PBP2b found that $PBP2b_{T446A}$ had lower activity than PBP2b found in both the wild-type R6 strain, a highly resistant clinical isolate (*S. pneumoniae* 5204), and a PBP2b hybrid between 5205 and R6 (Calvez et al., 2017), which could explain the reduced growth of MH91. Both the hybrid

and the 5204 strain included the $T_{446}A$ mutation, in addition to several other substitutions. The authors argued that some of these additional substitutions in *pbp2b*$_{5204}$ and *pbp2b*$_{hybrid}$ were most likely mutations compensating for this reduced activity, although the mechanisms behind this are not fully understood. This might shed some light as to why the same reduction in growth was not observed in MH83, which also harbours a low-affinity PBP2b in addition to low-affinity PBP2x and PBP1a. However, while MH83 did not display any growth defects when grown under standard conditions, the temperature sensitivity analysis revealed a significant difference between the growth of MH83 and the wild-type *S. pneumoniae* R6 when incubated at 43°C. This suggest that there is a certain biological cost to the acquisition of one or more low-affinity PBPs, but that the cost of these mutations is more prominent when exposed to cellular stress.

Another interesting aspect of the Calvez study, was the surprising observation that the hybrid PBP2b, which consisted of the N-terminal region from the resistant 5204 strain and the C-terminal region from R6 , displayed both a higher enzymatic activity, and a lower affinity for β-lactams, than the original resistant isolate *S. pneumoniae* 5204. This result might shed some light on why the low-affinity PBPs obtained in this work consistently resulted in hybrid sequences rather than the transfer of the whole PBP genes from *S. oralis* Uo5. The mosaics obtained might confer a higher resistance in the *S. pneumoniae* R6 background, than the whole Uo5 PBP genes would. The different theories are not mutually exclusive.

5.4 Inactivation of *murMN* does not always result in loss of β-lactam resistance

MurM is a well-known penicillin resistance determinant in *S. pneumoniae*. As previously discussed, the deletion or inactivation of MurM has been found to significantly decrease the resistance level of clinical isolates, even in the presence of low-affinity PBPs (Filipe and Tomasz, 2000). However, the effect of MurM on penicillin resistance has been shown to depend on the nature of the PBPs expressed in the cells (du Plessis et al., 2002), and specific sets of low-affinity PBPs are often found with a specific version of MurM (del Campo et al., 2006). The results obtained in this work demonstrates that MurM does not always confer increased resistance to β-lactams. With the sole exception of MH83, none of the strains harbouring different low-affinity PBP combinations displayed a significant reduction in MIC values upon the deletion of *murMN*. Comparison of the stem peptide composition in the cell wall of MH56 (low-affinity PBP2x and 1a) and MH83 (low-affinity PBP2x, 1a and 2b) with that of the wild-type RH1, revealed that MH83 had a cell wall enriched in branched muropeptides. The

muropeptide composition of MH56 did not display any substantial differences from that of RH1. This is especially interesting given that the sequences of *murM*, *pbp2x* and *pbp1a* are identical between MH56 and MH83, suggesting that PBP2b is the determining factor for the increased level of branching observed in MH83. This might be due to reduced activity of the low-affinity PBP2b. PBP2b depletion experiments in an R6 background revealed that the level of branched stem peptides in the cell wall increased when PBP2b became scarce(Berg et al., 2013). It is interesting that deletion of *murMN* reduced penicillin resistance only in the one strain building a cell wall with higher degree of branched stem peptides. Due to time limitations, both MIC determination and analysis of the cell wall was only performed on a small selection of the transformants. Resistance level and cell wall analysis of more of the transformants that contained a low-affinity PBP2b, in combination with the study of relative enzymatic activity, could provide additional insight to the relationship between low-affinity PBPs and cell wall branching. Especially, the analysis of the cell wall and PBP2b activity of MH68 (low-affinity PBP2x and PBP2b), in which the deletion of *murMN* did not result in a significant reduction in resistance level, could further enlighten this relationship.

5.5 MurM, low-affinity PBPs and the tolerance for temperature-induced stress

Under standard cultivation conditions, the Δ*murMN* strains did not display any growth or morphological defects. The deletion of *murMN* from MH83 (low-affinity PBP2x, PBP1a and PBP2b), however, resulted in a strain (MH108) that appeared be more sensitive to heat.. This was based on the fact that MH108 cells did not tolerate being inoculated in agar during the overlay process in MIC determination, which was tolerated by the other Δ*murMN* cells expressing different versions of low-affinity PBPs. Unexpectedly, the temperature sensitivity analysis of MH108 (Figure 4.19) showed that it was not more vulnerable to heat compared to the other Δ*murMN* mutants. Therefore, we could not conclude that the high temperature of the agar alone (47°C) prevented this mutant from growing in soft-agar overlays. Since, it was not immediately clear which other aspects of this process that prevented the MH108 cells from growing in soft-agar assay, whole genome sequencing was performed to examine whether mutations in non-*pbp* genes had occurred. Such suppressor mutations could potentially give important clues about compensating mechanisms that take place in pneumococci as an adaptation of having low-affinity PBPs, which have been shown to be less efficient transpeptidases than their normal counterparts (Zhao et al., 1997). Alterations in a few genes were identified (see Table 4.2), but none that instantly suggested involvement in this behaviour, but further analysis is needed to clarify the roles of these additional mutations. Of note, the

complement strain in which *murMN* was reintroduced into MH108 fully restored both the ability to tolerate the overlay assay and the penicillin resistance level of MH83. This strongly suggest that the anomaly phenotype of MH108 was rescued by MurMN, highlighting the importance of MurM for both penicillin resistance and tolerance for temperature-induced stress.

The temperature sensitivity test also revealed that while the presence of the low-affinity PBPs in MH83 did not affect growth under optimal conditions, the cells displayed a significant reduction in growth at elevated temperatures compared to the wild-type. This suggest that the presence of one or more of the low-affinity PBPs in MH83 increases its sensitivity to temperature-induced stress. Similar results were obtained for the Δ*murMN* mutant MH110. The results obtained in this work could not differentiate between the growth-inhibiting temperature effects on MH83, MH108 or MH110, indicating that the effects of the low-affinity PBPs ($PBP2x_{mos}/1a_{mos}/2b_{mos}$) and/or lack of MurMN both reduce the cells tolerance for elevated temperatures. As mentioned above, the transpeptidase activity of low-affinity PBPs have been shown to be reduced *in vitro* (Zhao et al., 1997, Calvez et al., 2017), and cells expressing low-affinity PBPs usually construct a cell wall containing more branched peptide cross-bridges (Berg et al., 2013) . Although providing resistance to β-lactams, one might speculate that it could also result in a cell wall that is more vulnerable to other external stresses. Similarly, the same could be the case for a cell wall lacking branched interpeptide bridges, e.g. for the Δ*murMN* mutants. Comparison of the stem peptide composition of the cell wall between MH108 ($PBP2x_{mos}/1a_{mos}/2b_{mos}$, Δ*murMN*) and that of a Δ*murMN* mutant, revealed no significant differences. Both displayed a loss of branched peptides, as expected with the absence of *murMN*. It should be mentioned that because MurM also has been postulated to play a role in translation quality control by deacetylating mischarged tRNAs (Shepherd and Ibba, 2013), it is possible that the reduced tolerance to environmental stress in MH108 is not only linked to the loss of the structural integrity of the branched cell wall, but is also related to this hypothesized role of MurM.

5.6 $MurM_{Uo5}$ is not tolerated in an R6 background in the absence of MurN

Like for many penicillin resistant *S. pneumoniae* isolates, MurM is an important penicillin resistance determinant in *S. oralis* Uo5, which was supported by the drastic reduction in resistance observed in the Uo5 Δ*murM* strain. We wanted to study whether $MurM_{Uo5}$ would confer an increased level of resistance in *S. pneumoniae*, but intraspecies transfer of *murM* genes to *S. pneumoniae* have proven difficult. Repeated attempts to introduce $murM_{Uo5}$ over

murMN$_{R6}$ were unsuccessful, supporting the theory that MurM$_{Uo5}$ is not tolerated in the R6 background. Therefore, to study the effects of MurM$_{Uo5}$ in *S. pneumoniae*, we ectopically expressed *murM*$_{Uo5}$ from the inducible promoter P$_{comX}$, both in MH83 (*pbp2x*$_{mos}$, *pbp1a*$_{mos,}$ *pbp2b*$_{mos}$) and in the wild-type background SPH131. Our results did not find support for the hypothesis that MurM$_{Uo5}$ is toxic in a regular *S. pneumoniae* R6 background, nor that the presence of low-affinity PBPs in MH83 would increase the tolerance of MurM$_{Uo5}$. However, we found that overexpression of MurM, both from *S. oralis* Uo5 and *S. pneumoniae* R6, is detrimental to pneumococcal cells in the absence of MurN. This would explain why it was not possible to replace the full *murMN*$_{R6}$ operon with *murM*$_{Uo5}$. It was also clear that expression of MurM$_{Uo5}$ had a much more toxic effect on the Δ*murN* cells than MurM$_{R6}$. This might be explained by results from Lloyd et al., who showed that MurM$_{Uo5}$ has higher activity than MurM$_{R6}$ and that it only attaches an L-Ala residue while MurM$_{R6}$ also can attach L-Ser (Lloyd et al., 2008). Alternatively, it might interfere more negatively with other cell division proteins than the native MurM$_{R6}$.

Why the overexpression of MurM is tolerated in the presence of MurN, but is severely detrimental to cells in its absence, could be related to effects on the integrity of the cell wall. As MurM only adds the first amino acid residue of the peptidoglycan interpeptide bridge, the high expression of MurM without MurN would likely result in lipid II molecules rich in single-residue branched muropeptides. The fraction of stem peptides with single-branching in the cell wall of *S. pneumoniae* R6 is usually very small (Bui et al., 2012), so this abnormal peptidoglycan composition could potentially impact the integrity of the cell wall. Lipid II with muropeptides containing only one L-Ala branch could serve as an unfavourable substrate for the R6 PBPs. Our hypothesis that low-affinity PBPs would handle this single-branched muropeptide better was not confirmed in this study since the same toxic effect of MurM overexpression in Δ*murN* mutants expressing low-affinity PBPs was seen. Clearly, there are other mechanisms than the substrate preferences between low- and high-affinity PBPs involved. However, this theory needs further exploration, including the analysis of the cell wall of cells overexpressing MurM$_{Uo5}$ and MurM$_{R6}$.

As the results obtained in this work showed that MurM$_{Uo5}$ is tolerated in *S. pneumoniae*, as long as MurN is present, we attempted to replace *murM*$_{R6}$ with *murM*$_{Uo5}$ in pneumococci having the *murN* gene intact. As expected, this resulted in transformants with *murM*$_{Uo5}$*murN*$_{R6}$ in addition to low-affinity PBP2x, PBP1a and PBP2b (MH156). Surprisingly, the acquisition of *murM*$_{Uo5}$

did not further increase the resistance for neither penicillin G, oxacillin, piperacillin nor ceftazidime from that of its parental strain, MH83. This result corroborates the lack of increased resistance observed when overexpressing *murM*$_{Uo5}$ in MH138 (MH83, but P$_{comX}$:*murM*$_{Uo5}$). Due to time limitations, this strain was only further examined for effects on growth and morphology. The MH156 cells did not display any growth defects or deviating morphologies when grown under laboratory conditions.

6 Concluding remarks and further research

The experiments performed in this work show that transfer of low-affinity PBPs to the penicillin sensitive *S. pneumoniae* R6 results in increased resistance to β-lactams, but not close to the resistance level of the donor strain, *S. oralis* Uo5. We were unable to obtain transformants in which the whole low-affinity PBP from *S. oralis* Uo5 was transferred, indicating that some complementary mutations are required for the successful integration of these domains in *S. pneumoniae*. Additionally, the successful transfer of the resistance determinant $MurM_{Uo5}$ into MH83, which express three low-affinity PBPs, did not further increase the resistance. This is a puzzling result, but must mean that there are other unidentified proteins or other factors giving *S. oralis* Uo5 higher resistance than the MH156 strain constructed in this study. It would have been interesting to see if transfer of $MurE_{Uo5}$, which is also known to contribute to resistance, would result in resistance levels resembling that of *S. oralis* Uo5.

The results obtained in this work also show that the overexpression of MurM is toxic in the absence of MurN. Due to time limitations, this effect was only analysed with regards to cellular growth and morphology. Further analysis on the cell walls of strains overexpressing MurM in *S. pneumoniae* could provide additional insight into the causes of these detrimental effects.

As briefly described in the introduction, the preprint of a study exploring additional effects of *murMN* in *S. pneumoniae* was published online in late April. This study presented findings which indicate that *murMN* is involved in the regulation of the stringent response pathway activation in pneumococci, and thus mediates cellular response to environmental stress (Aggarwal et al., 2019). This could explain the abnormal phenotype of MH108 in response to temperature-related stress. Re-analysis of the results presented in this work in light of the Aggarwal study could potentially answer some of the unresolved questions regarding the effects of overexpressing MurM, and the role of MurM in antibiotic resistance.

Reference list

AGGARWAL, S. D., YERNENI, S. S., NARCISO, A. R., FILIPE, S. R. & HILLER, N. L. 2019. A Molecular Link between Cell Wall Modification and Stringent Response in a Gram-positive Bacteria. *bioRxiv*, 622340.

ANDERSSON, D. I. & LEVIN, B. R. 1999. The biological cost of antibiotic resistance. *Current Opinion in Microbiology,* 2**,** 489-493.

BARRETEAU, H., KOVAC, A., BONIFACE, A., SOVA, M., GOBEC, S. & BLANOT, D. 2008. Cytoplasmic steps of peptidoglycan biosynthesis. *FEMS Microbiol Rev,* 32**,** 168-207.

BENTLEY, S. D., AANENSEN, D. M., MAVROIDI, A., SAUNDERS, D., RABBINOWITSCH, E., COLLINS, M., DONOHOE, K., HARRIS, D., MURPHY, L., QUAIL, M. A., SAMUEL, G., SKOVSTED, I. C., KALTOFT, M. S., BARRELL, B., REEVES, P. R., PARKHILL, J. & SPRATT, B. G. 2006. Genetic analysis of the capsular biosynthetic locus from all 90 pneumococcal serotypes. *PLoS genetics,* 2**,** e31-e31.

BERG, K. H., BIORNSTAD, T. J., JOHNSBORG, O. & HAVARSTEIN, L. S. 2012. Properties and biological role of streptococcal fratricins. *Appl Environ Microbiol,* 78**,** 3515-22.

BERG, K. H., BIORNSTAD, T. J., STRAUME, D. & HAVARSTEIN, L. S. 2011. Peptide-regulated gene depletion system developed for use in *Streptococcus pneumoniae*. *J Bacteriol,* 193**,** 5207-15.

BERG, K. H., STAMSAS, G. A., STRAUME, D. & HAVARSTEIN, L. S. 2013. Effects of low PBP2b levels on cell morphology and peptidoglycan composition in *Streptococcus pneumoniae* R6. *J Bacteriol,* 195**,** 4342-54.

BERG, K. H., STRAUME, D. & HAVARSTEIN, L. S. 2014. The function of the transmembrane and cytoplasmic domains of pneumococcal penicillin-binding proteins 2x and 2b extends beyond that of simple anchoring devices. *Microbiology,* 160**,** 1585-98.

BIOLABS, N. E. 2019a. *OneTaq DNA Polymerase* [Online]. Available: https://international.neb.com/products/m0480-onetaq-dna-polymerase#Product%20Information [Accessed 05.04.19 2019].

BIOLABS, N. E. 2019b. *PCR Protocol for Phusion High-Fidelity DNA Polymerase* [Online]. Available: https://www.neb.com/protocols/0001/01/01/pcr-protocol-m0530 [Accessed 04.04.2019 2019].

BRUNELLE, J. L. & GREEN, R. 2014. One-dimensional SDS-polyacrylamide gel electrophoresis (1D SDS-PAGE). *Methods Enzymol,* 541**,** 151-9.

BUI, N. K., EBERHARDT, A., VOLLMER, D., KERN, T., BOUGAULT, C., TOMASZ, A., SIMORRE, J. P. & VOLLMER, W. 2012. Isolation and analysis of cell wall components from *Streptococcus pneumoniae*. *Anal Biochem,* 421**,** 657-66.

BYCROFT, B. W. & SHUTE, R. E. 1985. The molecular basis for the mode of action of Beta-lactam antibiotics and mechanisms of resistance. *Pharm Res,* 2**,** 3-14.

CALVEZ, P., BREUKINK, E., ROPER, D. I., DIB, M., CONTRERAS-MARTEL, C. & ZAPUN, A. 2017. Substitutions in PBP2b from beta-Lactam-resistant *Streptococcus pneumoniae* Have Different Effects on Enzymatic Activity and Drug Reactivity. *J Biol Chem,* 292**,** 2854-2865.

CARAPITO, R., CHESNEL, L., VERNET, T. & ZAPUN, A. 2006. Pneumococcal beta-lactam resistance due to a conformational change in penicillin-binding protein 2x. *J Biol Chem,* 281**,** 1771-7.

CHESNEL, L., CARAPITO, R., CROIZE, J., DIDEBERG, O., VERNET, T. & ZAPUN, A. 2005. Identical penicillin-binding domains in penicillin-binding proteins of *Streptococcus pneumoniae* clinical isolates with different levels of beta-lactam resistance. *Antimicrob Agents Chemother,* 49**,** 2895-902.

CHESNEL, L., PERNOT, L., LEMAIRE, D., CHAMPELOVIER, D., CROIZE, J., DIDEBERG, O., VERNET, T. & ZAPUN, A. 2003. The structural modifications induced by the M339F substitution in PBP2x from *Streptococcus pneumoniae* further decreases the susceptibility to beta-lactams of resistant strains. *J Biol Chem,* 278**,** 44448-56.

CLAVERYS, J. P., MARTIN, B. & HAVARSTEIN, L. S. 2007. Competence-induced fratricide in streptococci. *Mol Microbiol,* 64**,** 1423-33.

CONTRERAS-MARTEL, C., DAHOUT-GONZALEZ, C., MARTINS ADOS, S., KOTNIK, M. & DESSEN, A. 2009. PBP active site flexibility as the key mechanism for beta-lactam resistance in pneumococci. *J Mol Biol,* 387**,** 899-909.

CORNICK, J. E. & BENTLEY, S. D. 2012. *Streptococcus pneumoniae*: the evolution of antimicrobial resistance to beta-lactams, fluoroquinolones and macrolides. *Microbes Infect,* 14**,** 573-83.

COWLEY, L. A., PETERSEN, F. C., JUNGES, R., JIMSON, D. J. M., MORRISON, D. A. & HANAGE, W. P. 2018. Evolution via recombination: Cell-to-cell contact facilitates larger recombination events in *Streptococcus pneumoniae*. *PLoS Genet,* 14**,** e1007410.

DALHOFF, A., JANJIC, N. & ECHOLS, R. 2006. Redefining penems. *Biochem Pharmacol,* 71**,** 1085-95.

DAVIES, J. & DAVIES, D. 2010. Origins and evolution of antibiotic resistance. *Microbiology and molecular biology reviews : MMBR,* 74**,** 417-433.

DE PASCALE, G., LLOYD, A. J., SCHOUTEN, J. A., GILBEY, A. M., ROPER, D. I., DOWSON, C. G. & BUGG, T. D. 2008. Kinetic characterization of lipid II-Ala:alanyl-tRNA ligase (MurN) from *Streptococcus pneumoniae* using semisynthetic aminoacyl-lipid II substrates. *J Biol Chem,* 283**,** 34571-9.

DEL CAMPO, R., CAFINI, F., MOROSINI, M. I., FENOLL, A., LINARES, J., ALOU, L., SEVILLANO, D., CANTON, R., PRIETO, J. & BAQUERO, F. 2006. Combinations of PBPs and MurM protein variants in early and contemporary high-level penicillin-resistant *Streptococcus pneumoniae* isolates in Spain. *J Antimicrob Chemother,* 57**,** 983-6.

DENAPAITE, D., BRUCKNER, R., HAKENBECK, R. & VOLLMER, W. 2012. Biosynthesis of teichoic acids in *Streptococcus pneumoniae* and closely related species: lessons from genomes. *Microb Drug Resist,* 18**,** 344-58.

DESMARAIS, S. M., DE PEDRO, M. A., CAVA, F. & HUANG, K. C. 2013. Peptidoglycan at its peaks: how chromatographic analyses can reveal bacterial cell wall structure and assembly. *Mol Microbiol,* 89**,** 1-13.

DU PLESSIS, M., BINGEN, E. & KLUGMAN, K. P. 2002. Analysis of penicillin-binding protein genes of clinical isolates of *Streptococcus pneumoniae* with reduced susceptibility to amoxicillin. *Antimicrobial agents and chemotherapy,* 46**,** 2349-2357.

DURAND, G. A., RAOULT, D. & DUBOURG, G. 2019. Antibiotic discovery: history, methods and perspectives. *Int J Antimicrob Agents,* 53**,** 371-382.

EC 2017. The new EU one health action plan against antimicrobial resistance. *In:* COMMISSION, E. (ed.).

ELDHOLM, V., JOHNSBORG, O., STRAUME, D., OHNSTAD, H. S., BERG, K. H., HERMOSO, J. A. & HAVARSTEIN, L. S. 2010. Pneumococcal CbpD is a murein hydrolase that requires a dual cell envelope binding specificity to kill target cells during fratricide. *Mol Microbiol,* 76**,** 905-17.

FILIPE, S. R., SEVERINA, E. & TOMASZ, A. 2000. Distribution of the mosaic structured murM genes among natural populations of *Streptococcus pneumoniae*. *Journal of bacteriology,* 182**,** 6798-6805.

FILIPE, S. R., SEVERINA, E. & TOMASZ, A. 2001. The role of murMN operon in penicillin resistance and antibiotic tolerance of *Streptococcus pneumoniae*. *Microb Drug Resist,* 7**,** 303-16.

FILIPE, S. R., SEVERINA, E. & TOMASZ, A. 2002. The murMN operon: a functional link between antibiotic resistance and antibiotic tolerance in Streptococcuspneumoniae. *Proc Natl Acad Sci U S A,* 99**,** 1550-5.

FILIPE, S. R. & TOMASZ, A. 2000. Inhibition of the expression of penicillin resistance in *Streptococcus pneumoniae* by inactivation of cell wall muropeptide branching genes. *Proc Natl Acad Sci U S A,* 97**,** 4891-6.

FISER, A., FILIPE, S. R. & TOMASZ, A. 2003. Cell wall branches, penicillin resistance and the secrets of the MurM protein. *Trends Microbiol,* 11**,** 547-53.

FLEMING, A. 1929. On the Antibacterial Action of Cultures of a Penicillium, with Special Reference to their Use in the Isolation of B. influenzæ. *British journal of experimental pathology,* 10**,** 226-236.

FONTAINE, L., BOUTRY, C., DE FRAHAN, M. H., DELPLACE, B., FREMAUX, C., HORVATH, P., BOYAVAL, P. & HOLS, P. 2010. A novel pheromone quorum-sensing system controls the development of natural competence in Streptococcus thermophilus and Streptococcus salivarius. *J Bacteriol,* 192**,** 1444-54.

GARIBYAN, L. & AVASHIA, N. 2013. Polymerase chain reaction. *The Journal of investigative dermatology,* 133**,** 1-4.

GUIRAL, S., MITCHELL, T. J., MARTIN, B. & CLAVERYS, J. P. 2005. Competence-programmed predation of noncompetent cells in the human pathogen *Streptococcus pneumoniae*: genetic requirements. *Proc Natl Acad Sci U S A,* 102**,** 8710-5.

HAKENBECK, R., BRUCKNER, R., DENAPAITE, D. & MAURER, P. 2012. Molecular mechanisms of beta-lactam resistance in *Streptococcus pneumoniae*. *Future Microbiol,* 7**,** 395-410.

HAKENBECK, R., TORNETTE, S. & ADKINSON, N. F. 1987. Interaction of non-lytic beta-lactams with penicillin-binding proteins in *Streptococcus pneumoniae*. *J Gen Microbiol,* 133**,** 755-60.

HANSMAN, D. & BULLEN, M. M. 1967. A RESISTANT PNEUMOCOCCUS. *The Lancet,* 290**,** 264-265.

HARDIE, J. M. & WHILEY, R. A. 1997. Classification and overview of the genera Streptococcus and Enterococcus. *J Appl Microbiol,* 83**,** 1s-11s.

HÅVARSTEIN, L. S. 2010. Increasing competence in the genus Streptococcus. *Mol Microbiol,* 78**,** 541-4.

HÅVARSTEIN, L. S., COOMARASWAMY, G. & MORRISON, D. A. 1995. An unmodified heptadecapeptide pheromone induces competence for genetic transformation in *Streptococcus pneumoniae*. *Proc Natl Acad Sci U S A,* 92**,** 11140-4.

HÅVARSTEIN, L. S., MARTIN, B., JOHNSBORG, O., GRANADEL, C. & CLAVERYS, J. P. 2006. New insights into the pneumococcal fratricide: relationship to clumping and identification of a novel immunity factor. *Mol Microbiol,* 59**,** 1297-307.

JENSEN, A., VALDÓRSSON, O., FRIMODT-MØLLER, N., HOLLINGSHEAD, S. & KILIAN, M. 2015. Commensal streptococci serve as a reservoir for β-lactam resistance genes in *Streptococcus pneumoniae*. *Antimicrobial agents and chemotherapy,* 59**,** 3529-3540.

JOB, V., CARAPITO, R., VERNET, T., DESSEN, A. & ZAPUN, A. 2008. Common alterations in PBP1a from resistant *Streptococcus pneumoniae* decrease its reactivity toward beta-lactams: structural insights. *J Biol Chem,* 283**,** 4886-94.

JOHNSBORG, O., ELDHOLM, V., BJORNSTAD, M. L. & HAVARSTEIN, L. S. 2008. A predatory mechanism dramatically increases the efficiency of lateral gene transfer in *Streptococcus pneumoniae* and related commensal species. *Mol Microbiol,* 69**,** 245-53.

JOHNSBORG, O., ELDHOLM, V. & HAVARSTEIN, L. S. 2007. Natural genetic transformation: prevalence, mechanisms and function. *Res Microbiol,* 158**,** 767-78.

KAWAMURA, Y., HOU, X. G., SULTANA, F., MIURA, H. & EZAKI, T. 1995. Determination of 16S rRNA sequences of Streptococcus mitis and Streptococcus gordonii and phylogenetic relationships among members of the genus Streptococcus. *Int J Syst Bacteriol,* 45**,** 406-8.

KILIAN, M., POULSEN, K., BLOMQVIST, T., HAVARSTEIN, L. S., BEK-THOMSEN, M., TETTELIN, H. & SORENSEN, U. B. 2008. Evolution of *Streptococcus pneumoniae* and its close commensal relatives. *PLoS One,* 3**,** e2683.

KOCAOGLU, O., TSUI, H. C., WINKLER, M. E. & CARLSON, E. E. 2015. Profiling of beta-lactam selectivity for penicillin-binding proteins in *Streptococcus pneumoniae* D39. *Antimicrob Agents Chemother,* 59**,** 3548-55.

KOVÁCS, M., HALFMANN, A., FEDTKE, I., HEINTZ, M., PESCHEL, A., VOLLMER, W., HAKENBECK, R. & BRÜCKNER, R. 2006. A functional dlt operon, encoding proteins required for incorporation of d-alanine in teichoic acids in gram-positive bacteria, confers resistance to cationic antimicrobial peptides in *Streptococcus pneumoniae*. *Journal of bacteriology,* 188**,** 5797-5805.

KUK, A. C. Y., HAO, A., GUAN, Z. & LEE, S.-Y. 2019. Visualizing conformation transitions of the Lipid II flippase MurJ. *Nature Communications,* 10**,** 1736.

LE BOURGEOIS, P., BUGAREL, M., CAMPO, N., DAVERAN-MINGOT, M. L., LABONTE, J., LANFRANCHI, D., LAUTIER, T., PAGES, C. & RITZENTHALER, P. 2007. The unconventional Xer recombination machinery of Streptococci/Lactococci. *PLoS Genet,* 3**,** e117.

LEE, P. Y., COSTUMBRADO, J., HSU, C.-Y. & KIM, Y. H. 2012. Agarose gel electrophoresis for the separation of DNA fragments. *Journal of visualized experiments : JoVE***,** 3923.

LLOYD, A. J., GILBEY, A. M., BLEWETT, A. M., DE PASCALE, G., EL ZOEIBY, A., LEVESQUE, R. C., CATHERWOOD, A. C., TOMASZ, A., BUGG, T. D., ROPER, D. I. & DOWSON, C. G. 2008. Characterization of tRNA-dependent peptide bond formation by MurM in the synthesis of *Streptococcus pneumoniae* peptidoglycan. *J Biol Chem,* 283**,** 6402-17.

MAESTRO, B. & SANZ, J. M. 2016. Choline Binding Proteins from *Streptococcus pneumoniae*: A Dual Role as Enzybiotics and Targets for the Design of New Antimicrobials. *Antibiotics (Basel, Switzerland),* 5**,** 21.

MASSIDDA, O., NOVAKOVA, L. & VOLLMER, W. 2013. From models to pathogens: how much have we learned about *Streptococcus pneumoniae* cell division? *Environ Microbiol,* 15**,** 3133-57.

MEESKE, A. J., RILEY, E. P., ROBINS, W. P., UEHARA, T., MEKALANOS, J. J., KAHNE, D., WALKER, S., KRUSE, A. C., BERNHARDT, T. G. & RUDNER, D. Z. 2016. SEDS proteins are a widespread family of bacterial cell wall polymerases. *Nature,* 537**,** 634-638.

MELLROTH, P., DANIELS, R., EBERHARDT, A., RONNLUND, D., BLOM, H., WIDENGREN, J., NORMARK, S. & HENRIQUES-NORMARK, B. 2012. LytA, major autolysin of *Streptococcus pneumoniae*, requires access to nascent peptidoglycan. *J Biol Chem,* 287**,** 11018-29.

MITCHELL, T. J. 2003. The pathogenesis of streptococcal infections: from tooth decay to meningitis. *Nat Rev Microbiol,* 1**,** 219-30.

MORLOT, C., NOIRCLERC-SAVOYE, M., ZAPUN, A., DIDEBERG, O. & VERNET, T. 2004. The D,D-carboxypeptidase PBP3 organizes the division process of *Streptococcus pneumoniae*. *Mol Microbiol,* 51**,** 1641-8.

MORLOT, C., PERNOT, L., LE GOUELLEC, A., DI GUILMI, A. M., VERNET, T., DIDEBERG, O. & DESSEN, A. 2005. Crystal structure of a peptidoglycan synthesis regulatory factor (PBP3) from *Streptococcus pneumoniae*. *J Biol Chem,* 280**,** 15984-91.

NAVARRE, W. W. & SCHNEEWIND, O. 1999. Surface proteins of gram-positive bacteria and mechanisms of their targeting to the cell wall envelope. *Microbiol Mol Biol Rev,* 63**,** 174-229.

O'BRIEN, K. L., WOLFSON, L. J., WATT, J. P., HENKLE, E., DELORIA-KNOLL, M., MCCALL, N., LEE, E., MULHOLLAND, K., LEVINE, O. S. & CHERIAN, T. 2009. Burden of disease caused by *Streptococcus pneumoniae* in children younger than 5 years: global estimates. *Lancet,* 374**,** 893-902.

OXOID. 2019. *Atmosphere Generation System* [Online]. Available: http://www.oxoid.com/UK/blue/prod_detail/prod_detail.asp?pr=AN0035&org=52&c=UK&lang=EN [Accessed 05.04.2019 2019].

PAGLIERO, E., CHESNEL, L., HOPKINS, J., CROIZE, J., DIDEBERG, O., VERNET, T. & DI GUILMI, A. M. 2004. Biochemical characterization of *Streptococcus pneumoniae* penicillin-binding protein 2b and its implication in beta-lactam resistance. *Antimicrob Agents Chemother,* 48**,** 1848-55.

PERLSTEIN, D. L., ZHANG, Y., WANG, T. S., KAHNE, D. E. & WALKER, S. 2007. The direction of glycan chain elongation by peptidoglycan glycosyltransferases. *J Am Chem Soc,* 129**,** 12674-5.

PESCHEL, A., OTTO, M., JACK, R. W., KALBACHER, H., JUNG, G. & GOTZ, F. 1999. Inactivation of the dlt operon in Staphylococcus aureus confers sensitivity to defensins, protegrins, and other antimicrobial peptides. *J Biol Chem,* 274**,** 8405-10.

PESCHEL, A., VUONG, C., OTTO, M. & GOTZ, F. 2000. The D-alanine residues of Staphylococcus aureus teichoic acids alter the susceptibility to vancomycin and the activity of autolytic enzymes. *Antimicrob Agents Chemother,* 44**,** 2845-7.

PHILIPPE, J., VERNET, T. & ZAPUN, A. 2014. The elongation of ovococci. *Microb Drug Resist,* 20**,** 215-21.

PINHO, M. G., KJOS, M. & VEENING, J. W. 2013. How to get (a)round: mechanisms controlling growth and division of coccoid bacteria. *Nat Rev Microbiol,* 11**,** 601-14.

PLOSMEDICINEEDITORS 2016. Antimicrobial Resistance: Is the World UNprepared? *PLoS medicine,* 13**,** e1002130-e1002130.

REICHMANN, P., XF, NIG, A., LI, XF, ARES, J., ALCAIDE, F., TENOVER, F. C., MCDOUGAL, L., SWIDSINSKI, S. & HAKENBECK, R. 1997. A Global Gene Pool for High-Level Cephalosporin Resistance in Commensal Streptococcus Species and *Streptococcus pneumoniae*. *The Journal of Infectious Diseases,* 176**,** 1001-1012.

ROWLAND, C. 2016. *Biosynthesis of peptidoglycan in Streptococcus pneumoniae* [Online]. Available: https://warwick.ac.uk/study/csde/gsp/eportfolio/directory/pg/lfulbc/research/ [Accessed].

SAIKI, R. K., SCHARF, S., FALOONA, F., MULLIS, K. B., HORN, G. T., ERLICH, H. A. & ARNHEIM, N. 1985. Enzymatic amplification of beta-globin genomic sequences and restriction site analysis for diagnosis of sickle cell anemia. *Science,* 230**,** 1350.

SANGER, F., NICKLEN, S. & COULSON, A. R. 1977. DNA sequencing with chain-terminating inhibitors. *Proc Natl Acad Sci U S A,* 74**,** 5463-7.

SAUERBIER, J., MAURER, P., RIEGER, M. & HAKENBECK, R. 2012. *Streptococcus pneumoniae* R6 interspecies transformation: genetic analysis of penicillin resistance determinants and genome-wide recombination events. *Mol Microbiol,* 86**,** 692-706.

SAUVAGE, E., KERFF, F., TERRAK, M., AYALA, J. A. & CHARLIER, P. 2008. The penicillin-binding proteins: structure and role in peptidoglycan biosynthesis. *FEMS Microbiol Rev,* 32**,** 234-58.

SAUVAGE, E. & TERRAK, M. 2016. Glycosyltransferases and Transpeptidases/Penicillin-Binding Proteins: Valuable Targets for New Antibacterials. *Antibiotics (Basel, Switzerland),* 5**,** 12.

SCHUSTER, C., DOBRINSKI, B. & HAKENBECK, R. 1990. Unusual septum formation in *Streptococcus pneumoniae* mutants with an alteration in the D,D-carboxypeptidase penicillin-binding protein 3. *Journal of bacteriology,* 172**,** 6499-6505.

SCIENTIFIC, T. 2009. NanoDrop 2000/2000c Spectophotometer V1.0 User Manual.

SEVERIN, A. & TOMASZ, A. 1996. Naturally occurring peptidoglycan variants of *Streptococcus pneumoniae*. *J Bacteriol,* 178**,** 168-74.

SHAM, L. T., BUTLER, E. K., LEBAR, M. D., KAHNE, D., BERNHARDT, T. G. & RUIZ, N. 2014. Bacterial cell wall. MurJ is the flippase of lipid-linked precursors for peptidoglycan biogenesis. *Science,* 345**,** 220-2.

SHEPHERD, J. & IBBA, M. 2013. Lipid II-independent trans editing of mischarged tRNAs by the penicillin resistance factor MurM. *J Biol Chem,* 288**,** 25915-23.

SIGMA-ALDRICH. 2019. *RedTaq ReadyMix PCR Reaction Mix with MgCl2* [Online]. Available: http://bioresurs.uu.se/wp-content/uploads/2016/09/bilagan2013_3_d1s80tekniskbulletin.pdf [Accessed 05.04.19 2019].

SMITH, A. M. & KLUGMAN, K. P. 1998. Alterations in PBP 1A essential-for high-level penicillin resistance in *Streptococcus pneumoniae*. *Antimicrob Agents Chemother,* 42**,** 1329-33.

SMITH, A. M. & KLUGMAN, K. P. 2001. Alterations in MurM, a cell wall muropeptide branching enzyme, increase high-level penicillin and cephalosporin resistance in *Streptococcus pneumoniae*. *Antimicrob Agents Chemother,* 45**,** 2393-6.

SOUCY, S. M., HUANG, J. & GOGARTEN, J. P. 2015. Horizontal gene transfer: building the web of life. *Nature Reviews Genetics,* 16**,** 472.

STRAUME, D., STAMSAS, G. A. & HAVARSTEIN, L. S. 2015. Natural transformation and genome evolution in *Streptococcus pneumoniae*. *Infect Genet Evol,* 33**,** 371-80.

SUNG, C. K., LI, H., CLAVERYS, J. P. & MORRISON, D. A. 2001. An rpsL cassette, janus, for gene replacement through negative selection in *Streptococcus pneumoniae*. *Appl Environ Microbiol,* 67**,** 5190-6.

TAGUCHI, A., WELSH, M. A., MARMONT, L. S., LEE, W., SJODT, M., KRUSE, A. C., KAHNE, D., BERNHARDT, T. G. & WALKER, S. 2019. FtsW is a peptidoglycan polymerase that is functional only in complex with its cognate penicillin-binding protein. *Nature Microbiology,* 4**,** 587-594.

TEO, A. C. K. & ROPER, D. I. 2015. Core Steps of Membrane-Bound Peptidoglycan Biosynthesis: Recent Advances, Insight and Opportunities. *Antibiotics (Basel, Switzerland),* 4**,** 495-520.

TODOROVA, K., MAURER, P., RIEGER, M., BECKER, T., BUI, N. K., GRAY, J., VOLLMER, W. & HAKENBECK, R. 2015. Transfer of penicillin resistance from Streptococcus oralis to *Streptococcus pneumoniae* identifies murE as resistance determinant. *Mol Microbiol,* 97**,** 866-80.

TROEGER, C. 2017. Estimates of the global, regional, and national morbidity, mortality, and aetiologies of lower respiratory tract infections in 195 countries: a systematic analysis for the Global Burden of Disease Study 2015. *Lancet Infect Dis,* 17**,** 1133-1161.

VAN DER POLL, T. & OPAL, S. M. 2009. Pathogenesis, treatment, and prevention of pneumococcal pneumonia. *Lancet,* 374**,** 1543-56.

VAN DIJK, E. L., AUGER, H., JASZCZYSZYN, Y. & THERMES, C. 2014. Ten years of next-generation sequencing technology. *Trends Genet,* 30**,** 418-26.

VERHAGEN, L. M., DE JONGE, M. I., BURGHOUT, P., SCHRAA, K., SPAGNUOLO, L., MENNENS, S., ELEVELD, M. J., VAN DER GAAST-DE JONGH, C. E., ZOMER, A., HERMANS, P. W. M. & BOOTSMA,

H. J. 2014. Genome-wide identification of genes essential for the survival of *Streptococcus pneumoniae* in human saliva. *PloS one,* 9**,** e89541-e89541.

VOLLMER, W. 2008. Structural variation in the glycan strands of bacterial peptidoglycan. *FEMS Microbiol Rev,* 32**,** 287-306.

VOLLMER, W., BLANOT, D. & DE PEDRO, M. A. 2008. Peptidoglycan structure and architecture. *FEMS Microbiol Rev,* 32**,** 149-67.

WAHL, B., O'BRIEN, K. L., GREENBAUM, A., MAJUMDER, A., LIU, L., CHU, Y., LUKSIC, I., NAIR, H., MCALLISTER, D. A., CAMPBELL, H., RUDAN, I., BLACK, R. & KNOLL, M. D. 2018. Burden of *Streptococcus pneumoniae* and Haemophilus influenzae type b disease in children in the era of conjugate vaccines: global, regional, and national estimates for 2000-15. *Lancet Glob Health,* 6**,** e744-e757.

WEIL-OLIVIER, C., VAN DER LINDEN, M., DE SCHUTTER, I., DAGAN, R. & MANTOVANI, L. 2012. Prevention of pneumococcal diseases in the post-seven valent vaccine era: a European perspective. *BMC Infect Dis,* 12**,** 207.

ZAPUN, A., CONTRERAS-MARTEL, C. & VERNET, T. 2008a. Penicillin-binding proteins and beta-lactam resistance. *FEMS Microbiol Rev,* 32**,** 361-85.

ZAPUN, A., PHILIPPE, J., ABRAHAMS, K. A., SIGNOR, L., ROPER, D. I., BREUKINK, E. & VERNET, T. 2013. In vitro reconstitution of peptidoglycan assembly from the Gram-positive pathogen *Streptococcus pneumoniae*. *ACS Chem Biol,* 8**,** 2688-96.

ZAPUN, A., VERNET, T. & PINHO, M. G. 2008b. The different shapes of cocci. *FEMS Microbiol Rev,* 32**,** 345-60.

ZERFASS, I., HAKENBECK, R. & DENAPAITE, D. 2009. An important site in PBP2x of penicillin-resistant clinical isolates of *Streptococcus pneumoniae*: mutational analysis of Thr338. *Antimicrobial agents and chemotherapy,* 53**,** 1107-1115.

ZHAO, G., MEIER, T. I., KAHL, S. D., GEE, K. R. & BLASZCZAK, L. C. 1999. BOCILLIN FL, a sensitive and commercially available reagent for detection of penicillin-binding proteins. *Antimicrobial agents and chemotherapy,* 43**,** 1124-1128.

ZHAO, G., YEH, W. K., CARNAHAN, R. H., FLOKOWITSCH, J., MEIER, T. I., ALBORN, W. E., JR., BECKER, G. W. & JASKUNAS, S. R. 1997. Biochemical characterization of penicillin-resistant and -sensitive penicillin-binding protein 2x transpeptidase activities of *Streptococcus pneumoniae* and mechanistic implications in bacterial resistance to beta-lactam antibiotics. *J Bacteriol,* 179**,** 4901-8.

Appendix

A1 Sequence alignments of *S. pneumonia* R6 and *S. oralis* Uo5 genes

PBP transpeptidase active site catalytic motifs highlighted in yellow. Substitutions known to confer increased β-lactam resistance in *S. pneumoniae* highlighted in green.

A1.1 Sequence alignment of *PBP2x*$_{R6}$ and *PBP2x*$_{Uo5}$

84.67% identity.

```
PBP2xR6       -MKWTKRVIRYATKNRKSPAENRRRVGKSLSLLSVFVFAIFLVNFAVIIGTGTRFGTDLA  59
PBP2xUo5      MKTWKEKIVHFAIKNRKTTLENRRRVGKSLSLLAVFLFAVFLVNFAVIIGTGKKFGVDLV  60
                .*.:::::::* ****:  ************:**:**:************.:**.**.

PBP2xR6       KEAKKVHQTTRTVPAKRGTIYDRNGVPIAEDATSYNVYAVIDENYKSATGKILYVEKTQF  119
PBP2xUo5      KEASRVHQTTRTVPAKRGTIYDRNGTPIAEDATSYNVYAVIDKDYKSANGDILYVEESQY  120
              ***.:*********************.*****************::****.*.*****::*:

PBP2xR6       NKVAEVFHKYLDMEESYVREQLSQPNLKQVSFGAKGNGITYANMMSIKKELEAAEVKGID  179
PBP2xUo5      NKVAEIFHKYLDMEESYVKEQLSQPNLKQVSFGAKGNGITYANMMSIKQDLEAAKVEGVN  180
              *****:************:******************************::****:*:*::

PBP2xR6       FTTSPNRSYPNGQFASSFIGLAQLHENEDGSKSLLGTSGMESSLNSILAGTDGIITYEKD  239
PBP2xUo5      FTTSPNRSYPNGKFASSFIGLAQLHENEDGSKSLIGTSGIESSLNSLLAGTDGIITYEKD  240
              ************:**********************:****:******:**************

PBP2xR6       RLGNIVPGTEQVSQRTMDGKDVYTTISSPLQSFMETQMDAFQEKVKGKYMTATLVSAKTG  299
PBP2xUo5      RVGNIVPGTELVSQQTVDGKDVYTTLSSPLQSFMETQMDAFLEKVKGKYMTATLVSAKTG  300
              *:********* ***:*:********:*************** ******************

PBP2xR6       EILATTQRPTFDADTKEGITEDFVWRDILYQSNYEPGSTMKVMMLAAAIDNNTFPGGEVF  359
PBP2xUo5      EILATTQRPTFNADTKEGITEDFVWRDILYQSNYEPGSGMKVMTLASSIDNNTFPSGEYF  360
              ***********:************************** **** **::*******.** *

PBP2xR6       NSSELKIADATIRDWDVNEGLTGGRMMTFSQGFAHSSNVGMTLLEQKMGDATWLDYLNRF  419
PBP2xUo5      NSSEFKMADATIRDWDVNEGLTTGSMMTFLQGFAHSSNVGMSLLEQKMGDATWLDYLKRF  420
              ****:*:**** ********** * **** ***********:***************:**

PBP2xR6       KFGVPTRFGLTDEYAGQLPADNIVNIAQSSFGQGISVTQTQMIRAFTAIANDGVMLEPKF  479
PBP2xUo5      KFGVPTRFGLTDEYAGQLPADNIVSIAQSSFGQGISVTQTQMLRAFTAIANDGVMLEPKF  480
              ************************.*****************:*****************

PBP2xR6       ISAIYDPNDQTARKSQKEIVGNPVSKDAASLTRTNMVLVGTDPVYGTMYNHSTGKPTVTV  539
PBP2xUo5      ISAIYDTNNQSVRKSQKEIVGNPVSKEAASTTRNHMILVGTDPLYGTMYNHYTGKPIITV  540
              ****** *:*:.***************:*** **.:*:*******:******* **** :**

PBP2xR6       PGQNVALKSGTAQIADEKNGGYLVGLTDYIFSAVSMSPAENPDFILYVTVQQPEHYSGIQ  599
PBP2xUo5      PGQNVAVKSGTAQIADEKNGGYLVGSTNYIFSVVTMNPAENPDFILYVTVQQPEHYSGIQ  600
              ******:****************** *:****.*:*.**********************

PBP2xR6       LGEFANPILERASAMKDSLNLQTTAKALEQVSQQSPYPMPSVKDISPGDLAEELRRNLVQ  659
PBP2xUo5      LGEFATPILERASAMKESLNLQSPAKNLDKVTTESSYAMPSIKDISPGELAEALRRNIVQ  660
              *****.**********:*****: ** *::*: :* * ***:******:*** ****:**

PBP2xR6       PIVVGTGTKIKNSSAEEGKNLAPNQQVLILSDKAEEVPDMYGWTKETAETLAKWLNIELE  719
PBP2xUo5      PIVVGTGTKIKETSVEEGTNLAPNQQVLLLSDKVEEIPDMYGWKKETAETFAKWLDIELE  720
              ***********::*.***.*********:****.**:******.******:****:****

PBP2xR6       FQGSGSTVQKQDVRANTAIKDIKKITLTLGD      750
PBP2xUo5      FEGSGSVVQKQDVRTNTAIKNIKKIKLTLGD      751
              *:*****.*******:*****:****.*****
```

A1.2 Sequence alignment of *PBP2b*$_{R6}$ and *PBP2b*$_{Uo5}$

83.68 % identity.

```
PBP2bR6       MRKFNSHSIPIRLNLLFSIVILLFMTIIGRLLYMQVLNKDFYEKKLASASQTKITSSSAR  60
PBP2bUo5      MRKFNSHSIPIRLNLLFAIVILLFMAIIGRLLYMQVLNKDFYETKLASASQTRVTTSSAR  60
              ******************:*******:*****************.********::*:****

PBP2bR6       GEIYDASGKPLVENTLKQVVSFTRSNKMTATDLKETAKKLLTYVSISSPNLTERQLADYY  120
PBP2bUo5      GQIYDAAGKPLVENTVKQVVSFTRNNKMTAAELKETAKKLLTYVNVTSPDLTDRQIADYY  120
              *:*****:********:********.*****::************.::**:**:**:****

PBP2bR6       LADPEIYKKIVEALPSEKRLDSDGNRLSESELYNNAVDSVQTSQLNYTEDEKKEIYLFSQ  180
PBP2bUo5      LADQDIYKKTVESLPSDKRLDSDGNRLSEATLYNNAVESIDVSQLNYTDDQKKEIYLFSQ  180
              *** :**** **:***:************: ******:*:::.******:*:*********

PBP2bR6       LNAVGNFATGTIATDPLNDSQVAVIASISKEMPGISISTSWDRKVLETSLSSIVGSVSSE  240
PBP2bUo5      LNAVENFATSTISTDALDDTQVALVASASKELPGISISTSWDRKVLDTSLSTIVGSVSNE  240
              **** ****.**:** *:*:***::** ***:**************:****:******.*

PBP2bR6       KAGLPAEEAEAYLKKGYSLNDRVGTSYLEKQYEETLQGKRSVKEIHLDKYGNMESVDTIE  300
PBP2bUo5      KSGLPAEEVDAYLKKGYSLNDRVGTSYLEKQYEEVLQGKRTVKEIHLDKHGDMESVENIE  300
              *:*******.:************************.*****:********:*:****:.**

PBP2bR6       EGSKGNNIKLTIDLAFQDSVDALLKSYFNSELENGGAKYSEGVYAVALNPKTGAVLSMSG  360
PBP2bUo5      EGSKGKNIKLTIDLAFQDSVDSLLKSYFNSELANGGARYSEGVYAVALNPKTGAVLAMSG  360
              *****:****************:********** ****:******************:***

PBP2bR6       IKHDLKTGELTPDSLGTVTNVFVPGSVVKAATISSGWENGVLSGNQTLTDQSIVFQGSAP  420
PBP2bUo5      MKHNVETGELTTDSLGTVTNVFVPGSVVKAATISSGWENGVLSGNQTLTDQPIVFQGSAP  420
              :**:::***** ****************************************** ********

PBP2bR6       INSWYTQAY-GSFPITAVQALEYSSNTYMVQTALGLMGQTYQPNMFVGTSNLESAMEKLR  479
PBP2bUo5      INSWYTPYYDGSFPITAVEALEYSSNAYMVQTVLGIMGQTYQPNMTVGTNNLESAMGKLR  480
              ******  * ********:*******:*****.**:********** ***.****** ***

PBP2bR6       STFGEYGLGTATGIDLPDESTGFVPKEYSFANYITNAFGQFDNYTPMQLAQYVATIANNG  539
PBP2bUo5      STFGEYGLGVSTEIDLPDESTGFIPQKFDLANYLTNAFGQFDNYTPMQLAQYVATIANNG  540
              *********.:* **********:*::::.:***:**************************

PBP2bR6       VRVAPRIVEGIYGNNDKGGLGDLIQQLQPTEMNKVNISDSDMSILHQGFYQVAHGTSGLT  599
PBP2bUo5      VRLAPHIVEGIYDNNDKGGLGELIQAIDTKEINKVNISESDMAILHQGFYQVSHGTSPLT  600
              **:**:******.********:*** :: .*:******:***:*********:**** **

PBP2bR6       TGRAFSNGALVSISGKTGTAESYVADGQQATNTNAVAYAPSDNPQIAVAVVFPHNTNLTN  659
PBP2bUo5      TGRAFSDGATVSISGKTGTGESYVAGGQDANNTNAVAYAPTENPQIAVAVVFPHNTNLTK  660
              ******:** *********.*****.**:*.**********::*****************:

PBP2bR6       GVGPSIARDIINLYQKYHPMN       680
PBP2bUo5      NVGPAIARDIINLYNQHHPMN       681
              .***:*********:::****
```

A1.3 Sequence alignment of *PBP1a*$_{R6}$ and *PBP1a*$_{Uo5}$

84.38% identity.

```
PBP1aR6       MNKPTILRLIKYLSISFLSLVIAAIVLGGGVFFYYVSKAPSLSESKLVATTSSKIYDNKN  60
PBP1aUo5      MNKQTFLRIAKYVSISLLTVFIAAVMLGGGLFLYYVSKAPELSESKLVATTSSKIYDSND  60
              *** *:**: **:***:*::.***::****:*:*******.***************.::

PBP1aR6       QLIADLGSERRVNAQANDIPTDLVKAIVSIEDHRFFDHRGIDTIRILGAFLRNLQS-NSL  119
PBP1aUo5      ELIADLGSERRVNAQANEIPTDLVNAIVSIEDHRFFNHRGIDTIRILGATLRNLRGGGGL  120
              :*****************:******:***********:************ ****:. ..*

PBP1aR6       QGGSALTQQLIKLTYFSTSTSDQTISRKAQEAWLAIQLEQKATKQEILTYYINKVYMSNG  179
PBP1aUo5      QGASTLTQQLIKLTYFSTSTSDQTLSRKAQEAWLAVQLEQKATKQEILTYYINKVYMSNG  180
              **.*:*******************:**********:************************

PBP1aR6       NYGMQTAAQNYYGKDLNNLSLPQLALLAGMPQAPNQYDPYSHPEAAQDRRNLVLSEMKNQ  239
PBP1aUo5      NYGMQTAAQSYYGKDLKDLSIPQLALLAGMPQAPNQYDPYSHPEAAQERRNLVLSEMKGQ  240
              *********.******::**:**************************:**********.*

PBP1aR6       GYISAEQYEKAVNTPITDGLQSLKSASNYPAYMDNYLKEVINQVEEETGYNLLTTGMDVY  299
PBP1aUo5      GYISAEQYEKAINTPITDGLQSLKSANSYPPYMDNYLKEVIDQVEQETGYNLLTTGMDVY  300
              ***********:**************..** **********:***:**************

PBP1aR6       TNVDQEAQKHLWDIYNTDEYVAYPDDELQVASTIVDVSNGKVIAQLGARHQSSNVSFGIN  359
PBP1aUo5      TNVDPKVQQHLWDIYNTDEYVNYPDDEMQVASTIVDVTNGKVIAQLGSRHQASNVSFGTN  360
              **** :.*:************ *****:*********:*********:***:****** *

PBP1aR6       QAVETNRDWGSTMKPITDYAPALEYGVYESTATIVHDEPYNYPGTNTPVYNWDRGYFGNI  419
PBP1aUo5      QAVETNRDWGSSMKPITDYAPALEYGVYDSTASIVHDVPYNYPGTDTPLYNWDHVYFGNI  420
              ***********:****************:***:**** *******:**:****: *****

PBP1aR6       TLQYALQQSRNVPAVETLNKVGLNRAKTFLNGLGIDYPSIHYSNAISSNTTESDKKYGAS  479
PBP1aUo5      TIQYALQQSRNVTAVETLNKVGLDRAKTFLNGLGIDYPSMHYANAISSNTTESNKQYGAS  480
              *:********** **********:***************:**:**********:*:****

PBP1aR6       SEKMAAAYAAFANGGTYYKPMYIHKVVFSDGSEKEFSNVGTRAMKETTAYMMTDMMKTVL  539
PBP1aUo5      SEKMAAAYAAFANGGIYHKPMYINKIVFSDGSSKEYADSGTRAMKETTAYMMTEMMKTVL  540
              *************** *:*****:*:******.**::: **************:******

PBP1aR6       SYGTGRNAYLAWLPQAGKTGTSNYTDEEIENHIKTSQFVAPDELFAGYTRKYSMAVWTGY  599
PBP1aUo5      AYGTGRGAYLPWLPQAGKTGTSNYTDEEIENYIKNTGYVAPDEMFVGYTRKYSMAVWTGY  600
              :******.*** ********************:**.: :******:*.**************

PBP1aR6       SNRLTPLVGNGLTVAAKVYRSMMTYLSEGSNPEDWNIPEGLYRNGEFVFKNGARSTWSSP  659
PBP1aUo5      SNRLTPIVGDGFYVAAKVYRSMMTYLSEDNNPGDWTMPEGLYRSGEFVFKNGARSAWTAP  660
              ******:**:*: ***************..** **.:*******.***********:*::*

PBP1aR6       APQQPPSTESSSSSSDSSTSQSSSTTPSTNNSTTTNPNNNTQQSNTTPDQ------QNQN  713
PBP1aUo5      APQQAPTPESSSSTSESSTSQSSSTTPSTNNSANNNTN--NQQPNTTPGQQNQNQNQNQN  718
              **** *: *****:*:****************:..* *  .** ****.*      ****

PBP1aR6       PQPAQP      719
PBP1aUo5      PQPAQP      724
              ******
```

A2 Sequence alignment of *murM*$_{R6}$ and *murM*$_{Uo5}$

50.25% identity.

```
MurMR6          MYRYQIGIPTLEYDQFVKEHELANVLQSSAWEEVKSNWQHEKFGVYREEKLLATASILIR   60
MurMUo5         MFTYKMNVDVQEWDLFLQNHYQGNLLQSSDWAKIKDTWGNERVGFYKDNQLVGVANILIQ   60
                *: *::.: . *:* *:::*  .*:**** * ::*..* :*:.*.*::::*:..*.***:

MurMR6          TLPLGYKMFYIPRGPILDYGDKELLNFAIQSIKSYARSKRVVFVTFDPSICLSQSLINQE   120
MurMUo5         PLPLGLSMFYIPRGPVVDYEDKELLKFVLLTIKKLAKKSRAIMVKFDPSLFVSRGLIGQE   120
                 **** .********::** *****:*.: :**. *:..*.::*.****: :*:.**.**

MurMR6          KTEFPENLAIIDSLQQMGVRWSGKTEEMGDTIQPRIQAKIYKENFEEDKLSKSTKQAIRT   180
MurMUo5         TVQNSRTLEIVEELKKNKVYWTGLTKDMAENIQPRFQANIHKENFSLDQLSKSTRQAIRT   180
                ..:  ..* *::.*::  * *:* *::*.:.****:**:*:****. *:*****:*****

MurMR6          ARNKGLEIQYGGLELLDSFSELMKKTEKRKEIHLRNEAYYKKLLDNFKDKAYITLATLDV   240
MurMUo5         ARNKGLEVKFGGLDLLDEFSFLMKKTESRKNISLRGKDYYQKLLTTYPNHCFITMSYLDL   240
                *******:::***:***.** ******.**:* **.: **:*** .: ::.:**:: **:

MurMR6          SKRSQELEEQLAKNRALEETFTESTRTSKVEAQKKEKERLLEELTFLQEYIDVGQARVPL   300
MurMUo5         PNRLKEVEKQLEKNLKIAQKFTDKTKEGKVKDNHQERKRLEEEISFLKSYIDRGDSVVPL   300
                 :* :*:*:** **  : :.**:.*: .**: :::*::** **::**:.*** *:: ***

MurMR6          AATLSLEFGTTSVNIYAGMDDDFKRYNAPILTWYETARYAFERGMVWQNLGGVENSLNGG   360
MurMUo5         SGTLTVEFGETSENLYAGMNEEFRHYQPAIPTWFETAQHSFERGAETHNMGGLENNLDGG   360
                :.**::*** ** *:****:::*::*:  * **:***::**** :*:**:**.*:**

MurMR6          LYHFKEKFNPTIEEYLGEFTMPTHPLYPLLRLALDFRKTLRKKHRK 406
MurMUo5         LFNFKSKFNPTIEEFVGEFNYPTSSLYFLFNIAYKIRKKLRSRN-- 404
                *::**.********::***. **  ** *:.:* .:**.**.::
```

A3 Abbreviations

Abbreviations	
AMR	Anti-Microbial Resistance
CBD	Choline-Binding Domain
CBP	Choline-Binding Protein
ddNTP	Di-DeoxyNucleotideTriPhosphate
dNTP	DeoxyNucleotideTriPhosphate
EDTA	EthyleneDiamineTetraAcetic acid
FD	Functional Domain
gDNA	Genomic DNA
HMM	High Molecular Mass
HPLC	High-Performance Liquid Chromatography
LMM	Low Molecular Mass
LTA	LipoTeichoic Acid
MIC	Minimal Inhibitory Concentration
NGS	Next Generation Sequencing
PAGE	PolyAcrylamide Gel Electrophoresis
PASTA	PBP And Serine/Threonine kinase Associated
PBP	Penicillin-Binding Protein
PC	Phase Contrast (microscopy)
PCR	Polymerase Chain Reaction
TAE	Tris-Acetate EDTA
TFA	TriFluorAcetic acid
TG	TransGlycosylase
TM	TransMembrane
TP	TransPeptidase
WGS	Whole Genome Sequencing
WTA	Wall Teichoic Acid

Norges miljø- og biovitenskapelige universitet
Noregs miljø- og biovitskapelege universitet
Norwegian University of Life Sciences

Postboks 5003
NO-1432 Ås
Norway